

STUDY ON THE MATERIAL ENGINEERING ASPECTS OF MICROWAVE SINTERED ALUMINIUM CENOSPHERES COMPOSITES

THESIS

Submitted in partial fulfillment of the requirements for the
degree of

DOCTOR OF PHILOSOPHY

by

M. G. Ananda Kumar



**DEPARTMENT OF METALLURGICAL
AND
MATERIALS ENGINEERING**

**NATIONAL INSTITUTE OF TECHNOLOGY KARNATAKA
SURATHKAL, MANGALORE-575025**

JULY 2016

Declaration

by the

Ph.D. RESEARCH SCHOLAR

I hereby declare that the Research Synopsis Thesis entitled “**Study on the Material Engineering aspects of Microwave sintered Aluminum– Cenospheres Composites** ” which is being submitted to the **National Institute of Technology-Karnataka, Surathkal** in partial fulfillment of the requirements for the award of the Degree of **Doctor of Philosophy in Materials Engineering** is a bonafide report of the research work carried out by me. The material contained in this Research Thesis has not been submitted to any University or Institution for the award of any degree.

M. G. Ananda Kumar

Register Number: **081013MT08P01**

Department of Metallurgical and Materials Engineering,

National Institute of Technology Karnataka, Surathkal

Place: NITK-Surathkal

Date: 29.07.2016

CERTIFICATE

This is to certify that the Research Synopsis Thesis entitled “**Study on the Material Engineering aspects of Microwave sintered Aluminum– Cenospheres Composites**” submitted by M. G. Ananda Kumar (Register Number: **081013MT08P01**) as the record of the research work carried out by him, is accepted as the **Research Thesis** submission in partial fulfillment of the requirements for the award of degree of **Doctor of Philosophy**

Dr. Jagannath Nayak

Research Guide (Internal)

Department of Metallurgical

and Materials Engineering,

National Institute of Technology Karnataka,

Surathkal

Dr. S. Seetharamu

Research Guide (External)

Director (Retd.)

Central Power Research Institute

Bangalore

Date: 29.07.2016

ACKNOWLEDGEMENTS

I would like to express my sincere gratitude to **Dr. Jagannath Nayak**, Professor and Head, Department of Metallurgical and Materials Engineering, NITK, Surathkal for allowing me to carry out the research work under his supervision and for his valuable guidance throughout the project work. I express my sincere thanks and gratitude to the RPAC members **Dr. Subhash Yaragal** and **Dr. S. M. Kulkarni** for their kind guidance and advice during my course work. My heartfelt thanks are also due to all **Faculty Members** of the **Department of Metallurgical and Materials Engineering, NITK Surathkal**.

I am grateful to **Dr. S. Seetharamu**, Former Director, Central Power Research Institute, Bangalore for his kind guidance and supervision for carrying out this research work at CPRI. I thank **Dr. M. Shekhar Kumar**, Head MTD, **Sri T. R. Venkatesh** Joint Director, Materials Technology Division, CPRI Bangalore for their encouragement and permission for me to carry out the project work in the department and to use the laboratory facilities.

I immensely thank the **Director General and Management of Central Power Research Institute, Bangalore** for permitting me to pursue my PhD work from the Institute. I specially thank **Sri S. Vynatheya, Sri Arvind Kumar**, Engineering Officers from CPRI for helping me in the material characterization work and other colleagues of CPRI for their suggestions, comments and guidance. I would like to whole heartedly thank **Sri S. Dhanraj**, Technician, MTD CPRI for his kind help and involvement in sample preparation and sintering work. I also thank the technicians of **Sri J. Shanker, Sri Chinnappa** and **Sri Anjanayya** who helped me in the times of need during the experimental works.

I immensely thank the support and help of **Dr. P. Sampath Kumaran**, Joint Director (Retd.) and Professor Sambhram Institute of Technology, Bangalore and **Dr. Nataraj J.R** Professor, RV College of Engineering, Bangalore and for correcting the manuscript and for their valuable guidance and suggestion for preparing the thesis.

I profusely thank **Dr. B.K. Muralidhara**, Dean and Professor, Department of Mechanical Engineering, UVCE, Bangalore, **Dr. C. D.Madhusoodana**, AGM, BHEL CTI, Bangalore **Dr. L. N. Satapathy**, AGM, BHEL CTI Bangalore for their critical comments and

suggestions during the research work.

I thank very much Mr. **Basavaraj** and Mr. **Siddanagouda Patil** for their kind help in conducting the FEM analysis.

Thanks to my family members especially my mother **Smt Sreelakshmi** and my brother **Late Sri Raghunandan**, for their blessings, my wife **Smt. Veena** and my daughter **Kum. Sharanya** for all their support and encouragement during my PhD course.

Finally, I thank all those who directly & indirectly helped me to complete the research work and submit the thesis.

M G ANANDA KUMAR

List of Figures

Fig.2.1 Coal Fired Thermal Power Plant	9
Fig.2.2 Fly ash pond	9
Fig.2.3 Ash pile up near ash pond	10
Fig.2.4 Cenospheres particles in fly ash	11
Fig.2.5 Stir Casting Apparatus	19
Fig.2.6 The Electromagnetic Spectrum and MW frequencies for processing	27
Fig.2.7 Microwave material interaction	29
Fig.2.8 Illustration of microwave and conventional sintering of material	33
Fig.2.9 Illustration of rapid microwave sintering with that of conventional sintering of material	34
Fig.2.10 Flow chart for the study on the composite	38
Fig.3.1 Aluminium Powder	42
Fig.3.2 As received cenospheres	42
Fig. 3.3 Planetary bowl mill	43
Fig.3.4 Pressed composite pellets round specimen samples	46
Fig.3.5 Pressed composites rectangular specimen samples	46
Fig.3.6 Hydraulic press	47
Fig.3.7 Microwave sintering cycle (90 min) for composite sintered at 665 deg C	48
Fig.3.8 Microwave sintering facility at CPRI	48
Fig.3.9 Sintered composite sample	49
Fig.3.10 Scanning Electron Microscope	50
Fig.3.11 X-Ray Fluorescence (XRF) Spectrometer	51
Fig.3.12 X-ray Diffractometer	51

Fig.3.13 Schematic of Pin on Disc machine	54
Fig.3.14 Jet Erosion Test Rig	55
Fig.3.15 Ash Fusion Temperature Determinator equipment	58
Fig.3.16 Sequences of ash fusion temperature test	59
Fig.4.1 X-ray Diffraction (XRD) pattern of Cenospheres	64
Fig.4.2 Cenospheres particles	65
Fig.4.3 Individual Hollow Cenospheres particle	66
Fig.5.1 Microstructure and XRD of conventionally sintered mix at 650 ⁰ C	71
Fig.5.2 Microstructure and XRD of conventionally sintered mix at 750 ⁰ C	72
Fig.5.3 Microstructure and XRD of conventionally sintered mix at 850 ⁰ C	72
Fig.5.4 Microstructure and XRD of conventionally sintered mix at 950 ⁰ C	72
Fig.5.5 Microstructure and XRD of conventionally sintered mix at 1050 ⁰ C	73
Fig.5.6 Microstructure and XRD of conventionally sintered mix at 1150 ⁰ C	73
Fig.5.7 Microstructure and XRD of microwave sintered mix at 650 ⁰ C	76
Fig.5.8 Microstructure and XRD of microwave sintered mix at 750 ⁰ C	76
Fig.5.9 Microstructure and XRD of microwave sintered mix at 850 ⁰ C	76
Fig.5.10 Microstructure and XRD of microwave sintered mix at 950 ⁰ C	77
Fig.5.11 Microstructure and XRD of microwave sintered mix at 1050 ⁰ C	77
Fig.5.12 Microstructure and XRD of microwave sintered mix at 1150 ⁰ C	77
Fig.5.13 XRD graphs of Un-sintered and microwave sintered mix at various Temperatures	78
Fig.5.14 Sintering Temperature versus Brinell Hardness Number for Conventional and Microwave Sintered Composites	79
Fig.5.15 Sintering Temperature versus Water Absorption for Conventional and Microwave Sintered Composites	79

Fig.6.1 XRD of conventionally sintered aluminium powder at 665 ⁰ C	88
Fig.6.2 XRD of microwave sintered aluminium powder at 665 ⁰ C	89
Fig.6.3 XRD of conventionally sintered composite at 665 ⁰ C	89
Fig.6.4 XRD of microwave sintered composite at 665 ⁰ C	89
Fig.6.5 Microstructure aluminium cenospheres interface at 665 ⁰ C	91
Fig.6.6 Dispersed cenospheres seen in aluminium matrix in microwave sintered composite at 665 ⁰ C	92
Fig.6.7 Bulk Density (g/cc) graph of samples	93
Fig.6.8 Water Absorption (%) values of samples	94
Fig.6.9 Porosity (%) values of samples	95
Fig.7.1 Erosion test samples of conventionally sintered samples	101
Fig. 7.2 Erosion test samples of microwave sintered samples	101
Fig.7.3 Erosion loss comparison of 1C and 1M samples	102
Fig.7.4 Erosion loss comparison of 2C and 2M samples	103
Fig.7.5 Erosion loss comparison of 3C and 3M samples	103
Fig.7.6 Erosion loss comparison of 4C and 4M samples	104
Fig.7.7 Erosion loss comparison of 5C and 5M samples	105
Fig.7.8 Erosion loss comparison of 6C and 6M samples	105
Fig.7.9 Erosion Loss of conventionally sintered samples at 30°, 45°, 60° and 90°	106
Fig.7.10 Erosion Loss of microwave sintered samples at 30°, 45°, 60° and 90°	106
Fig.7.11 Wear loss comparison of 1C and 1M samples at 1, 2 and 3kg load	107
Fig.7.12 Wear surface of conventionally sintered 1C at 3kg load (100X)	108
Fig.7.13 Wear surface of microwave sintered 1M sample at 3kg load (100X)	108
Fig.7.14 Wear loss comparison of 2C and 2M samples at 1, 2 and 3kg load	109
Fig.7.15 Wear surface of 2C (10 vol.% cenospheres) sample at 100X	110

Fig.7.16 Wear surface of 2M (10 vol.% cenospheres)sample at 100X	110
Fig.7.17 Wear loss comparison of 3C and 3M samples at 1, 2 and 3kg load	111
Fig.7.18 Wear loss comparison of 4C and 4M samples at 1, 2 and 3kg load	112
Fig.7.19 Wear surface of 4C (30 vol.% cenospheres) sample at 150X	113
Fig.7.20 Wear surface of 4M (30 vol.% cenospheres) sample at 100X	113
Fig.7.21 Wear loss comparison of 5C and 5M samples at 1, 2 and 3kg load	114
Fig.7.22 Wear surface of 5C (40 vol.% cenospheres) sample at 115X	115
Fig.7.23 Wear surface of 5M (40 vol.% cenospheres) sample at 100X	115
Fig.7.24 Wear loss comparison of 6C and 6M samples at 1, 2 and 3kg load	116
Fig.7.25 Wear Loss of conventionally sintered sample at 1, 2 and 3 kg load	116
Fig.7.26 Wear Loss of microwave sintered sample at 1, 2 and 3 kg load	117
Fig.8.1 Compressive Yield Strength (MPa) of composites prior to thermal shock	127
Fig.8.2 Compressive Yield Strength (MPa) of composites after thermal shock cycles	128
Fig.8.3 Comparison of Co-efficient of Thermal Expansion of composites	129
Fig.9.1 Comparison of Compression Strength of composites	134
Fig.9.2 FEA of Stress vs. Displacement of 1C sample	135
Fig.9.3 FEA of Stress vs. Displacement of 2C sample	136
Fig.9.4 FEA of Stress vs. Displacement of 3C sample	137
Fig.9.5 FEA of Stress vs. Displacement of 4C sample	137
Fig.9.6 FEA of Stress vs. Displacement of 5C sample	138
Fig.9.7 FEA of Stress vs. Displacement of 6C sample	139
Fig.9.8 Comparison of tested and FEA of conventionally sintered composites	139

Fig.9.9 FEA of Stress vs. Displacement of 1M sample	140
Fig.9.10 FEA of Stress vs. Displacement of 2M sample	141
Fig.9.11 FEA of Stress vs. Displacement of 3M sample	142
Fig.9.12 FEA of Stress vs. Displacement of 4M sample	142
Fig.9.13 FEA of Stress vs. Displacement of 5M sample	143
Fig.9.14 FEA of Stress vs. Displacement of 6M sample	144
Fig.9.15 Comparison of tested and FEA of Microwave sintered composites	144
Fig.9.16 Comparison of Modulus of Rupture of composites	146
Fig.9.17 Fracture surface of the 1C tested sample	147
Fig.9.18 Fracture surface of the 1M tested sample	148
Fig.9.19 Fracture surface of the 5C test sample	149
Fig.9.20 Fracture surface of the 5M test sample	149
Fig.9.21 Brinell Hardness Number (BHN) of samples	150

List of Tables

	Page No.
Table 2.1 Physical properties of Cenospheres	12
Table 2.2 Use of Cenospheres in various fields Table No.2 Physical properties of Cenospheres	14
Table 3.1 Properties of Aluminum powder	41
Table 3.2 Composition & Designation	45
Table 3.3 Specification of BHEL make Microwave Sintering Facility	48
Table 4.1 Cenospheres elemental oxide analysis (%)	64
Table 4.2 Major mineral phases in Cenospheres	65
Table 4.3 Particle size distribution of cenospheres	66
Table 4.4 Fusion Temperature of Cenospheres	67
Table 5.1 Phases of Aluminium Cenospheres mix at various temperatures	78
Table 5.2 Comparison of properties of Microwave and Conventional sintered composites samples at various temperatures from 650 to 1050 ⁰ C	78
Table 5.3 Comparison of properties of Microwave and Conventional sintered composites samples at 650 ⁰ C only.	79

Nomenclature

AFT	Ash Fusion Temperature
ALFA	Aluminium Fly Ash Composite
AMMC	Aluminium Metal Matrix Composite
ASTM	American Society for Testing and Material
BHEL	Bharat Heavy Electricals Limited
BHN	Brinell Hardness Number
CMC	Ceramic Matrix Composite
CTE	Co-efficient of Thermal Expansion
CYS	Compression Yield Strength
DIN	Deutsches Institut für Normung (German Institute for Standardization)
EMI	Electromagnetic Interference
ESP	Electro Static Precipitator
FEA	Finite Element Analysis
FEM	Finite Element Method
FT	Fluid Temperature
GHz	Giga Hertz
HRC	Rockwell Hardness C Scale
HT	Hemispherical Temperature
IDT	Initial Deformation Temperature
ISO	International Organization for Standardization
MHz	Mega Hertz
MMC	Metal Matrix Composite

MOR	Modulus of Rupture
MW	Mega Watt
MW	Microwave
MW	Microwave
NTPC	National Thermal Power Corporation
OMC	Organic Matrix Composite
PAMC	Particle reinforced Aluminium Metal Matrix Composite
PIT	Pressure Infiltration Technique
PM	Powder Metallurgy
PMC	Polymer Matrix Composite
PVA	Poly Vinyl Alcohol
RFI	Radio Frequency Interference
RT	Room Temperature
SCIT	Squeeze Cast Infiltration Techniques
SEM/EDAX	Scanning Electron Microscope/ Energy Dispersive X-ray Analysis
SF	Syntactic Foam
SRM	Standard Reference Material
ST	Softening Temperature
TPS	Thermal Power Station
TPS	Thermal Power Station
UTM	Universal Testing Machine
XRD	X-Ray Diffractometer
XRF	X-Ray Fluorescence spectrometer
MWSF	Microwave Sintering Facility

Abstract

The thesis brings out the findings from the study undertaken on development of Aluminium based Metal Matrix composite through Powder Metallurgy route. The composite has been fabricated reinforced with various volume percentages of Fly ash Cenospheres particulates ranging from 0 to 50 vol %. The densification of the composites has been achieved through a non conventional sintering route known as Microwave sintering which is different from the well known conventional processing routes. The microwave sintering process appears rapid and economical.

The Aluminium composites reinforced with Cenospheres and sintering through Microwave sintered composites have been later characterized for physical properties such as Density, Porosity, Hardness and Water Absorption, Chemical characteristics and Morphology of the synthesized composites and that of the raw materials through Scanning Electron Microscopy and Energy Dispersive X-ray Fluorescence methods. The Phase Analysis of the composites has been carried through Powder route X-ray Diffraction. The composites have also been studied for Mechanical properties such as Compression Strength with Finite Element Analysis and Modulus of Rupture. The composites have been studied for Tribological properties such as Wear and Erosion Resistance, Thermal properties such as Co-efficient of Thermal Expansion, Thermal Shock Resistance and Fusion Temperatures. The above test results have been compared with the results of conventionally prepared AMCs.

The study on the various properties on the PM based Aluminium Cenospheres composites sintered in Microwave at 665⁰C have indicated that Apparent Porosity was about 35% compared to conventionally sintered ones which was around 40.7%. The Bulk Density was seen to reduce from 2.2 to 1.75 g/cc and the BHN values were found decreasing from 46 to 24% for the Microwave sintered samples. The conventionally sintered sample showed Bulk Density reducing from of 2.1 to 1.75 g/cc and BHN values were found decreasing from 46 to 24. The BHN values were better than the conventional ones by about 26 %. The CTE of the composites decreased from 25.6 to 7.4 x 10⁻⁶/⁰C with increase in cenospheres content from 0 to 50 vol % for

the conventionally sintered composites. For the microwave sintered composites, the CTE of the composites decreased as the cenospheres content from 25.6 to $3.6 \times 10^{-6}/^{\circ}\text{C}$ which is much lower than the conventionally sintered samples by 51%.

The microwave sintered composites showed lesser erosion loss by about 12-15% compared to conventionally sintered samples. The slide wear data shows that conventionally sintered samples has higher slide wear losses compared to conventionally sintered ones by about 86%. The Flexural strength of the conventionally sintered composites was seen decreasing from 52 to 8.8 MPa while Flexural strength of microwave sintered composites were decreasing from 71.9 to 31.5 MPa with increase in cenospheres content from 10 to 50 vol %. MW sintered was better by about 40% in Flexural Strength compared to the conventionally sintered composites. The Compression strength of the composites containing Cenospheres from 10 vol. % to 50 vol. % was found to decrease from 140.3 to 71.7 MPa with the increase in Cenospheres content, for microwave sintered samples. For the conventionally sintered composites the strength reduced from 140.3 to 71.7 MPa. The compressive strength of microwave sintered samples was more by 17.4 % compared to the conventionally sintered samples.

Aluminium metal matrix composites can be fabricated through powder metallurgy route sintered in microwave sintering which is found to be adoptive & effective rapid sintering method. It is possible to fabricate Aluminium Cenospheres 'Syntactic Foams' through powder metallurgy microwave sintering and the properties for the same match with those materials for applications in automotives.

Key words: Syntactic Foams, Cenospheres, microwave sintering, mechanical properties, flexural strength, porosity, density, metal matrix composite, powder metallurgy.

CONTENTS

	Page No.
Declaration	
Certificate	
Acknowledgement	
LIST OF FIGURES	i
LIST OF TABLES	vi
NOMENCLATURE	vii
ABSTRACT	ix
CHAPTER 1: INTRODUCTION	1
CHAPTER 2: LITERATURE REVIEW	4
2.1 Composites	4
2.2 Matrix	4
2.3 Fillers	5
2.4 Metal Matrix Composites (MMCs)	6
2.4.1 Aluminium Metal Matrix Composites Matrix (AMCs)	7
2.4.2 Particle reinforced Aluminium metal matrix composites (PAMCs)	8
2.5 Cenospheres as particulate filler	8
2.5.1 Advantages of using Cenospheres	13
2.5.2 Cenospheres Application	13
2.6 Aluminium Cenospheres metal matrix composites	14

2.7 Syntactic Foams	16
2.7.1 Aluminium metal matrix Syntactic Foams	16
2.8 Processing of Metal Matrix Composites	18
2.8.1 Liquid State Method	18
2.8.1.1 Stir Casting	18
2.8.1.2 Liquid infiltration technique	19
2.8.2 Solid State processing	19
2.8.2.1 Powder Metallurgy	19
2.8.2.2 Aluminium Powder Metallurgy	21
2.9 Sintering	22
2.9.1 Solid state sintering	23
2.9.2 Vitrification	23
2.9.3 Viscous Sintering	23
2.9.4 Liquid phase sintering	23
2.10 Microwave Sintering	24
2.10.1 Microwave	27
2.10.2 Microwave material interaction	29
2.10.3 Microwave versus conventional heating	33
2.11 Summary on literature review	35
2.12 Gaps in the Technology	36
2.13 Scope and Objectives of the present investigation	38
2.14 Contents of the Thesis	39
CHAPTER 3 EXPERIMENTAL TECHNIQUES	41
3.1 Materials	41

3.1.1 Aluminium	41
3.1.2 Cenospheres	42
3.2 Initial Study on High Temperature Sintering Behavior of Aluminium Cenospheres Mix	43
3.3 Aluminium Cenospheres MMC's processing methodology	44
3.3.1 Materials	44
3.3.2 Mix preparation	45
3.3.3 Pressing	46
3.3.4 Sintering	47
3.4 Evaluation of properties of the sintered Aluminium Cenospheres Metal Matrix Composites (ACMMCs)	49
3.4.1 Micro-structural, Phase and Chemical characterization using SEM, EDAX, XRF and XRD	50
3.4.2 Physical Properties	51
3.4.2.1 Bulk Density	52
3.4.2.2 Water Absorption	52
3.4.2.3 Apparent Porosity	52
3.4.2.4 Particle Size Distribution	53
3.4.3 Tribological studies	54
3.4.3.1 Sliding Wear study	54
3.4.3.2 Jet Erosion Resistance Test	55
3.4.4 Thermal Properties	57
3.4.4.1 Linear Co-efficient of Thermal Expansion (α)	57
3.4.4.2 Thermal Shock Resistance Test	57
3.4.4.3 Ash Fusion Temperature	58
3.4.5 Mechanical Properties	60

3.4.5.1	Compression strength (σ_{cs})	60
3.4.5.2	Analysis of Compressive strength results using Finite Element Method (FEM)	60
3.4.5.3	Flexural strength (σ_{fs})	61
3.4.5.4	Brinell Hardness Number	61
3.5	Equipment used for research work	62
CHAPTER 4 RESULTS AND DISCUSSIONS ON CENOSPHERES MATERIAL CHARACTERIZATION		63
4.1	SEM, XRF and XRD Analysis of Cenospheres	63
4.2	Morphological Analysis of Cenospheres	65
4.3	Particle Size Distribution Analysis Cenospheres	66
4.4	Fusion Temperature determination of Cenospheres	67
4.5	Discussions on the study	67
CHAPTER 5 RESULTS AND DISCUSSIONS ON INITIAL STUDY ON HIGH TEMPERATURE SINTERING BEHAVIOR OF ALUMINIUM CENOSPHERES MIX		69
5.1	Results and Discussions of Conventionally sintered aluminium cenospheres mix	69
5.1.1	Microstructural and Phase Analysis of mix conventionally sintered at 650 ⁰ C	69
5.1.2	Microstructural and Phase Analysis of mix conventionally sintered at 750 ⁰ C	69
5.1.3	Microstructural and Phase Analysis of mix conventionally sintered at 850 ⁰ C	70
5.1.4	Microstructural and Phase Analysis of mix conventionally sintered at 950 ⁰ C	70
5.1.5	Microstructural and Phase Analysis of mix conventionally sintered at 1050 ⁰ C	70

5.1.6 Microstructural and Phase Analysis of mix conventionally sintered at 1150 ⁰ C	71
5.2 Results and Discussions of microwave sintered aluminium cenospheres mix	73
5.2.1 Microstructural and Phase Analysis of mix sintered in microwave at 650 ⁰ C	73
5.2.2 Microstructural and Phase Analysis of mix sintered in microwave at 750 ⁰ C	74
5.2.3 Microstructural and Phase Analysis of mix sintered in microwave at 850 ⁰ C	74
5.2.4 Microstructural and Phase Analysis of mix sintered in microwave at 950 ⁰ C	75
5.2.5 Microstructural and Phase Analysis of mix sintered in microwave at 1050 ⁰ C	75
5.2.6 Microstructural and Phase Analysis of mix sintered in microwave at 1150 ⁰ C	75
5.3 Discussions on the study	80
CHAPTER 6 RESULTS AND DISCUSSIONS ON PHYSICAL, MORPHOLOGICAL AND MICROSTRUCTURAL PROPERTIES	88
6.1 Results and Discussions on morphological and microstructural Analysis	88
6.2 Physical Properties evaluation	92
6.2.1 Bulk Density measurements	92
6.2.2 Water Absorption evaluation	93
6.2.3 Porosity evaluation	94
6.3 Discussions on physical morphological and micro-structural properties	95
CHAPTER 7 RESULTS AND DISCUSSIONS ON THE TRIBOLOGICAL PROPERTIES	101

7.1 Jet Erosion Study	101
7.1.1 Jet Erosion Study of 1C and 1M composite samples	102
7.1.2 Jet Erosion Study of 2C and 2M composite samples	102
7.1.3 Jet Erosion Study of 3C and 3M composite samples	103
7.1.4 Jet Erosion Study of 4C and 4M composite samples	104
7.1.5 Jet Erosion Study of 5C and 5M composite samples	104
7.1.6 Jet Erosion Study of 6C and 6M composite samples	105
7.2 Dry Sliding Wear behaviour	106
7.2.1 Dry Sliding Wear behavior of 1C and 1M composite samples	107
7.2.2 Dry Sliding Wear behavior of 2C and 2M composite samples	109
7.2.3 Dry Sliding Wear behavior of 3C and 3M composite samples	110
7.2.4 Dry Sliding Wear behavior of 4C and 4M composite samples	111
7.2.5 Dry Sliding Wear behavior of 5C and 5M composite samples	113
7.2.6 Dry Sliding Wear behavior of 6C and 6M composite samples	115
7.2.7 Dry Sliding Wear behavior of conventional and microwave sintered composite samples	116
7.3 Discussions on Jet Erosion Study	117
7.4 Discussions on Dry Sliding Wear Behaviour	120
CHAPTER 8 RESULTS AND DISCUSSIONS ON THERMAL PROPERTIES	126
8.1 Compressive Yield Strength (MPa) of conventionally sintered samples before and after thermal shock cycles	126
8.2 Compressive Yield Strength (MPa) of microwave sintered samples before and after thermal shock cycles	128
8.3 Linear Co-efficient of Thermal Expansion (α)	129

8.3 Discussions on thermal properties	129
CHAPTER 9 RESULTS AND DISCUSSIONS ON MECHANICAL PROPERTIES	133
9.1 Compressive strength	133
9.1.1 Finite Element Method Analysis of conventionally sintered samples	135
9.1.1.1 FEA Stress vs. Displacement analysis of 1C sample	135
9.1.1.2 FEA Stress vs. Displacement analysis of 2C sample	135
9.1.1.3 FEA Stress vs. Displacement analysis of 3C sample	136
9.1.1.4 FEA Stress vs. Displacement analysis of 4C sample	137
9.1.1.5 FEA Stress vs. Displacement analysis of 5C sample	138
9.1.1.6 FEA Stress vs. Displacement analysis of 6C sample	138
9.1.2 Finite Element Method Analysis of microwave sintered samples	140
9.1.2.1 FEA Stress vs. Displacement analysis of 1M sample	140
9.1.2.2 FEA Stress vs. Displacement analysis of 2M sample	140
9.1.2.3 FEA Stress vs. Displacement analysis of 3M sample	141
9.1.2.4 FEA Stress vs. Displacement analysis of 4M sample	142
9.1.2.5 FEA Stress vs. Displacement analysis of 5M sample	143
9.1.2.6 FEA Stress vs. Displacement analysis of 6M sample	143
9.2. Flexural strength (Modulus of Rupture)	145
9.3 Study of the fracture surface	147
9.4 Brinell Hardness Number	150
9.5 Discussions on mechanical properties	150
CHAPTER 10 CONCLUSIONS FROM THE STUDY	162
10.1 Scope for future work	165

RESEARCH PUBLICATIONS	166
References	167
Bio data	178
Appendix	179

CHAPTER 1

INTRODUCTION

Composite is defined as a material which is a macroscopic combination of two or more distinct materials, and they have a recognizable interface between them. Composites are used not only for their structural properties, but for vast applications as an engineering material for electrical, thermal, mechanical, tribological, and environmental applications. Modern composite materials are usually optimized to achieve a particular balance of properties for a given range of applications.

Composites are classified at two distinct levels; the first level of classification is usually made with respect to the matrix constituent. The major matrices in the composite classes include organic-matrix composites (OMCs), metal-matrix composites (MMCs), and ceramic-matrix composites (CMCs) and the polymer-matrix composites (PMCs). The second level of classification refers to the type of reinforcement form that are embedded in the matrix such as particulate reinforcements, whiskers, continuous fiber laminated composites, and woven composites etc [Miracle D B 2001, ASM Handbook].

Amongst the various matrix composites, the metal matrix composite are notable and popular materials for their applications as a versatile material having vast and varied engineering applications. Metal Matrix Composites (MMCs) are composites composed of metals like Aluminum, Copper, Iron, Magnesium, Titanium, Cobalt etc as the matrix and having reinforcements such as ceramic, organic materials etc., and they exhibit exceptional engineering properties and aid design of components for specific purposes. Amongst the various metal matrix composites, the Aluminium Metal Matrix Composites (AMMC) are known to possess enhanced properties and offers variety of advantages including higher strength, higher stiffness, lower coefficient of thermal expansion, high fatigue and wear properties, lower density etc., and are cheaper compared to those of other matrix alloys [www.Aluminium.org].

In AMMC one of the constituent is aluminium/ aluminium alloy, which forms the matrix phase. The other constituent is embedded in this alloy matrix and serves as reinforcement, which is usually non-metallic and commonly ceramic in nature [Surappa 2003].

There has been an increasing interest in the MMCs containing low density and low cost reinforcements. Amongst the various reinforcements, Fly ash based 'Cenospheres' is one of those ceramic materials which has low density and are cheaper. Fly ash cenospheres are by product of combusted residue of pulverized coal in thermal power plant boilers which are hollow and porous structured spheres and are in the form of micro balloons. Cenospheres can make an effective reinforcement material in the metal matrix composites.

A similar class of materials which are also MMCs called the 'Syntactic Foams' are becoming popular. Syntactic foams are composed of various metals in the matrix of the composites and are dispersed with hollow ceramic reinforcements. They are gaining importance as a low density light weight materials [Rohatgi et.al 2011]. Amongst the syntactic foam materials, aluminium metal matrix reinforced with cenospheres have been fabricated through conventional stir casting and pressure infiltration techniques and studied. They are a popular class of light weight material and the use of these composite materials appears promising in automotive components.

MMCs are fabricated through various metallurgical processes such as stir casting, melt infiltration technique, powder metallurgy process etc. Amongst these processes, Powder Metallurgy (PM) is an attractive processing technique to produce near net shape products and is commonly used for the fabrication of engineering components and particulate reinforced metal matrix composites. The basic process involved in PM technology route is mixing and blending of powders, consolidation and sintering of the consolidated powders for densification. The densification process is generally carried out by conventional methods in an electric resistance furnace or furnaces fired

using various fuels. But other sintering methods such as, plasma arc sintering technique, microwave assisted sintering etc., are gaining importance presently.

Microwave sintering process is quite significant and unique in recent times for sintering material for densification because of its intrinsic advantages such as rapid heating rates, reduced processing times, uniform temperatures with minimal thermal gradients. Microwave sintering process leads to substantial energy savings with high efficiency, improved properties, finer microstructures, environmental friendly process and are less environmental hazards. The composites sintered through microwave process are expected to yield better properties compared to the composite products that are obtained through conventionally sintering methods.

In the present study, Aluminium Metal Matrix Composites (AMMCs) with Cenospheres as reinforcement have been synthesized through Powder Metallurgy route and sintered rapidly through Microwave sintering route for densification. These composites have been studied for various engineering properties. The study indicated that microwave sintered composites exhibited enhanced properties in terms of light weight, low density, high hardness, low wear loss, low coefficient of thermal expansion and good mechanical strength compared to conventionally sintered ones. Very less information is available from the literature survey on the study on the synthesis of aluminium based syntactic foams with cenospheres reinforcement that has been sintered through Microwave route and studied for their properties.

The present study also indicated that the properties of the Aluminium Cenospheres based Metal Matrix Composites fabricated through Powder Metallurgy route and Microwave sintered, are found to be similar to that of conventionally fabricated Aluminium metal matrix 'Syntactic Foams'. It is also observed that these composites possess better properties such as light weight, low density, high hardness, low wear loss, low thermal expansion and good mechanical strength. The use of these composite materials as a syntactic foam material appears promising and these composites can become a starting material for use in the automotive components.

CHAPTER 2

LITERATURE REVIEW

2.1 Composites

‘Composites’ are engineering materials made up of two or more different components having varied physical and chemical properties and when these components are combined together they produce material with characteristics that are different from those individual components. The composites are mainly composed of a continuous phase called the ‘matrix’ phase and which contains discrete constituent called the ‘filler’ that are reinforced or embedded and evenly distributed in the matrix. The composite derives its distinguishing characteristics from the properties of its constituents, the geometry and architecture of the constituents, and from the boundaries (interfaces) between different constituents. Composite materials are usually classified on the basis of the physical or chemical nature of the matrix phase, and depending on the type of matrix the composites are further classified as Metal Matrix Composites (MMC), Ceramic Matrix Composites (CMC), Polymer Matrix components (PMC) etc., The reinforcement in composites could be in the form of continuous/discontinuous fibres, whisker or particulates, in volume fraction ranging from few percent to 70%. The properties of the composites can be tailor made to the demands of different industrial applications by suitable combinations of matrix, reinforcement and processing route [Surappa 2003].

2.2 Matrix

Matrix is a completely continuous phase in a composite in which a filler or reinforcement of a different material is embedded. The matrix is a monolithic material which forms the bulk of the composite and is continuously connected to any point in the material through a path. Matrix in a composite may be composed of material such as a polymer, a ceramic or a metal and provides a compliant support for the reinforcement embedded in it. [Book: Composite Materials]

2.3 Fillers

Filler is a discrete constituent that is embedded and distributed in the matrix and are in the form of particulates, whiskers, and fibers etc., dispersed evenly in the matrix. Composites are loaded with these fillers to improve strength and/or stiffness. Fillers are particles added to material like (plastics, composite material, concrete etc.) to lower the consumption of more expensive binder material or to better some properties of the mixture material. Worldwide more than 50 million tons of fillers for different application areas, such as paper, plastics, rubber, paints and adhesives, are consumed annually. As such, fillers, produced by more than 700 companies, rank among the world's major raw materials and are contained in a variety of goods for daily consumer needs. Production of metal, ceramic or polymer composite materials employ fillers in their basic structures. [Book: Composite Materials]

Formerly, fillers were used predominantly to cheapen end products. Today, it has been proven that fillers are also able to enhance technical properties of the products. As a result, a number of optimized types of fillers, nano-fillers or surface treated goods have been developed. Industrial solid waste materials are increasingly used in the composite materials as fillers to enhance technical properties of the end product. Fibers are usually chopped, wound or woven and made of materials such as fabric, metal, glass, or fiberglass. Solid, self-lubricated, and bearing grade fillers are commonly available. Particulates vary in terms of shape and size. Powders are usually made of carbon, graphite, silicates, ceramics, and other organic or inorganic materials. Some matrix reinforcements provide improved electrical conductivity. Others offer improved thermal conductivity.

Selecting fillers in composites requires an analysis of physical, mechanical, electrical, and thermal properties. Physical properties include shape, size, morphology, porosity and water absorption. Mechanical properties for composites include tensile strength, tensile modulus, elongation and hardness. Electrical properties include electrical resistivity, dielectric strength, and dielectric constant. Use temperature, deflection

temperature, thermal conductivity, and the coefficient of thermal expansion (CTE) are important thermal properties. [Book: Composite Materials, Internet: Wikipedia]

2.4 Metal Matrix Composites (MMCs)

Metal Matrix Composites first emerged as a distinct technology in an era when improved performance for advanced military systems provided a primary motivation for materials development. In this paradigm, improved affordability and more widespread commercialization followed from the experience gained in the engineering, production and servicing of these initial military applications products. [Miracle et al 2001]. MMCs are composites composed of metals like Aluminum, Copper, Iron, Magnesium, Titanium, and Cobalt etc as the matrix, and having reinforcements such as ceramic, organic materials etc. MMCs exhibit exceptional engineering properties and aid design of components for specific purposes. They offer a unique balance of physical and mechanical properties such as good thermal and electrical conductivity, good fatigue properties, good impact and wear resistance. In addition to this, they add higher strength and stiffness than the matrix alloy alone and have excellent wear resistance and lower coefficient of thermal expansion (CTE). Composite products that are designed for electrical and electronics applications often provide protection against electrostatic discharge (ESD), electromagnetic interference (EMI), and radio frequency interference (RFI). Materials that are electrically conductive or resistive are also available. Thermal compounds, insulators, and interfaces are used between heat-generating devices and heat sinks. [Miracle D B et al 2005].

Additional functionalities can be designed into some MMCs through appropriate selection of constituents. Since the metal matrix and ceramic reinforcement have vastly different physical, thermal, electrical and mechanical properties, MMC properties can be varied over a very broad range that spans metals and ceramics. This confers a degree of tailorability that is unusual in engineering materials. Thermal and electrical properties, for example, can be varied from metal like to ceramic-like by appropriate adjustment of reinforcement volume fraction (V_f), morphology and

distribution [Miracle D B et al 2005]. With the increasing demand for light weight components primarily driven by the need to reduce energy consumption in a variety of societal and structural components, due to rising costs of fuel and demand for higher efficiency, materials selectors are actively looking into diversifying the use of lighter metals such as Aluminium material based composites in lightweight applications [Wu G H et al 2007]. MMCs are fabricated through various metallurgical processes such as stir casting, melt infiltration technique, powder metallurgy process etc.

2.4.1 Aluminium Metal Matrix Composites (AMMCs)

Aluminium alloys are cheap, have low density, excellent strength, ductility and corrosion behavior [Guo R Q et al 1998]. The Aluminium Metal Matrix Composites (AMMC) refer to the class of light weight high performance aluminium centric material systems, are known to possess enhanced properties and offers variety of advantages including higher strength, higher stiffness, lower thermal expansion, high fatigue and wear properties, lower density and cheaper compared to those of other matrix alloys. In AMCs one of the constituent is aluminium/ aluminium alloy, which forms the percolating network and is termed a matrix phase, The other constituent is embedded in this aluminium/ aluminium alloy matrix and serves as reinforcement, which is usually non-metallic and commonly ceramic in nature [Sudharshan et al 2008]. Aluminium composites are also very well known for their high use in several industries such as automotives, aeronautical to leisure and they owe their excellent behaviour from different points of view such as strength, ductility, resistance to corrosion etc., in addition to the fact that they can be modified in order to satisfy different applications. [Torralba et al 2003].

The major advantages of AMCs compared to un-reinforced materials are as follows:

- Greater strength
- Improved stiffness
- Reduced density
- Improved high temperature property

- Controlled thermal expansion co-efficient
- Thermal/ head management
- Enhanced and tailored chemical performance
- Improved abrasion and wear resistance
- Control of mass
- Improved damping capabilities

2.4.2 Particle reinforced Aluminium metal matrix composites (PAMCs)

These composites generally contain equiaxed ceramic reinforcement with an aspect ratio less than about 5. Ceramic reinforcements are generally oxides or carbides or borides and present in volume fraction less than 30% when used for structural and wear resistance applications. However in other engineering applications, the reinforcement volume fraction can be as high as 70 %. PAMCs are manufactured either by solid state (powder metallurgy) or liquid state (stir casting, infiltration and in-situ) processes and they are also less expensive.

The mechanical properties of PAMCs are inferior compared to whisker/ short fibre/ continuous fibre reinforced AMCs but far superior compared to unreinforced aluminium alloys. These composites are isotropic in nature and can be subjected to a variety of secondary forming processes such as extrusion, rolling and forging. [Surappa et al 2003]. Aluminium metal matrix composites are known to possess higher specific strength, high stiffness and low thermal expansion co-efficient when reinforced with suitable particles compared to their base alloy matrices. The densification process is generally carried out by conventional methods using a furnace, but other sintering methods such as microwave assisted sintering are gaining importance [Asokan P et al 2005, Nawathe et al 2009]

2.5 Cenospheres as particulate filler

To meet the electric power requirement, the world population is greatly dependent on fossil fuel. Presently, in India about 75% of the total electrical energy (~ 1,90,000 MW) is generated from fossil fuel [Central Electricity Authority Report 2015] and

about 130 million tons of coal combustion residues in the form of ash as solid waste/by product is being released annually during combustion of pulverized bituminous, sub-bituminous and lignite coal.

Coal –Once reproachfully discarded as a dirty fuel and considered destined for obscurity, but now sobriquet as black diamond. Indian coal typically has ash content of 30-60%. Out of the total ash generated 70 % of the ash comprises of Fly ash and 20 %-Bottom ash. Coal fired thermal power plants generate enormous ash as waste product and with very little utilization rate. The ash deposits of all the TPPs in the country are increasing every day leading to ash disposal problems and environmental hazards. The enormous quantity of ash is made into slurry and sluiced to the ash ponds for disposal.



Fig. 2.1: Coal Fired Thermal Power Plant (source: NTPC)



Fig. 2.2: Fly ash pond (Source: NTPC)



Fig. 2.3: Ash pile up near ash pond (Source: NTPC)

The pulverized coal is combusted the boiler and the combustion residue which is fly ash, gets carried away along the hot gas stream through the electrostatic precipitator (ESP) hoppers, where the fly ash gets trapped. This trapped dry ash is then evacuated, collected and stored in silos for further use in order to avoid environmental pollution. Fly ash is effectively being used in building materials, cement and concrete, roads and embankments, etc. [Ananda Kumar et al 2015]

Fly-ash contains primarily “Cenospheres” which are hollow ceramic micro spheres and is obtained primary by-product from the pulverized coal combustion in power generating thermal power plants. Cenospheres is a useful by-product to produce newer profitable materials which otherwise poses major environmental and disposable problems. Fly-ash cenospheres are unique in the way that they are low density, non-toxic, non metallic hollow micro particles, that are light in weight. Cenospheres have a size range from 1 to 500 microns with an average compressive strength up to 7000 psi. Their color ranges from white to dark grey [www.apitco.org]. They are also referred to as microspheres, hollow spheres, hollow ceramic microspheres, micro balloons, or glass beads [Matsunaga et al 2002].

It is also reported that fly ash particles are composed of two different types-precipitator ash which are solid spherical particles and the other ‘cenospheres’ (< 1% of the total fly ash) which are hollow particles with density less than 1.0 g cm^{-3} .

Another study shows that there are two main classes of microspheres- empty spheres, in which the cavity are filled with gas only called the ‘Cenospheres’ and the other ‘Plerospheres’ in which the cavities are filled with small mineral particles, foam, spongy and other porous frameworks. The term ‘Cenospheres’ comes from the Greek word ‘kenos’(hollow) + ‘spheres’ and reflects the most important feature of the cenospheres- the presence of a cavity surrounded by solid or a perforated mineral shell. The latter of microspheres are often called as network structured cenospheres or ‘Plerospheres’ from the Greek ‘pleres’(filled) + spheres. [V. B. Fenelonov et al 2010]

Traditionally, only particles having densities $< 1 \text{ gm/cm}^3$ have been called ‘cenospheric’. This terminology is probably because cenospheres float on water, allowing harvesting from wet ash impoundments. In the formation of fly ash, the relative amount of cenospheres is typically around 1%. However, cenospheres are really gas bubble-containing particles and their bulk density can be greater than 1 gm/cm^3 and their concentration in combustion ash can be greater than 1%. Cenospheres particles having bulk densities $< 2 \text{ gm/cm}^3$, also can be effectively separated from combustion fly ashes by the use of a specially-designed, pneumatic transport, tribo-electric separators [Matsunaga et al 2002]. Mineralogical analysis revealed that fly ash cenospheres is primarily composed of the crystalline compounds such as Mullite, Quartz and magnetic Spinel. The Quartz (SiO_2), Alumino Silicate, Gehlenite, ($\text{Ca}_2\text{Al}_2\text{SiO}_7$) and Hematite (Fe_2O_3) are the predominant phase constituents, which influenced the concentration of Alumina, Silica and Iron Oxide [Josph J Biernacki et al 2008].

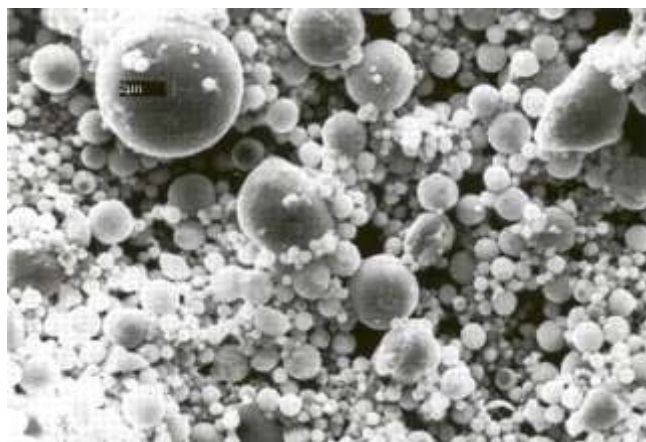


Fig. 2.4: Cenospheres particles in fly ash

Cenospheres are formed during coal combustion in the high temperature boilers when the coal ash is in molten state. The temperatures of these boilers may be as high as 1450°C. Flowing with the combustion gas stream, the temperature of the molten ash particles are rapidly quenched, thereby ‘freezing in’ a spherical shape. Any gas bubbles within the molten particles are also trapped inside the spheres. These bubbles cause the production of light weight sphere-cenospheres; bubbles may occur in multiple forms within the ‘frozen’ particles, or as single concentric forms and their thickness that are nearly as great as the diameter of the particles. The temperature at which the ash turns into molten state depends on the chemical constituents of the ash. The thickness of cenospheres walls may be very small-< 10 % of the particle diameter, typically in the range of 2 – 10 microns. Though considered as a waste, cenospheres is a useful by-product to be used to produce newer materials cheaply which otherwise poses major environmental and disposable problems. The Scanning Electron Micrograph shown in Fig.2.4 depicts the cenospheres dispersed in fly ash particles as received from the thermal power plant.

Table 2.1: Physical properties of Cenospheres [www.cenotechnologies.com]

Particle Density (g/cc)	0.50 to 0.70
Specific Gravity	0.68 –0.72
Bulk Density (g/cc)	0.35-0.42
Hardness (Mohs)	5-6
Thermal Conductivity ($Wm^{-1}K^{-1}$)	0.10- 0.20
Melting Point ($^{\circ}C$)	1200 to 1500
Shell Thickness (μm)	2 – 6
Crushing Strength (psi)	4100 - 7000
Colour	Off-white
Shape	mostly spherical
Moisture (%)	0.2 to 0.4 max
pH in water	8- 8.5
Loss on Ignition (%)	6.0 – 8.0

2.5.1 Advantages of using Cenospheres

The advantages of using cenospheres in the engineering materials application are:

- Spherical in Shape
- Light weight
- Inert Material
- Free flowing
- Insulating
- High Melting point
- Good Hardness
- Good Electrical properties
- Low Oil Absorption
- Good Packing factor

2.5.2 Cenospheres Application

Hollow spheres have been used for more than 20 years to improve the properties of a variety of finished consumer products. They were first introduced as an extender for plastic compounds, as they are compatible with plastisols, thermoplastics, latex, polyesters, epoxies, phenolic resins, and urethanes.

The compatibility of cenospheres with specialty cements and other building materials such as coatings and composites was also quickly identified. Since that time cenospheres have been used in a wide variety of other products, including sports equipment, insulations, automobile bodies, marine craft bodies, paints, and fire and heat protection devices. [www.apitco.org] The ESP fly ash, which has a density in the range of 2.0-2.6 g cm⁻³ are used as fillers to improve various properties of the matrix materials in composites contributing to its stiffness, strength, wear resistance and reduced density of the product [Matsunaga et al 2002].

Table 2.2: Use of Cenospheres in various fields [Source: www.apitco.org]

Ceramics	Refractories, Castables, Tile, Fire Bricks, Aluminum Cement, Insulating Materials, Coatings
Plastics	BMC, SMC, Injection Molding, Moulding, Extruding, PVC Flooring, Film, Nylon, High Density Polyethylene, Low Density Polyethylene, Polypropylene
Construction	Specialty Cements, Mortars, Grouts, Stucco, Roofing Materials, Acoustical Panels, Coatings, Shotcrete, Gunite
Recreation	Marine Craft, Flotation Devices, Bowling Balls, Surf Boards, Kayaks, Golf Equipment, Footwear, Lawn & Garden Décor
Automotive	Composites, Undercoatings, Tires, Engine Parts, Brake Pads, Trim Molding, Body Fillers, Plastics, Sound Proofing Materials
Energy & Technology	Oil Well Cements, Drilling Muds, Coatings, Grinding Materials, Aerospace Coatings & Composites, Explosives, Propeller Blades

2.6 Aluminium Cenospheres metal matrix composites

Various researchers have undertaken studies on cenospheres and their properties mainly to focus on the relationship that exists between the cenospheres chemical composition, its mineralogy, density, fired properties, water absorption characteristics and the morphology on the processed products. The influence of processing parameters like milling, compaction pressures, sintering temperature and time on the properties, microstructure and mineralogical changes of the sintered products have also been investigated [Asokan P et al 2005].

There has been an increasing interest in the MMCs containing low density and low cost reinforcements. The filler addition is the key factor which enhances the physical and mechanical properties of the composites. Among various dispersive reinforcements, fly ash ‘cenospheres’ is one of those ceramic materials which are lower in density, are cheaper and are available in large quantities as solid waste by product in coal fired thermal power stations which is in the form of hollow and porous structured spheres possess good physical, mechanical and tribological characteristics, is used as a filler material. Cenospheres can be incorporated into metal as the

dispersed phase to make low cost metal matrix composites with a range of useful properties [Surappa et al 2003], [Wu G H et al 2007]. Cenospheres can make an effective reinforcement material in the metal matrix composites.

Aluminium fly ash/ Cenospheres metal matrix composites have been fabricated through the low pressure infiltration technique in which molten aluminium is forced down through a bed of loose fly ash powder under pressure and forming a composite. In some other studies, other techniques like casting route have been adopted, in which the molten aluminium metal is reinforced with cenospheres particulates and then cast to form composites and then they have been studied for various properties.

Wu G.H. et al [2008] studied the damping properties of aluminium metal matrix- fly ash composites. The commercial Al alloy and cenospheres fly ash particles with varied diameter range were used in the matrix and studied. Rohatgi P K et al [2009] studied the dry sliding performance of A 206 Aluminium alloy containing silica sand particles and the wear rate of the composites. Guo R. Q. et al [1998] have carried out extensive study on the differential thermal analysis to establish the influence of processing and reheating on the stability of aluminium- fly ash composite systems. Sudharshan and M. K. Surappa et al [2008] have fabricated A 356 Aluminium- fly ash particle composites using stir cast techniques and hot extrusion. The hardness, tensile and compression strength, damping characteristics of the composites have been evaluated.

Kiran Kumar Ekka et al [2013] have studied the effects of ceramic particulates including cenospheres on sliding wear behavior of aluminium matrix composites using Taguchi design and neural network. Kwak J S et al [2008] have reported on the mechanical properties and grinding performance on aluminium based metal matrix composites. Hyo S. Lee et al [2000] have studied the fabrication process and thermal properties of SiCp/Al metal matrix composites for electronic packaging applications. Gaohui Wu et al [2007] have studied the electromagnetic interfering shielding of aluminium alloy- cenospheres composite. Ghosh S et al [2011] studied the characterization of microwave processed aluminium powder. Tjong S.C et al [1999]

have reported on the high temperature creep behaviour of powder-metallurgy aluminium composites reinforced with SiC particles of various sizes.

2.7 Syntactic Foams

A similar class of MMCs material called the ‘Syntactic Foams’ which are composed of various metal matrix composites dispersed with hollow ceramic reinforcements, are gaining importance as a low density light weight materials [Rohatgi et al 2011].

2.7.1 Aluminium metal matrix Syntactic Foams

Amongst the syntactic foam materials, Aluminium metal matrix reinforced with cenospheres have been fabricated through stir casting and pressure infiltration techniques and studied. Metallic Syntactic Foams possess similar properties that of Aluminium Cenospheres metal matrix composites such as light weight, low density, high hardness, low wear loss, low thermal expansion and good mechanical strength. The use of these composite materials appears promising in automotive components.

Anthony Macke et al [2012] have tried to develop Aluminium cenospheres composite for the automotive parts to reduce vehicle weight and improve performance. They have concluded that the composites can be used in automobile industry and can be customized for high-strength, wear-resistant, and self-lubricating lightweight MMCs for specific applications to make significant weight reductions and improve fuel efficiency. Dorian K Balch et al [2005] have studied the plasticity and damage mechanism in the Aluminium syntactic foams deformed under dynamic and quasi static conditions. Chandrakant Kini et al [2015] have tried to investigate the behavior of aluminium fly ash composites synthesized through melt casting route, for their mechanical and other properties. They have concluded that the aluminium fly ash composites have improved hardness, wear and tensile characteristics. Dou Z Y et al [2007] have studied the high strain rate compression behavior of cenospheres pure aluminium syntactic foams. Bhattacharya et al [2002] have studied the thermo physical properties of high porosity metal foams.

Bienias et al [2003] have studied the microstructure and corrosion behavior of aluminium fly ash composites. The outcome of their research findings is that fly ash particles as reinforcement in metal matrix composites and synthesis of Aluminium Fly ash (ALFA) composites by squeeze casting technology in comparison with gravity casting are advantageous for obtaining higher structural homogeneity with minimum possible porosity levels, good interfacial bonding and quite a uniform distribution of reinforcement. Altenaiji et al [2012] have studied the characterization of aluminium matrix syntactic foams under static and dynamic loading. Mondal et al [2009] have synthesized cenospheres filled aluminium syntactic foams made through stir casting technique and studied its properties. The outcome of their study is that the cenosphere primarily contains alumino-silicate phases and are not subjected to any phase transformation up to 900⁰C. Cenospheres also retains their shape and size during mechanical stirring and thus effectively could be used for making cenospheres filled aluminum Syntactic Foam using stir-casting technique. Souvignier C.W et al [2001] have reported on the freeform fabrication of aluminium metal matrix composites. Suresh N et al [2010] have studied the influence of cenospheres of fly ash on the mechanical properties and wear of permanent moulded eutectic Al–Si alloys.

Rohatgi et al [2011] have studied the synthesis, compressive properties and application of metal matrix syntactic foams. Wu G H, et.al [2008] studied the damping properties of aluminium metal matrix- fly ash composites. The commercial Al alloy and cenospheres fly ash particles with varied diameter range were used in the matrix and studied. Rohatgi P K et.al [2009] studied the dry sliding performance of A 206 aluminium alloy containing silica sand particles and the wear rate of the composites.

Guo R Q et.al [1998] have carried out extensive study on the differential thermal analysis to establish the influence of processing and reheating on the stability of aluminium- fly ash composite systems. Sudharshan and Surappa M K et al [2008] have fabricated A 356 Aluminium- fly ash particle composites using stir cast techniques and hot extrusion. Wu G H[2006] have extensively studied the damping characteristics of aluminium fly ash based cellular composites which are potential

material for application in automobile, aerospace and submarine industry. They have studied the damping characteristics using the forced vibration mode in frequency range of 0-8 Hz and the bending vibration mode in the resonant frequency range of the specimen at about 300-500 Hz and it are reported that aluminium fly ash composite material performed well as a damping material compared to other alloy materials.

Mondal et al [2009] have concluded that cenospheres which are primarily aluminosilicates are not subjected to any phase transformation up to 900°C and hence cenospheres can be a suitable material for aluminium based syntactic foam. Since cenospheres are mostly spherical in nature and are porous in nature. The porosity of the cenospheres may be around 10%. The cenospheres' shape does not get distorted during processing and also retains their shape and size even during mechanical stirring in the stir-casting technique for fabrication of syntactic foams. Raghavendra et al [2012] have studied the deformation behavior of aluminium cenospheres syntactic foams as a function of porosity, shell thickness, shell volume fraction and cenospheres volume fraction using FEM under both constrained and unconstrained conditions. Imre Norbert Orbulov [2012] has extensively studied and reported on the compressive properties of aluminium matrix syntactic foams. Nipendra P Singh et al [2003] have reported on the aluminum syntactic foams ALFA for automotive applications.

2.8 Processing of Metal Matrix Composites

MMCs are processed conventionally through metallurgical processes such as Liquid State Method which employs matrix metal in the molten or liquid state.

2.8.1 Liquid State Method

Under the Liquid State Method methods there are Stir Casting and Liquid Infiltration Techniques that are commonly followed for the composite manufacture.

2.8.1.1 Stir Casting

In this process, different dissimilar materials are mixed by stirring. The process involves melting or melting the matrix metal to sufficient liquid form and then

introducing the reinforcement material into the melt. The stirring of the melt is done by a stirrer which is having a rotating impeller such that there is uniform wetting and dispersion of the reinforced material in the matrix. This is a simple and commercial viable conventional technique to produce MMCs [Baskar B et al, 2015].

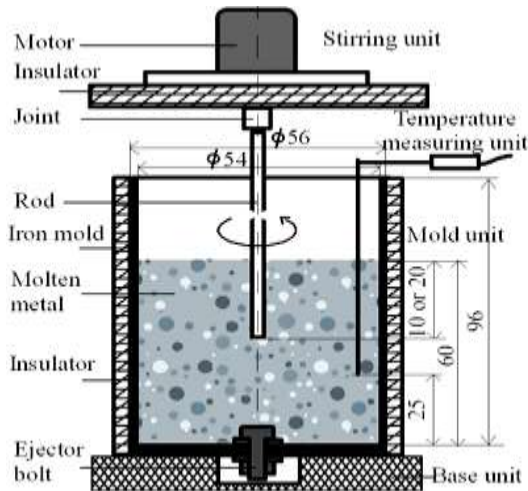


Fig. 2.5: Stir Casting Apparatus (after Baskar B 2015)

2.8.1.2 Liquid infiltration technique

In the Squeeze Cast Infiltration Techniques (SCIT) or Pressure Infiltration Technique (PIT), the molten metal is forced the infiltrate through a preformed reinforcement dispersed phase, by applying pressure on the molten metal through hydraulic or pneumatic pressure. The melt is forced to penetrate into the perform cavity which is placed in the lower fixed mould part.

2.8.2 Solid State processing

The Solid State method in one in which both the matrix and the reinforcement material are in solid state and under this process, Powder metallurgy method is commonly practiced for the fabrication of the composites.

2.8.2.1 Powder Metallurgy

Powder metallurgy (PM) is an attractive processing technique to produce near net shape products and is commonly used for the fabrication of engineering components

and particulate reinforced metal matrix composites. Powder Metallurgy is one of the most common approaches to the synthesis of high performance components for various applications. The PM technology route of processing of materials and engineering parts consists of powder production, powder processing, forming operations and sintering of pressure assisted hot consolidation. Ferrous alloys are widely used in powder metallurgy (PM) for various applications the predominant being the automotive parts. The PM copper and nickel steels are very extensively used for their high strength and excellent dimensional stability.

Powder of many metals, alloys, compounds and ceramic materials with particles sizes ranging from nanometers to several hundred micrometers are available from industrial sources or may be produced by the methods developed over decades in the field of PM or ceramics. One of the necessary steps in the PM approach is that of sintering. The main purpose of sintering is to improve bonding between the powders and to minimize porosity to realize an overall improvement in the properties. The basic steps involved in the synthesis of composites comprise of mixing and blending the powders, followed by consolidation of the powders in a die pressed in hydraulic/ pneumatic presses and finally sintering of the consolidated powders. Secondary processes such as extrusion or rolling may also be carried out after sintering.

Sintering plays an important role in the synthesis of the composites because it assists in improving density, reducing porosity and development of metal-metal bond between metallic powders and metal-ceramic bonds between matrix and reinforcement. The major advantage of the powder metallurgy route is the uniform distribution of the reinforcement in the matrix leading to better matrix particle bonding unlike the problems encountered in the process involving melting of matrix metals and stirring ceramic particles/ reinforcements in the melt such as stir casting, melts infiltration techniques etc. In these processes, the particles try to sink or float in the melt depending of the density relative to that of liquid metal leading to segregation and the particles are also not properly wetted by the liquid matrix material[Kok M 2004].

Although PM can be used to produce near net shape products, a common problem associated with processing aluminium using PM is the presence of thin oxide film on the surfaces of individual particles which prevents strong bond formation between particles. This leads to lower strength and toughness in the sintered products. With the increasing demand for light weight materials due to rising of costs of fuel and demand for higher efficiency, materials selectors are actively looking into diversifying the use of aluminium based materials in lightweight applications. Hence it is important to develop innovative and cost effective sintering techniques to process aluminium components using PM.

Sintering can be accomplished in a number of ways using radiant, plasma, induction and microwave heating sources. Among these methods microwave sintering is rapidly emerging as an energy efficient and environmentally friendly technique. Results of literature search indicated that the investigations on microwave sintering of metallic materials primarily focused on ferrous and copper based alloys with limited studies being carried out to study the effect on the microstructure and the properties of aluminium and its composites.

Nawathe et al [2009] used microwave to synthesize pure aluminium and metastable Al/Cu nano-composites with superior properties. The composites were processed through the powder metallurgy route.

MMCs are fabricated through various metallurgical processes such as stir casting, melt infiltration technique, powder metallurgy process etc. Amongst these processes, Powder Metallurgy (PM) is an attractive processing technique to produce near net shape products and is commonly used for the fabrication of engineering components and particulate reinforced metal matrix composites.

2.8.2.2 Aluminium Powder Metallurgy

Powder Metallurgy (P/M) offers components with exceptional mechanical and fatigue properties, low density, corrosion resistance, high thermal and electrical conductivity, excellent machinability, good response to a variety of finishing processes, and which

are competitive on a cost per unit volume basis. In addition, aluminium P/M parts can be further processed to eliminate porosity and improve bonding and yielding properties that compare favorably to those of conventional wrought aluminium products. The primary driver for the use of aluminium P/M is the unique properties of aluminium coupled with the ability to produce complex net or near net shape parts which can reduce or eliminate the operational and capital costs associated with intricate machining operations. Aluminium P/M can replace other P/M in certain applications on a direct basis. However, in terms of the potential for ferrous based product substitution, each potential application needs to be considered on a case by case basis. Typical economics tend to favor iron parts but the unique characteristics of aluminium such as strength, weight, corrosion resistance, and machinability can make the aluminium parts economical. The basic process involved in PM technology route is mixing and blending of powders, consolidation and sintering the consolidated powders for densification.

2.9 Sintering

Sintering is defined as a heat treatment step which is given to powders of metals and or ceramics which have been pressed into required shape by consolidation and converting this mass into dense solid. One of the necessary steps in the PM approach is that of sintering. The main purpose of sintering is to improve bonding between the powders and to minimize porosity to realize an overall improvement in the properties such as improved density, reduced porosity and development of metal-metal bond between metallic powders, and metal-ceramic bonds between matrix and reinforcement [Asokan P et al 2005].

Sintering occurs in materials by several mechanisms such as vapour transport, surface diffusion, lattice diffusion, grain boundary diffusion and dislocation motions. Sintering can be classified into 4 categories depending of the composition of the material that is sintered and on the extent of secondary phase that forms as a result of sintering.

2.9.1 Solid state sintering

In solid state sintering process the body to be heated to a temperature of about 0.5 to 0.9 of the melting point. In this sintering process there is no liquid phase present and the joining of particles and reduction in pores is due to atomic diffusion.

2.9.2 Vitrification

In vitrification sintering process relatively large amount of liquid phase typically greater than ~ 25% of the original volume is formed which is sufficient to fill the volume of the pores resulting in a denser product due to flow of liquid into the pores.

2.9.3 Viscous Sintering

In this viscous sintering process a consolidated mass of glass powder is heated to its softening temperature such that the densification process occurs by the viscous flow of the glass under surface tension.

2.9.4 Liquid phase sintering

In this sintering process, a small amount of liquid phase which is a few volume percent of the original solid mixture is formed at the sintering temperature. This liquid phase fills the pore space thereby leading to pore volume reduction and densification. [Lutgard C et al 2003].

Most of the MMCs are sintered through solid state sintering processes and they have certain disadvantages like higher processing time and are energy intense, and hence, this calls for adoption of advanced processing technique such as microwave sintering. The advantages of PM process become important especially in conditions where volume fractions of the particulates are to be increased and to achieve effective cohesion and bonding between matrix and reinforcement and achieving the properties. The densification process is generally carried out by conventional methods using a furnace, but other sintering methods such as, plasma arc sintering technique, microwave assisted sintering etc., are gaining importance.

2.10 Microwave Sintering

Microwave (MW) sintering is a process in which the materials to be sintered couple with microwaves, absorb the electromagnetic energy volumetrically, and transform into heat. This heating mechanism enhances diffusion process, reduces energy consumption, has rapid heating rates and reduces processing time. MW sintering improves physical and mechanical properties of the material [Nawathe S et al 2009, Gupta M et al 2005]. Microwave sintering will overcome certain difficulties connected with heating and is ideally suited to accommodate different particulates with vastly different properties compared to matrix.

The applicability of microwave sintering to metals has been simply ignored due to the fact that metals are known to reflect microwaves. The sintering community had explicitly ignored the possibility of sintering their metals using microwaves. Very few papers have reported microwave sintering of powders and alloys, although a couple of papers do report modest heating of metal powders using microwaves [Anklekar et al 2005].

Initially use of microwaves was to process microwave absorbing materials such as oxide or non-oxide ceramics only, but the concept has been extended to sinter metallic powders from commercial sources using a 2.45 GHz microwave field yielding dense products with improved mechanical properties compared to those sintered conventionally. These findings were surprising in view of the reflectivity of the bulk metals to the microwave frequencies. Over the past decade microwave sintering chambers capable of processing a variety of samples with different shapes and sizes, and maintaining any temperature ranges between RT to 1500°C has been developed, in exceptional cases up to 1800 to 2000°C.

The microwave generators are operated at a frequency of 2.45 GHz with power output ranging from 1 to 6 kW in both single and multimode operations are possible [Anklekar et al 2005]. A typical microwave oven has either an alumina or silicon carbide tube surrounded by ceramic high temperature insulation fibers. The primary

function of the insulation is to preserve the heat in the oven. Insulation does not absorb microwave at the lower temperature range. But at higher temperatures there is some portion of power dissipation between the insulation and the sample. Temperatures are read by optical pyrometers or sheathed thermocouples placed very close to the surface of the sample. The relative temperature readings are accurate to $\pm 5^{\circ}\text{C}$. The absolute temperature monitoring is not established to anywhere near that precision. Different controlled atmospheres such as air to H_2 , to forming gas to oxygen can be used. Typically the total sintering time would be ~ 90 minutes. With the use of microwave susceptors, the heating cycle can be rapid.

Microwave sintering process is quite significant and unique in recent times for sintering material for densification because of its intrinsic advantages such as rapid heating rates, reduced processing times, uniform temperatures with minimal thermal gradients. Microwave sintering process leads to substantial energy savings with higher efficiency, improved properties, finer microstructures, environmental friendly process and with less environmental hazards. The microwave sintered composites are expected to yield better properties compared to the composite products that are obtained through conventionally sintering methods [Gupta M et al 2005, Ramesh P D et al 2002, Piluso P et al 1996].

Microwave sintered aluminium cenospheres composites have good microstructure that helps to produce materials with better properties such as light weight, dense, hard, better engineering properties including effective EMI shielding and vibration damping properties. The composites have also been reported to give rise to significant improvements in mechanical properties such as high strength, high stiffness, better thermal properties like low coefficient of thermal expansion and lower thermal conductivity, better acoustic property and damping characteristics. In the conventional heat treatment, the heat penetrates the body from outside to inside creating a temperature gradient; therefore it is not possible to heat those samples at a very high heating rate. This results in long cycle time and makes the process energy intensive [Lutgard C]. The consolidation of metal matrix composites has been reported to give rise to significant improvements in mechanical properties such as high strength, high

stiffness, better thermal properties like low coefficient of thermal expansion and lower thermal conductivity, better acoustic property and damping characteristic and EMI shielding properties. The microwave sintered composites are expected to yield better properties compared to the composite products that are obtained through conventionally sintering methods.

M. Gupta et al [2005] have reported the enhanced overall mechanical performance of metallic materials processed using two directional microwave assisted rapid sintering. The feasibility of densifying α SiC powder compacts based on a liquid assisted sintering approach by the use of microwave furnaces was examined by A. Goldstein et al [2002]. They have also reported the properties of the material. Ramesh D. et al [2002] studied the microwave induced reaction sintering of NiAl₂O₄. The anisothermal reaction condition leading to enhanced reaction kinetics of NiAl₂O₄ formation have been achieved by the group when they carried out simultaneous synthesis and sintering of NiAl₂O₄ from NiO + Al₂O₃ powder mixture in just 15 minutes in a 2.45 GHz microwave field. Mullitization and Densification of powder compacts of 3 Al₂O₃ and 2 SiO₂ by microwave sintering were achieved by P. Piluso et al [1996]. T Ebadzadeh et al [2009] also reported the microwave assisted synthesis and sintering of ceramics like mullite. A comparative study of microwave and conventional processing of MgAl₂O₄ based spinel material has been reported by Idalia Gomez et al [2004]. Hermann Riedel et al have studied on the simulation of microwave sintering with advanced sintering models and reported at the 8th International Conference on Microwave & High Frequency Heating. Panneerselvam M and Rao K. J [2002] have studied on the preparation of Si₃N₄SiC composite by microwave route. Sintering of metal powder In an unprecedented approach, sintering of fine metallic powders, intermetallic compounds and alloys was achieved by this process wherein the sintered products showed better properties [Gerdes et al 1996]; [Gedevanishvili et al 1999]; [Roy et al 1999]; [Saitou et al 2006]. Recently, Mg–Cu nanocomposites have been developed using microwave assisted sintering method [Wong, Gupta et al 2010]. Unlike bulk metals that act as reflector, it is believed that in finely divided metallic powder, multiple scattering coupled with eddy current loss play a significant role in microwave absorption [Das S et al 2004]

2.10.1 Microwave

Microwaves can be defined as that part of the electromagnetic radiation spectrum having a wavelength ranging from about 1 mm to 1 metre in free space and the frequency ranging from 300 MHz to 300 GHz. However, only narrow frequency bands centered at 915 MHz and 2.45 GHz, 28-30 GHz and 80-81 GHz are actually permitted for research purposes. They are coherent and polarized waves obeying the laws of optics. Depending upon the type of material the microwave may get transmitted, absorbed or reflected by the materials [Sutton W.H 1989].

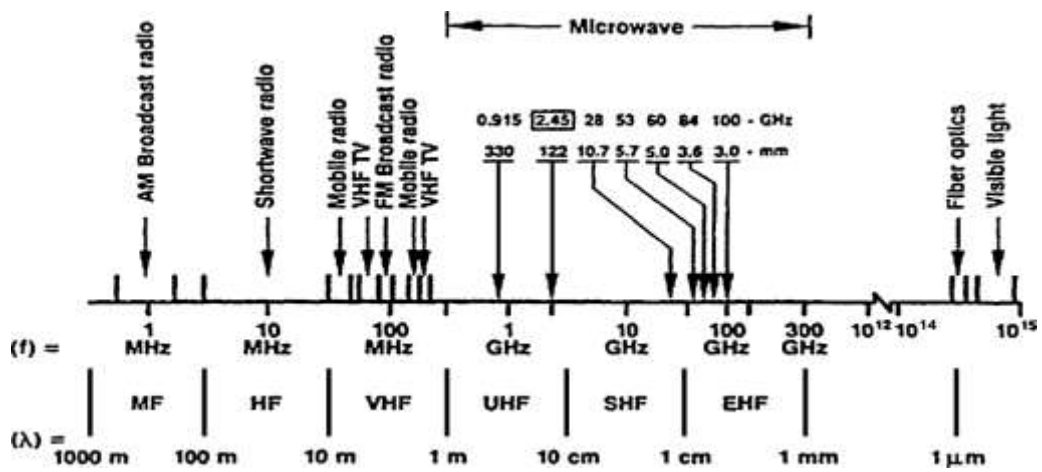


Fig. 2.6: The Electromagnetic Spectrum and MW frequencies for processing (After Morteza Oghabaei, Omid Mirzaee 2010)

Microwave energy is transferred to the material by interaction of the electromagnetic field at the molecular level. The dielectric properties determine the effect of the electromagnetic field on the material. The interaction of microwaves with a dielectric material results in translational motions of free or bound charges and rotation of the dipoles. The resistance of these induced motions due to inertial, elastic, and frictional forces causes losses resulting in volumetric heating.

The power absorbed per unit volume, P (W/m^3) is expressed as [Sutton 1989, Morteza Oghabaei et al 2010].

$$P = \sigma |E|^2 = 2\pi f \epsilon_0 \epsilon' r \tan \delta |E|^2 \quad (2.1)$$

where \mathbf{E} (V/m) is the magnitude of the internal field, σ the total effective conductivity (S/m), f the frequency (GHz), ϵ_0 the permittivity of free space ($\epsilon_0 = 8.86 \times 10^{-12}$ F/m), ϵ'_r the relative dielectric constant and $\tan \delta$ the loss tangent. Equation (1) demonstrates that the power absorbed varies linearly with the frequency, the relative dielectric constant, loss tangent and the square of the electric field.

The penetration depth of microwaves (D) at which the incident power is reduced by one half is expressed as [Sutton 1989]

$$D = 3\lambda_0 / 8.686 \pi \tan \delta (\epsilon'_r / \epsilon_0)^{1/2} \quad (2.2)$$

where λ_0 is the incident or free-space wavelength. The relative dielectric constant and the loss tangent are the parameters that describe the behaviour of a dielectric material under the influence of the microwave field. During heating, the relative dielectric constant and the loss tangent change with temperature [Das S et al 2004]

The degree of absorption by dielectric material is related to the materials complex permittivity ϵ^* (F/m) which is composed of two components i.e. ϵ' (dielectric constant) the real part and an imaginary part ϵ'' (dielectric loss factor) by:

$$\epsilon^* = \epsilon' - j \epsilon'' = \epsilon_0 (\epsilon'_r - j \epsilon''_{\text{eff}}) \quad (2.3)$$

where $j = (-1)^{1/2}$, ϵ_0 is the permittivity of free space ($\epsilon_0 = 8.86 \times 10^{-12}$ F/m), ϵ'_r is the relative dielectric constant, and ϵ'' is the effective relative dielectric loss factor. The dielectric constant \mathbf{K} or the relative permittivity ϵ_r , the dissipation factor ($\tan \delta$) and the dielectric loss ($\epsilon_r \times \tan \delta$) of the material that is being processed and their dependence on temperature generally dictates to a large extent the microwave power absorption characteristics during microwave sintering of ceramic materials. For dielectric heating the generated power density per volume is calculated by

$$p = \omega \cdot \epsilon''_r \cdot \epsilon_0 \cdot E^2 \quad (2.4)$$

where ω is the angular frequency ϵ''_r is the imaginary part of the complex relative permittivity, ϵ_0 is the permittivity of free space and E the electric field strength. The

imaginary part of the complex relative permittivity is a measure for the ability of dielectric material to convert radio frequency electromagnetic field energy into heat.

2.10.2 Microwave material interaction

Various types of materials interact with microwave in which the microwave may get transmitted (transparent), absorbed or reflected by the materials depending upon the material type. Metals reflect microwave since they are opaque to microwave whereas ceramic materials such as Silica, Alumina, Magnesium Oxide and other glasses are transparent to microwave at ambient temperatures. Above a critical temperature (T_{crit}) these materials absorb and couple effectively with microwave. [Anklekar et al 2005, Sutton 1989].

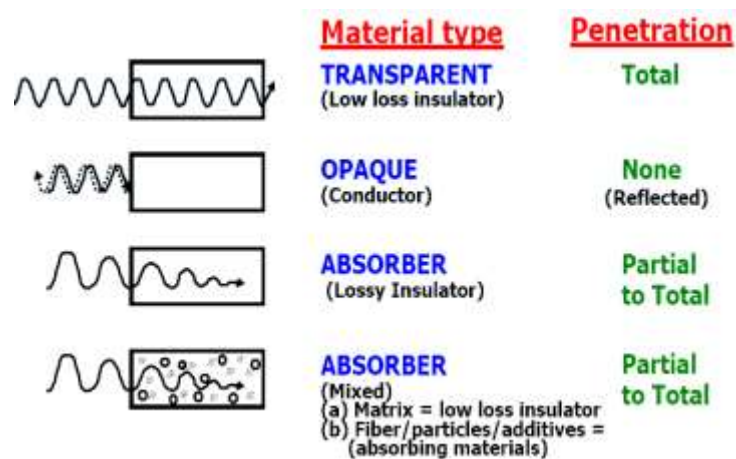


Fig. 2.7: Microwave material interaction (after Sutton 1989)

The microwave transparent materials are those which have low dielectric losses where in the microwaves pass through them and there is no loss of microwave energy. Whereas in an opaque material the microwave energy gets reflected from the material surface and does not penetrate into the bulk of the material. This property of the material that is opaqueness is used in the radar detection. The microwave absorber materials are high loss materials in which the microwave energy is absorbed into the material depending on its dielectric loss factor. There are a fourth type of material in which there is a mixed absorb of the microwave energy. This type of interaction is common in composite materials which are multiphase material having different materials where one is high loss material and the other is a low loss material. This

mixed type absorber material take advantage of the significant characteristic of microwave processing that is selective heating [Morteza Oghbaei et al 2010].

Microwave heating is fundamentally different from conventional heating methods, as it uses microwave interactions with materials at molecular or atomic levels to generate heat. The degree of interaction between the microwaves and the material of choice strongly determine whether a material can be heated and how to design the microwave heating equipment and parameters used. Therefore, it is very important to understand how different materials absorb microwave energy. Theoretically, the degree of microwave interaction with a material can be inferred through its dielectric and magnetic properties. For a material that is not significantly magnetic, the microwave interaction with that material depends on the complex permittivity ϵ , which is defined as follows:

$$\epsilon = \epsilon' - i\epsilon'' \quad (2.5)$$

where ϵ' is the real component of the complex permittivity and ϵ'' is the imaginary component of the complex permittivity.

The real permittivity is a measure of a material's ability to store electrical energy, while the imaginary permittivity represents the loss of electric field energy in a material. The power absorbed by a material per unit volume (P) is proportional to the frequency of the applied electric field, as well as to the loss factor and to the square of the local electric field intensity. It can be expressed as follows:

$$P = 2\pi f \epsilon_0 \epsilon'' E^2 \quad (2.6)$$

where f is the microwave frequency and E is the root mean square (rms) internal electric field intensity, which is related to the local geometry and ϵ' . When the microwave energy heats a material, the rate of temperature increase in the material can be derived as follows:

$$dT/dt = P/(C_p \rho) \quad (2.7)$$

where C is the specific heat of the material and ρ is the density of the material. [Chun Li He et al, 2013]

Microwaves induce rapid heating in the material depending upon its dielectric property. When the microwave propagates or penetrates through the material, the internal electric fields within the affected volume induces translational motions of free and bound charges in the material such as electrons or ions and rotate the charge complexes such as the dipoles. These induced translational motions are resisted by elastic and frictional forces within the material thereby causing loss and attenuation of the field generating heat within. This causes rapid and uniform heating throughout [Sutton, 1989].

Microwave heating is a very sensitive function of the material being processed and depends upon such factors such as size, geometry and mass of the sample. Microwave processing has gained a lot of significance in recent times for material synthesis and sintering mainly because of its intrinsic advantages such as rapid heating rates, reduced processing times, uniform temperatures with minimal thermal gradients, substantial energy savings with high efficiency, novel and improved properties, finer microstructures and its environmental friendly process and less environmental hazards. Materials that have a high dielectric loss couple well with microwaves while the poor lossy materials with no absorption at room temperature require initial heating using some kind of secondary susceptors. For most powder metals, no susceptor is needed, but it is mainly used to provide uniform temperature distribution throughout the sample to obtain uniform sintering.

The Microwave Research Group at the Materials Research Institute of the Pennsylvania State University, however, made the first step advance in the microwave sintering of many traditional and advanced ceramic materials such as alumina, mullite and hydroxyl apatite, by demonstrating rapid sintering in time intervals varying from 3-20 min. leading to transparency and almost full density. This same step function advance in ceramic processing has been extended to other commercial ceramics such as zirconia, zinc oxide, perovskites, and silicon nitride. Microwave sintering can lead to near theoretical densities in most materials in less than 30 min [Anklekar et al 2005].

Morteza Oghbaei et al have reported that metal powders are used for diversified products and applications in the engineering industries. Before the microwave sintering of metal powders, there was a misconception among the researchers that metals reflect microwave or cause plasma formation. The metal powders cannot be heated since microwave has a limited surface penetration on metals. It is reported that this argument is valid only for sintered or bulk metals at room temperatures and not for the metal powders. Presently it is found that the microwave sintering can be efficiently carried out on metal powders as is been done with ceramics. It is also reported that the penetration of microwave in the bulk of the metals is very less which is in the order of a few microns where as the penetration is good and that rapid heating can occur when microwave interacts with metal powders. It is predicted that if the metal powders particle size is less than 100 microns, they effectively absorb microwave at 2.45 GHz and this absorption depends on the electrical conductivity, temperature and frequency.

Further literature survey reports that the following theories put forth by various researchers with regard to the microwave material reactions and their sintering kinetics are as follows:

- a. Ponder motive Force Interaction in which Microwave-excited ionic currents become locally rectified (near the interface), giving rise to an additional driving force for mass transport [Booske, Rybakov et al].
- b. Materials with substantial amount of porosity, an enhancement in the electric field at convex surfaces of the pores, providing a non-ohmic and a localized plasma contribution to the driving force for pore removal and thereby accelerated material diffusion [Willert-Porada et al].
- c. Anisothermal heating caused in two different phases of widely varying microwave absorption characteristics, would provide a strong driving force to cause enhancement in the reaction kinetics followed by sintering [Roy and Agrawal].

- d. Effect of Electric and Magnetic fields at the grain boundaries [Roy and Agrawal].

Morteza Oghbaei (2010) and Sutton et al 1989 have concluded that sintering materials with microwave consumes much lower energy than conventional sintering. Due to the enhanced mechanism while sintering in microwave, the diffusion process is intensified leading to better microstructure. Higher heating rates can be attained rapidly which reduces the sintering time by using microwave. The material will attain higher density and better grain distribution through microwave sintering leading to better physical and mechanical properties.

2.10.3 Microwave versus conventional heating

Conventional heating usually involves the use of a furnace or oil which heats the walls of the reactors by convection or conduction. The core of the sample takes much longer to achieve the target temperature. On the other hand microwave penetrates inside the material and heat is generated through direct microwave-material interaction. Moreover volumetric heating, reaction rate acceleration, higher chemical yield, lower energy usage and different reaction selectivity the advantages microwave heating has over conventional methods.

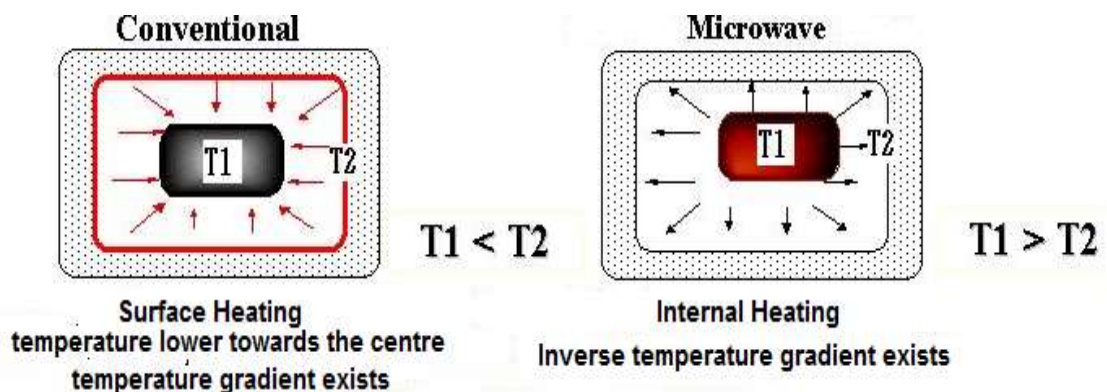


Fig. 2.8: Illustration of microwave and conventional sintering of material. (after Satapathy, 1989)

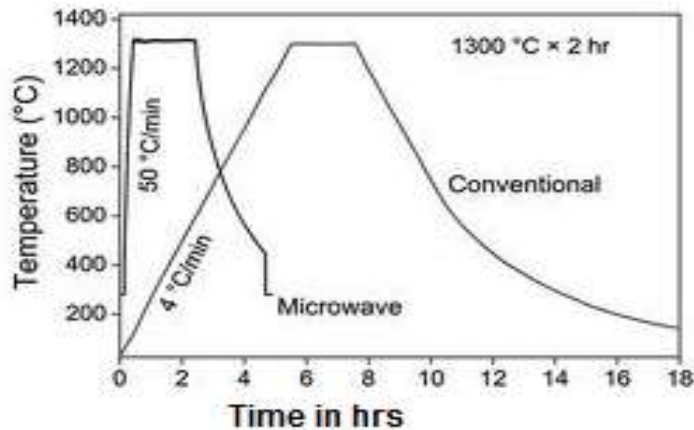


Fig. 2.9: Illustration of rapid microwave sintering with that of conventional sintering of material (Source: Internet Google search)

High integrity advanced engineering materials demand for finer microstructure coupled with near theoretical densities in special powder metallurgy products, which are difficult to attain and is a costly process. Microwave sintering offers this need of obtaining finer microstructures in an economical and energy saving process. The reason for microwave sintered products yield better mechanical properties in the powder pressed samples is that it produces finer grain size with shape of the porosity which is different compared to conventionally sintered products. Microwave sintered powder metallurgy products have round edged porosities which is responsible for high ductility and toughness [Rustum Roy et al 1999].

Chandrasekaran et al [2011] have reported that the time and energy required for melting of metals was half when using microwave as compared to conventional heating. The melting of metals could be achieved in a microwave sintering furnace of 1300 W capacity where as to melt the metals of the same quantity, it required 2500 W conventional furnace. A temperature of 1673-2073 K can be reached in a low power microwave oven operating at 2-6 kW as compared to conventional induction heating which required 10-15kW power. They have also reported that a microwave oven of 1300W took 9 minutes to melt aluminium at a temperature raise rate of 82⁰C/min where as conventional 2500W capacity conventional furnace took 29 minutes to melt the same quantity of aluminium at a heating rate of 29⁰C/min. Conventional heating is much slower compared to microwave sintering which is rapid.

While comparing the conventional heating to that of microwave heating, the energetic aspects need to be considered to understand the heating sequence in each of the processes. In case of conventional sintering, the sample has equalized its temperature with the furnace surroundings before the actual heat energy goes into the sample for actual synthesis. This is time consuming since the source of heat is supplied from outside the material during sintering. In case of microwave sintering, the absorption of heat energy is not limited by the furnace surroundings, and in fact the sample itself becomes the source of heat energy rather than the supply of heat energy from external source. The maximum temperature achieved by microwave sintering depends on the thermal balance between the heat losses and the heat required for synthesis against the microwave input. [Idalia Gomez et al 2004]

2.11 Summary on literature review

From the above literature survey it appears that attempts are being made by various scientists all over the world to meet the demand for materials with enhanced efficiency and cost effectiveness in manufacturing. The introduction of new materials and improvement of properties of materials manufactured so far call for development and implementation of new synthesis and processes. The basic selection criteria for these processes are the quality maximization with simultaneous minimization of costs with quality. The appropriate selection of material for a particular application is based on a multi criterion optimization which takes into account chemical species, manufacturing process and conditions, price dependant issues related with transforming the material into a product, generation of waste and its disposal as well as modeling and process parameter optimization.

There is an increasing interest in the lightweight materials for the automotive industry, coupled with a need for a cost effective processes have combined to create a significant opportunity for aluminium powder metallurgy which adds light weight, high compressibility, low sintering temperatures, easy machinability and good corrosion resistance to all the advantages of conventional P/M.[G.B. Schaffer 2004]. More efficient use of materials and energy efficient processes and technologies are the

order of the day keeping in view the environmental hazards and also minimizing the effect of industrial solid wastes and effective utilization of these wastes into value added products [Leszek A et al 2006].

Metal matrix syntactic foams materials have been less studied and not as extensively as the polymer matrix composites. This may be due to cost of manufacture and the associated difficulties in producing cheaply. The benefits accrued from the use of hollow or porous particles such as cenospheres are less pronounced than polymer matrix syntactic foams, especially in terms of mechanical properties.

Metal matrix syntactic foams have potential for many applications and the foams developed so far are finding vast applications as a structural application material where weight reduction and resistance to impact is desirable. Several metals have been used as matrix materials with various ceramic particles as reinforcements in composites and have been studied. Aluminum and magnesium alloy are generally used, and syntactic foams with steel or titanium have also been developed. There are very limited choices of hollow or porous ceramic particles, including micro balloons, cenospheres, and E-spheres, which are all silica and alumina-based. The availability of high quality ceramic particles is deemed crucial for the development of new metal matrix syntactic foams. The properties of composites depend not only on the matrix materials but on the type, composition, volume percentage, and distribution of the ceramic particles. All these factors dictate the choice of cost-effective manufacturing technologies, which have a significant influence on the quality and properties of the resultant materials [Yuyuan Zhao].

2.12 Gaps in the Technology

Sufficient studies have been carried out on development of Aluminium cenospheres light weight composites and syntactic foams which are fabricated through stir casting and melt infiltration techniques but also it is seen that synthesis of aluminium cenospheres composite through PM route and MW sintering needs to be studied since little information is available on that.

MMCs comprising of Aluminium metal as matrix embedded with fly ash cenospheres particulates can be fabricated through Powder Metallurgy (PM) route. Keeping in view the definite advantages foreseen in MW sintering process to promote matrix properties as required for tailoring syntactic foams, the proposed study is an attempt made to fabricate Aluminium Cenospheres Composite through Powder Metallurgy route and achieving densification of the composites through Microwave Sintering. The properties of these composites are studied to assess the suitability of using them as 'Syntactic Foams' for applications in automotives and other engineering applications and fill the gap on the information which is not fully available.

The composite need to be studied for its physical properties such as porosity, water absorption, and density, morphological features through SEM, mineralogical properties through XRD, thermal properties such as thermal shock resistance and coefficient of thermal expansion, mechanical properties such as compression and flexural strength, and tribological characteristics such as wear and erosion resistance tests. All these studies enable to comprehensively generate information on the engineering properties of the composites which has been less studied. The flow chart of the proposed research activity is given in Fig. 2.10. Keeping in view the desired advantages of using cenospheres, this study covers the possibility of making the starting level composite agglomerate for further evaluation of physical, mechanical and thermal properties. This can find place as a part of a bigger component.

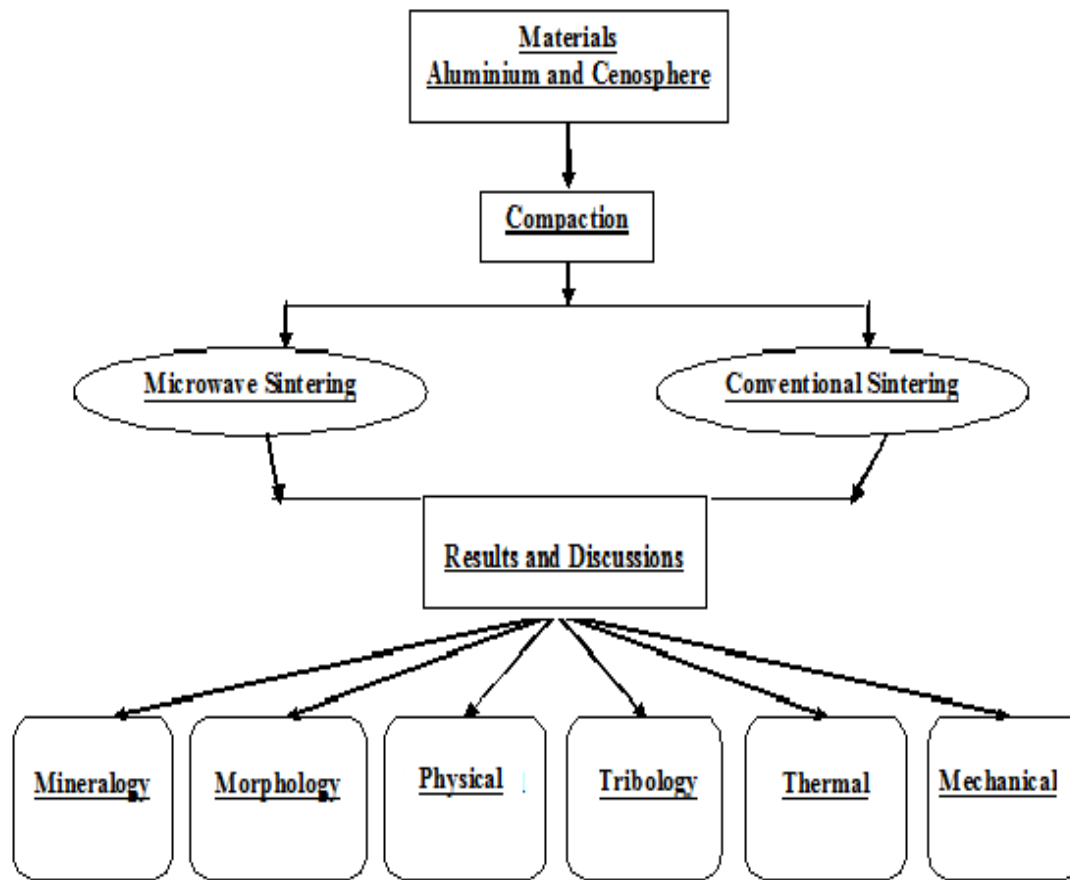


Fig 2.10: Flow chart for the study on the composite

2.13 Scope and Objective of the Present Investigation

The scope and objectives of the present investigation will be:

1. To understand all the process variables required to develop successfully Aluminium- Cenospheres Metal Matrix Composites (MMCs) processed through Powder Metallurgy route and sintered rapidly through Microwave sintering.
2. The Powder Metallurgy based Aluminium Cenospheres MMCs rapidly sintered in Microwave will be subsequently studied for engineering properties such as physical, morphological, mechanical, thermal and tribological properties.

3. Comparison of the properties of the Aluminium- Cenospheres Metal Matrix Composites with that of the base material and discussions on the enhancement or improvement in properties, if any will be discussed.
4. Comparison of properties of the Aluminium- Cenospheres Metal Matrix Composites sintered in microwave with that of Aluminium- Cenospheres Metal Matrix Composites composites sintered through conventional route will be undertaken.
5. Feasibility studies will be undertaken to explore the possibility of using Aluminium- Cenospheres Metal Matrix Composites sintered in microwave as a Syntactic Foam (SF) material for various engineering applications.

2.14 Content of the Thesis

- a) A detailed review of the available literature on Aluminium Cenospheres based Metal Matrix Composites fabricated through various conventional routes, their properties and applications have been discussed in Chapter 2.
- b) The experimental undertaken for the present work which include synthesis of aluminium cenospheres composites through powder metallurgy mix, sintering of the same in conventional and microwave routes and the details on material characterization methods adopted such as Scanning Electron Microscopy, X-ray Diffractometry, Energy Dispersive X-Ray Analysis, X-ray Fluorescence, processing route for the synthesis of composite material such as microwave and conventional sintering, raw material processing, testing and evaluation of various engineering properties such as chemical, morphological characterization, physical, tribological, thermal and mechanical properties evaluation etc., are discussed in Chapter 3.
- c) The cenospheres material characteristics such as chemical constituents by SEM, XRD, XRF etc., particle size distribution analysis, ash fusion temperature along with analysis and interpretation of the results have been discussed in Chapter 4.

- d) The initial study carried out on the high temperature sintering behavior of aluminium cenospheres mix both in conventional and microwave sintering and its phase and morphological analyses along with physical property evaluation such as brinell hardness number, bulk density and water absorption studies undertaken has been discussed in Chapter 5.
- e) The physical, morphological and micro-structural analysis of conventionally and microwave sintered composites by SEM, EDAX, XRD and physical properties evaluation such as bulk density, water absorption, brinell hardness measurement and porosity evaluation studies have been discussed in Chapter 6.
- f) The evaluations of the tribological characteristics such as wear loss and erosion loss and study of the wear surface by SEM for conventionally and microwave sintered samples, and interpretation of their results have been discussed in Chapter 7.
- g) The thermal properties evaluation such as thermal shock resistance measurement of the conventionally and microwave sintered samples, along with compressive yield strength of the composites before and after thermal shock resistance tests, co-efficient of thermal expansion, interpretation of their results have been discussed in Chapter 8.
- h) The evaluations of the mechanical properties of the composite such as compression and flexural strength, FEM analysis for the compressive strength, and study of the fracture surfaces of failed samples of both conventionally and microwave sintered samples along with analysis of results and interpretation have been discussed in Chapter 9.
- i) The conclusions drawn from the study undertaken have been discussed in Chapter 10.

CHAPTER 3

EXPERIMENTAL TECHNIQUES

3.1 Materials

3.1.1 Aluminium

In this study, atomized Aluminium metal powder of 99.5 % purity from M/s. NICE Chemicals, which had a particle size range of ASTM 200 mesh (75 μm) was used as the matrix material for the development of the composite. This aluminium powder also called as pyro-powder is flaky in shape when observed at micro level. The powder is silver white to grayish in color thereby indicating a possibility of presence of some amount of aluminium oxide (alumina) since the aluminium is having high affinity towards oxygen thereby forming a thin layer of oxide on the metal surface that affects the colour of the powder from whitish to brown (Fig.3.1). The Table 3.1 shows the general properties of the aluminium powder obtained from the literature.

Table 3.1: Properties of Aluminum powder [Adefemi O. Adeodu]

Shape	Flaky
Composition	Al
Appearance	Whitish/ Greyish, odour less powder
Particle Size (μm)	< 1 μm
True Density (g/cm^3)	2.70
Boiling Point ($^{\circ}\text{C}$)	2467
Melting Point ($^{\circ}\text{C}$)	660.1
Molecular Weight (g/mol)	29.92
Specific Heat@25$^{\circ}\text{C}$ ($\text{Cal}/\text{g}^{\circ}\text{C}$)	0.215
Thermal Conductivity @20$^{\circ}\text{C}$ ($\text{Cal}/\text{s. cm. }^{\circ}\text{C}$)	0.50
Co-efficient of Expansion@20-100 deg.C	24.0
Modulus of Elasticity	69
Specific gravity	2.6989
Crystallography	Cubic structure, face centered



Fig. 3.1 Aluminium powder (source: Siva Sakthi Chemicals, Salem)

3.1.2 Cenospheres

In the present work, cenospheres obtained from fly-ash collected from M/s. NTPC Simhadri Thermal Power Station, Vishakhapatnam was used for the study. The fly-ash was processed in the lab for harvesting the cenospheres present in it. The process involved preparation of ash slurry, stirring the same with mechanical stirrer for known period of time to assist good dispersion of the ash in the slurry. A permanent magnet is introduced into the slurry which removes free form of magnetic iron oxide ($\text{Fe}_2\text{O}_3 + \text{Fe}_3\text{O}_4$) particles present in the fly ash. The agitated slurry was then allowed to settle in settling tanks to a standstill. Later, the light weight floating material of the ash comprising of cenospheres and other material were removed. The removed material was dried thoroughly in an oven. The dried material was then sieved to remove cenospheres of various size fractions. Cenospheres with an average particle size of 10- 100 μm has been used in this study and Fig.3.2 depicts as received cenospheres.



Fig. 3.2: As received cenospheres

3.2 Initial study on high temperature sintering behavior of Aluminium Cenospheres mix

This study was undertaken to assess the behavior of aluminium cenospheres mix when subjected to sintering at various high temperatures. The temperature range of 650⁰C to 1150⁰C was chosen for the study since 650⁰C is the temperature at which Aluminium begins to melt and 1150⁰C is the initial deformation temperature of the Cenospheres. The aluminium and cenospheres mix was subjected to these temperature starting with 650⁰C up to 1150⁰C in increments of 100⁰C. The study was aimed at assimilating the information on the changes that are observed the mix undergoes at various temperatures in terms of its physical, morphological and chemical characteristics. This study was deemed to be important as this would enable fixing of the process parameters that are important for the synthesis of the composites. By the information gathered it was possible to design the mix, processing route and the sintering temperatures and environment for design of experiments for the present study for successful synthesis of the aluminium cenospheres composite in lab.

Aluminium metal powder of 60 volume % and Cenospheres of 40 volume % was blended in the RETSCH Planetary Bowl Mill-400 laboratory mixer cum grinding machine (Fig.3.3) at 100 rpm for 15 minutes using rubber balls to aid effective blending of the materials. The blended mixture of aluminium and cenospheres was then mixed with 5% Poly Vinyl Alcohol (PVA) solution to aid workability and wetting for pressing of samples in the form of pellets.



Fig. 3.3: Planetary bowl mill

The mix was cold compacted in a laboratory make hydraulic press for preparation of pellets of size 15 mm dia with 3 mm height. Pure Aluminium powder was also

compacted using the same parameters without blending with Cenospheres. The composite mix was pressed into pellets of size 12.5 mm dia x 5mm in height at a pressure of 5 MPa. The compacted pellets were then taken up for sintering.

One set of pellets were sintered in a BHEL make Multimode Microwave Sintering Facility which operates at 1.1 kW and microwave frequency 2.45 GHz. The equipment is programmable with thyristor based controller for sintering cycles, soaking time and temperature. The microwave sintering equipment was operated at power level of 100 % with a 90 minutes sintering cycle with soaking time of 42 minutes at maximum set temperature. The sintering time comprised of total 90 minutes from room temperature (RT) to maximum set temperature with inclusion of soaking/ dwell time. The sinter cycle comprised of rate of heating at 12⁰C per minute for sintering and the mix was sintered at various temperatures of 650⁰C, 750⁰C, 850⁰C, 950⁰C, 1050⁰C and 1150⁰C for the study. The pellets were soaked at the maximum temperature of sintering for a dwell time of 42 minutes. Silicon Carbide crucible which is a microwave susceptor was used to hold the pellets in the microwave sintering unit to aid sintering. The crucible was thoroughly packed with glass wool insulation to arrest the heat losses.

Another set of Aluminium Cenospheres pellets were sintering conventionally in a laboratory make muffle type resistance furnace heated with kanthal element. Both the type of sintered samples was later taken up for characterization of various properties. The mix pellets sintered at various temperatures were later studied for their morphological features by SEM, mineralogical phases by XRD, physical properties such as Bulk Density, Brinell Hardness Number and Apparent Porosity. The findings on the studies have been presented in the results and discussions section at Chapter 4.

3.3 Aluminium Cenospheres MMC's Processing Methodology

3.3.1 Materials

In the present study, atomized Aluminium metal powder of 99.5 % purity from M/s. NICE Chemicals, with a particle size range of ASTM 200 mesh (75 µm) was used for the metal matrix for the composite. The Cenospheres beneficiated from fly-ash

collected from M/s. NTPC Simhadri Thermal Power Station was used as the filler in the composite. Cenospheres with an average particle size of 10- 100 μm was used in this study.

3.3.2 Mix preparation

Mix consisting of aluminium powder: cenospheres in various batches with cenospheres content ranging from 0 to 50 vol. % as shown in Table No. 3.2 were prepared for the study. The materials were mixed thoroughly in laboratory make mechanical mixer using 5% Poly Vinyl Alcohol (PVA) solution to aid workability and wetting for pressing of samples in the form of round and rectangular shaped samples for study.

Table 3.2: Composition & Designation

Sample Composition (vol. %)		Sample designation	
Aluminium	Cenospheres	Conventional Sintering	Microwave Sintered
100	0	1C	1M
90	10	2C	2M
80	20	3C	3M
70	30	4C	4M
60	40	5C	5M
50	50	6C	6M

Two sets of composite samples were prepared with compositions as shown in Table no.3.2, for densification through microwave and conventional sintering. The samples were coded as ‘M’ samples for microwave sintered samples and ‘C’ samples for the conventionally sintered ones. The samples were designated as 1C, 2C, 3C, 4C, 5C and 6C for the conventionally sintered samples. The microwave sintered samples were designated as 1M, 2M, 3M, 4M, 5M and 6M. The cenospheres content was varied from 0, 10, 20, 30, 40 and 50 volume % respectively and the remaining portion of the mix being aluminium powder. The reason for fixing the maximum volume % of cenospheres to 50 vol. % in the composition is that as per the literature review, if the matrix to cenospheres size ratio is nearer or less than 1, clustering of the cenospheres

particles is observed in the composite. The clustering of ceramic phase i.e. cenospheres leads to deterioration of mechanical properties of the composite [Vogiatzis et al]. Hence the ration of matrix to cenospheres content was kept above 1.

3.3.3 Pressing

The mix was pressed through cold compaction into cylindrical shaped samples of size 40 mm x 8 mm diameter at a pressure of 25 MPa in a laboratory Enkay make hydraulic press through single ended uniaxial compaction. The cylindrical shaped samples were prepared for evaluating the compression strength, hardness and porosity of the composites. Another set of samples of size having length 50mm x 15mm width x 12 mm depth rectangular bar shaped specimens were prepared for the evaluation of flexural strength. The cylindrical and rectangular shaped composite samples are shown in Fig.3.1 and 3.2 respectively.



Fig. 3.4: Pressed composite pellets round specimen samples

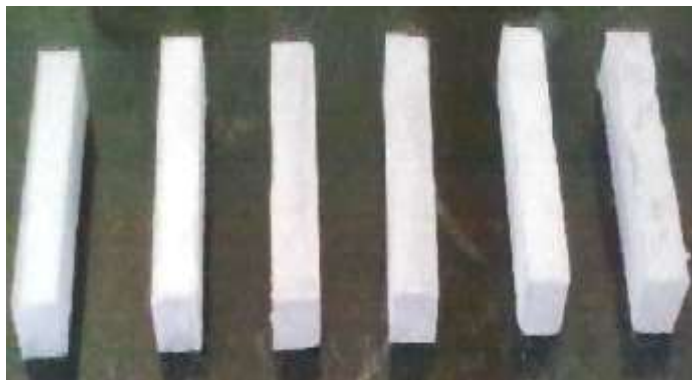


Fig. 3.5: Pressed composites rectangular specimen samples



Fig. 3.6: Hydraulic press

The Fig. 3.3 shows the hydraulic pellet press which was used for the cold compaction of the composites. The green composites were then thoroughly dried in oven at 108⁰C for 2 hours to remove the moisture prior to sintering.

3.3.4 Sintering

One set of dried samples were sintered in BHEL make Microwave Sintering Facility shown in Fig.3.5. The microwave sintering facility is rated at 1.1 kW power with microwave frequency of 2.45 GHz, at a power level of 100 %. The samples were sintered at a temperature of 665⁰C. The sintering cycle for each batch of materials comprised of 90 minutes which included soaking time of 42 minutes at the maximum temperature. The sintering temperature is measured using a calibrated, Alumina sheathed R type Platinum-Rhodium thermocouple. In this system the susceptor in the form of a silicon carbide cylindrical crucible gets heated by the microwaves which in turn heats the charge. The specifications for the BHEL make Microwave Sintering Facility same is shown in Table 3.3. The Fig. 3.4 shows the graph depicting the microwave sintering cycle (90 min) vs.time for composite sintered at 665 deg C.

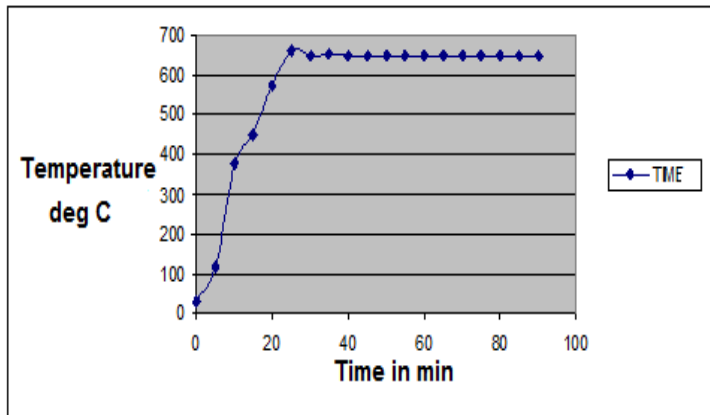


Fig. 3.7: Microwave sintering cycle (90 min) for composite sintered at 665 deg C



Fig. 3.8: Microwave Sintering Facility

Table 3.3: Specification of BHEL make Microwave Sintering Facility

Maximum Temperature	Up to 1600 ⁰ C
Sample size	1 " diameter and height of 3 to 5 mm
Chamber	Microwave oven of capacity 1.1 kW/2.45 GHz
Susceptor	Cast SiC- Alumina crucible
Temperature measurement	PID controller with R type thermocouple
Parameter	Soft touch button panel with timer for process time settings
Cooling	Fan provided

The other set of samples were sintered separately in a conventional laboratory make resistance type muffle furnace which is heated with kanthal heating element. The

temperature of sintering was also kept at 665⁰C for the conventional sintering. The sintering cycle comprised of 7 hours with soaking time of 2 hours for the composites at the peak temperature and the same is shown in Fig. 2.9 at page 34. Both the microwave and conventionally sintered samples were later characterized for various properties and comparison studies.



Fig. 3.9: Sintered composite sample

3.4 Evaluation of properties of the sintered Aluminium Cenospheres Metal Matrix Composites (ACMMCs)

The conventionally and microwave sintered Aluminium Cenospheres Metal Matrix Composites (ACMMCs) have been evaluated for the following properties and a comparison study has been made which are discussed in Chapter 4.

- Micro-structural, Phase, Chemical characterization using SEM, EDAX, XRF and XRD respectively.
- Physical Properties such as Bulk Density and Apparent Porosity, Water Absorption Measurements,
- Tribological studies such as Sliding Wear and Jet Erosion Resistance studies to determine wear and erosion losses.
- Thermal Properties such as Linear Co-efficient of Thermal Expansion (α), Thermal Shock Resistance Test and Ash Fusion Temperature.
- Mechanical Properties such as Compression strength, Flexural strength and Brinell Hardness Number

3.4.1 Micro-structural, Phase and Chemical characterization using SEM, EDAX, XRF and XRD

Microstructural characterization was carried out using Scanning Electron and Optical Microscopes on the polished samples of the composite pellets to determine the presence of porosity, reinforcement distribution and matrix-reinforcement interfacial integrity.

Scanning Electron Microscope equipped with Energy Dispersive X-ray Spectroscopy equipment Leica make Q500MC Model, which operates at a typical accelerating voltage of 15 kV was used for the study. The SEM with EDAX attachment is shown in Fig.3.6



Fig.3.10: Scanning Electron Microscope

In energy dispersive spectrometers (EDX or EDS), the sample for analysis may either be in solid, powder or liquid form. The material taken for the study was in powder form and in order to ensure proper analysis, the sample powders were pressed into pellets in the hand operated laboratory hydraulic press and analyzed.

The chemical characterization of the raw materials was carried out using an X-Ray Fluorescence Spectrometer (XRF) to study the basic elemental oxides of cenospheres. The XRF which is show in Fig. 3.7 and the EDAX attchment were calibrated using Standard Reference Material (SRM) which are similar materials with analysis report

of the quantities of the elements present in them have been analyzed. A minimum of 4 samples were used for calibration of the equipment to provide reasonably accurate results of analysis of the unknown sample. The elemental compositions of the unknown samples are determined as percentages.



Fig. 3.11: X-Ray Fluorescence (XRF) Spectrometer

The mineralogical phase analysis of aluminium cenospheres powders and the sintered composite samples has been carried out in PANalytical make XPert PRO Model X-ray Diffractometer using Cu-K α radiation. The XRD equipment is shown in Fig. 3.8.



Fig.3.12: X-ray Diffractometer

3.4.2 Physical Properties

The density, water absorption and porosity of sintered pellets were measured using the Archimedes principle. Three samples were randomly selected from the sintered

lot which were weighed in air and immersed in water. A Sartorius make electronic balance which is calibrated with an accuracy of $\pm 0.0001\text{g}$ was used for the weighing purpose of the samples for measurement of the above properties.

3.4.2.1 Bulk Density

Bulk Density of the microwave and conventionally sintered aluminium cenospheres composites was calculated through Archimedes principle using the following formula:

$$\text{Bulk Density (BD)} = \frac{\text{Mass of the sample (M) in g}}{\text{Volume of the sample (V) in cc}} \quad (3.1)$$

which is given in the units g/cc.

3.4.2.2 Water Absorption

Water Absorption of the microwave and conventionally sintered aluminium cenospheres composites was calculated through Archimedes principle using water immersion method as follows:

$$\text{Water Absorption (\%)} = \frac{m_2 - m_1}{m_1} \times 100 \quad (3.2)$$

Where m_1 is the mass of a dried sample in air (g); m_2 is the mass saturated with water.

3.4.2.3 Apparent Porosity

Porosity is classified into open or closed types. The open porosity is defined as the ratio of the volume of void space that is accessible from exterior to bulk volume, also known as Apparent Porosity (P_a) and the closed porosity is defined by the ratio of the volume of void space that is not accessible from exterior to bulk volume. The porosity of composites depends on the shape and size of the pores. The porosity of metal matrix composite, however, is determined by the porosity of the cellular spheres or porous material that is impregnated as fillers. The strength of the porous composites could be tailored through the appropriate selection of the wall thickness and the radius of cenospheres. [M. Altenaiji et al 2012]

Apparent Porosity (P_a) of the microwave and conventionally sintered aluminium cenospheres composites samples was calculated by water immersion method using Archimedes's principle as follows.

$$\text{Apparent Porosity (Pa) \%} = \frac{(m_3 - m_1)}{(m_3 - m_2)} \times 100 \quad (3.2)$$

Where m_1 is the mass of a dried sample in air (g); m_2 is the mass of the saturated suspended weight of sample in water (g); m_3 is the mass of the sample saturated with water.

3.4.2.4 Particle Size Distribution

The particle size distribution analysis gives us an idea of the range of particle size and the percentage of the initial material used for processing in the study. The particle size analysis has been carried out using Malvern make Laser Beam Particle Size Analyzer. The unit consists of 3 units- sample preparation unit, monitoring unit and the laser producing unit. Two types of analyzing techniques can be carried out in the equipment namely wet method analysis and dry method analysis.

Wet method analysis is preferred for those samples which get dispersed into a homogeneous solution such that the sample should not dissolve in the liquid substance. Dry method is adopted for those samples that do not get dispersed to a uniform solution in the liquid medium used. The light from a low power helium-neon laser is used to form a collimated and monochromatic beam of light, which is known as analyzer beam and any particle present within it will scatter this laser light. The particles are introduced into the analyzer beam by simultaneously observing the concentration from monitor, which should be in the range of 10-15% after the size distribution. Results are plotted in terms of the cumulative and distributive analysis which is recorded in the monitoring unit device. By this technique, the particle size ranging from 0.1 to 2000 μm can be measured. For the study wet method analysis was used.

3.4.3 Tribological characteristics

3.4.3.1 Sliding Wear behaviour

The experimental work involved studying the Sliding Wear Behavior of the aluminium-cenospheres metal matrix composites system as a function of sliding distance for a constant sliding velocity and applied load. The wear properties of the composite samples were carried out on a computer interfaced Pin on Disc apparatus, the schematic of the apparatus is shown in Fig 3.9 as below.

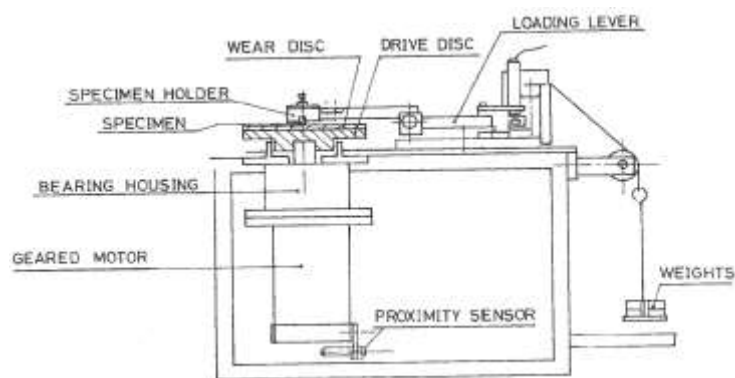


Fig. 3.13: Schematic of Pin on Disc machine (ASTM G 99)

The test was carried out as per the ASTM standard No. G 99 test procedure. The tribological property study included wears loss. The tribo-surfaces of the composite have been observed under the optical and scanning electron microscopes to determine the wear type mechanism and an attempt was made to correlate the weight loss with the SEM observations on the worn surfaces.

Smoothly finished composite cylindrical pin samples of size 10mm diameter and 15mm length aluminium cenospheres composite specimens were prepared and loaded in the pin- on -disc wear testing rig using suitable adhesive. Before testing, the surface of the specimens was polished by using 1000 grit paper. The initial weights of the samples were recorded using a high precision Sartorius make Electronic Digital Weighing Balance after thorough cleaning. A hardened alloy steel material such as EN 32 (62HRC) steel and diameter 75 mm having surface roughness of $R_a = 10 \mu\text{m}$ was used as the disc. After fixing both the disc and the sample pin in their respective positions, the normal load to the pin was applied through a pivoted loading lever with

a string and pan assembly. The mounting arrangement of the sample consists of making the flat face of the sample to come in good contact with the rotating hardened steel disc. The disc rotates continuously till select distances in the range 500- 6000 m are reached. Wear tests were carried out at room temperature for 20 minutes and the weight loss recorded. After the set time is reached, the test was stopped using the inbuilt timer mechanism provided to the machine. The difference in the weight of the sample after completion of the test with respect to initial weight of the sample was measured, to calculate the material loss due to wear. The normal load of 1, 2 and 3kg and sliding speed of: 1.0 m/s were used as test parameters.

3.4.3.2 Jet Erosion Resistance Test

The conventionally and microwave sintered samples were subjected to Jet Erosion studies to assess the erosion properties of the composites as per ASTM G76 -04 standard which specifies the standard test method for ‘Conducting Erosion Tests by Solid Particle Impingement Using Gas Jets’. The test was conducted in the Jet Erosion test rig shown in Fig. 3.10 available in the laboratory to assess the erosion properties of the composites. Silica sand particles were used for impingement using gas jets supplied through an air compressor.



Fig. 3.14: Jet Erosion Test Rig

This test method covers the determination of material loss by gas-entrained solid particle impingement erosion with jet nozzle type erosion equipment. This test method is used in the laboratory to measure the solid particle erosion of different

materials and has been used as a screening test for ranking solid particle erosion rates of materials in simulated service environments. Actual erosion service involves particle sizes, velocities, attack angles, environments, and so forth, that will vary over a wide range.

The standard test conditions specified as per ASTM G-76 were maintained for the jet erosion test. The jet nozzle tube is 1.5 mm \pm 0.075 mm with inner diameter at about 50 mm long. The test gas was kept dry air, with dew point at -50°C or lower. The silica abrasive particles with nominal 50- μm angular or equivalent was used only once. The abrasive particle velocity was maintained at $30 \pm 2 \text{ m}\cdot\text{s}^{-1}$ which is measured at the specimen location. At this velocity the gas flow rate would be approximately 8 $\text{L}\cdot\text{min}^{-1}$ and the system pressure will be approximately 140 kPa (20 psig). The test time was kept at 10 min to achieve steady state conditions. Longer times are permissible as per the standard so long the final erosion crater is no deeper than 1 mm. The angle between the nozzle axis and the specimen surface was adjusted at $90 \pm 2^{\circ}$. The test temperature was kept at normal ambient value which is typically between 18°C to 28°C .

The particle feed rate was about $2.0 \pm 0.5 \text{ g}\cdot\text{min}^{-1}$. This corresponds to a particle flux at the specimen surface of about $2 \text{ mg}\cdot\text{mm}^{-2}\cdot\text{s}^{-1}$ under standard conditions. Particle flux determination requires measurement of the eroded area on the specimen and is subject to considerable error. A measured width and depth profile of an erosion crater produced using stated conditions are then derived which indicates a typical eroded width/depth relation. The distance from specimen surface to nozzle end was kept at $10 \pm 1 \text{ mm}$. The erosion tests were conducted at angles of 30, 45, 60 and 90 deg for 15 minute duration each.

3.4.4 Thermal Properties

3.4.4.1 Linear Co-efficient of Thermal Expansion (α)

The Co-efficient of Thermal Expansion (CTE) test was conducted on the composite samples using Orton Dilatometer, USA make. The samples were cut into cylindrical shape of size 10 mm dia and length 25 mm. The samples were heated to a temperature of 500°C with rate of heating at 3°C/min in oxidizing atmosphere. The change in length Δl of the samples were measured at 500°C for all the composites.

The Co-efficient of Thermal Expansion (α) was calculated as:

$$\text{Co-efficient of Thermal Expansion } (\alpha) = \frac{l}{l_0} \frac{dl}{dt} \quad (3.4)$$

where l_0 is the initial specimen height and t is time and dl/dt denotes the slope of the change in specimen height over change in temperature.

3.4.4.2 Thermal Shock Resistance Test

The conventionally and microwave sintered samples were subjected to compressive yield strength (CYS). The test was performed in the Universal Testing Machine (UTM) of Enkay make of capacity 100T. The compressive yield strength was evaluated for the sintered samples prior to, and after the thermal shock resistance test. The thermal shock resistance test comprised of heating the composite samples in a laboratory make resistance type muffle furnace which is heated with kanthal element. The samples were heated to a temperature of 500°C and held at this temperature for 15 minutes soaking time. Immediately the heated samples are quenched in water bath held at ambient temperature. This constitutes 1 thermal shock cycle. The composites samples are then evaluated for their compression strength after the thermal shock cycles. The composites containing 100 vol. % aluminum (1C and 1M samples) and Aluminum- Cenospheres composite samples having 10 and 50 vol. % of Cenospheres (2C, 2M, 6C and 6M samples respectively) only were studied for the test. The conventionally and microwave sintered samples were subjected to thermal shock

resistance tests comprising of 5, 10 and 25 thermal shock cycles and the compression strength values before and after thermal shock cycles were measured.

3.4.4.3 Ash Fusion Temperature

The determination of Ash Fusion Temperature (AFT) of the ash cenospheres is of prime importance to assess its high temperature behavior, for design of composite sintering temperature or for use of cenospheres for refractory application. The ash fusion test gives an indication of the softening and melting behavior of coal ash at high temperatures in oxidizing atmosphere. Ash fusion temperature is determined by heating a prepared sample of molded ash in a cone form, in a high-temperature furnace to temperatures exceeding 1,000°C in both reducing and oxidizing conditions. Ash fusion point is also one significant parameter as far as ash analysis is concerned. Ash fusion temperatures are determined by viewing a moulded specimen of the coal ash through an observation window in a high-temperature furnace known as the Ash Fusion Temperature Determinator. The ash, in the form of a cone, pyramid or cube, is heated steadily past 1000 °C to as high a temperature as possible, preferably 1,600 °C . The AFT test was conducted as in a LECO make AF 700 equipment as shown in Fig. 3.11.



Fig. 3.15: Ash Fusion Temperature Determinator (courtesy: LECO corporation)

The test was conducted as per the guidelines of the ASTM D1857M- 04(2010) standard which describes the ‘Standard Test Method for Fusibility of Coal and Coke Ash’ in an oxidizing atmosphere. The following temperatures are recorded.

a. Initial Deformation Temperature (IDT): This is reached when the corners of the cone first become rounded.

b. Softening Temperature (ST): This is reached when the when the height of the deformed cone becomes equal to the base

c. Hemispherical Temperature (HT): This is reached when the height of the deformed cone becomes half the size of the base

d. Flow (fluid) Temperature (FT): This is reached when the molten cone collapses to a flattened button of thickness less than 1.6mm on the furnace floor.

The Fig. 3.12 below shows the schematic of the ash cones depicting IDT, ST, HST and FT sequences.

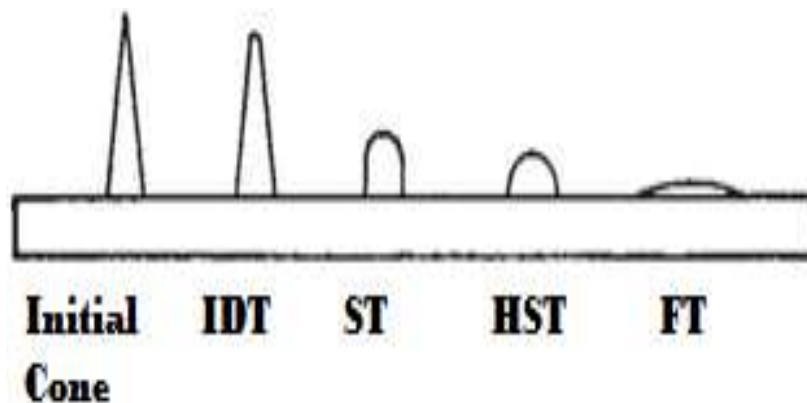


Fig. 3.16: Sequences of ash fusion temperature test

The Ash Fusion Determinator equipment automatically monitors ash cone deformation temperatures in coal ash, coke ash, and mold powders with easy to operate software. The ash fusibility temperatures such as Initial Deformation Temperature(IT), Softening Temperature(ST), Hemi-spherical Temperature(HT) and

Fusion Temperature(FT) is automatically determined using the software's Image Recognition Functions (IRF).

3.4.5 Mechanical Properties

3.4.5.1 Compression strength (σ_c)

The compression strength measurements were carried out in Enkay make hydraulically operated Universal Testing Machine of capacity 100T. The compression strength was calculated by dividing the maximum load in kN by the original cross section area (cm^2) of the sample and the values are converted and given in MPa.

3.4.5.2 Analysis of Compressive strength results using Finite Element Method (FEM)

To understand the behavior of the structure and to solve any engineering problem three methods are available, the analytical method, experimental method and numerical method. Numerical method is the mathematical representation and real life complicated problems are solved using this method. But limitation of this method is the results cannot be accepted instantaneously and must be verified with experimental results or by hand calculation to know the range of results.

The results of the conventionally and microwave sintered composites samples tested for mechanical property viz. compression strength was validated through FEM. The Finite Element Method analysis was carried out using MSC NASTRAN software package (MSC Nastran 2007). The matrix was identified by 8 noded hexahedron elements called CHEXA8 in NASTRAN.

The test results obtained from the mechanical properties evaluated by static compression test in the laboratory as the input for defining the material. The physical properties, linear elastic and plasticity of the material used were defined for the material in MSC Nastran software simulation. The material had a valid density defined for the explicit or implicit simulation. Isotropic elasticity was used to define linear elastic material behavior by defining Young's modulus and Poisson's ratio.

However, the plastic deformation was computed by reference to Von Mises yield criterion. The multi-linear isotropic model was used to define the yield stress (σ_y) as a piecewise linear function of plastic strain, ϵ_p . The Load vs. Displacement behavior of both the types of samples sintered differently was also incorporated for the simulation studies.

3.4.5.3 Flexural strength (σ_f)

Flexural Strength also known as Modulus of Rupture (MOR), bend strength, or fracture strength, is a mechanical parameter for brittle material. This is defined as material's ability to resist deformation under load. The transverse bending test is most frequently employed, in which a specimen having either a circular or rectangular cross-section is bent until fracture or yielding using a three point flexural test technique. The flexural strength represents the highest stress experienced within the material at its moment of rupture. The Flexural Strength test has been carried out as per the guidelines of ASTM D790 – 15 standards.

Flexural Strength (σ_{fs}) is measured in terms of stress, here given the symbol σ . was calculated as follows:

$$\text{Flexural Strength } (\sigma_{fs}) = \frac{3PL}{2BD^2} \quad (3.5)$$

Where P= the actual load at the fracture point, L is the length of the supports holding the test specimen, B is the width of the test specimen and D is the depth or thickness of the test specimen and the units of flexural strength is kg/cm^2 or MPa. Flexural Strength measurements of the composites were carried out in a Laboratory make 3 point bending machine of capacity ranging from 1 to 20 kg.

3.4.5.4 Brinell Hardness Number

Hardness number of the composite materials was determined using Zwick Werkstoff-Prufmaschinen T 3212 B Digital Hardness tester. This hardness testing machine is designed according to DIN 51225 and ISO/R 146 for hardness testing machines with optical indentation measuring devices. A precision measuring microscope with bright field illumination was used to measure the Brinell impressions.

The Brinell Hardness Number is used to determine the hardness of metals and alloys. The test is performed on the sample by applying a known load on the surface of the material to be tested. The load of 3kgf is applied through a steel ball which has a diameter of 10 mm. The ball makes an indentation on the surface of the sample and the diameter of this indentation is measured. The Brinell Hardness Number is then calculated using the formula:

$$\text{Brinell Hardness Number (BHN)} = 2 P / (\pi D (D - (D^2 - d^2)^{1/2})) \quad (3.6)$$

where P = load on the indenting tool (kg) on the sample, D = diameter of steel ball (mm), d = measure diameter at the rim of the impression (mm)

3.5 Equipment used for research work

A. Equipment used for material processing

- Microwave Sintering Facility
- Planetary bowl mill/mixer
- Precision Weighing Balances, Mixers, Hot air oven
- Hydraulic press
- Electric resistance type furnace

B. Facilities used for material testing and characterization

- Scanning Electron Microscope with EDAX
- X-ray Diffractometer, X-ray Fluorescence spectrometer
- Dynamic Testing Machine, Hardness Tester
- Particle Size Analyzer,
- Ash Fusion Temperature determinator
- Abrasion Index machine-Pin on Disc machine, Jet Erosion test rig
- Thermo-mechanical Analyzer

CHAPTER 4

RESULTS AND DISCUSSIONS ON CENOSPHERES MATERIAL CHARACTERIZATION

4.1 SEM, XRF and XRD Analysis of Cenospheres

The SEM with EDAX and the XRF equipment were primarily used for the cenospheres ash elemental oxides analysis for major oxides. It is seen that the primary 11 oxides present in the cenospheres are SiO_2 , Al_2O_3 , CaO , Fe_2O_3 , TiO_2 , K_2O , Na_2O , MgO , MnO , P_2O_5 , and SO_3 . The ash elemental analysis provides a quantitative evaluation of oxides that adversely affect the high temperature characteristics of cenospheres.

The chemical composition of fly ash cenospheres, received from M/s. NTPC Simhadri TPS, Vishakhapatnam, shown in Table 4.1 indicates the presence of Silica (SiO_2) and Alumina (Al_2O_3) as the predominant elements forming Alumino-silicates. The mass content of Silica was observed to be more than 50% in cenospheres. The analysis indicates the presence of Alumina as the next predominant compound present at around 24 %. The other major oxides present in cenospheres include Calcia (CaO) up to 15.5% with Iron Oxide (Fe_2O_3) up to 3.54 % which determines its refractoriness and color. Potassium oxide (K_2O) and the Titania (TiO_2) are in the range 2.25 and 1.84 wt % respectively while the oxides of Magnesium (MgO), Manganese (MnO), Phosphorous(P_2O_5), Sulphur (SO_3) and Sodium(Na_2O) are less than 1 wt.%.

The chemical compositions of the study materials exhibited that the chemical components were in specified proportions with less impurities within the maximum permissible limits for application as a composite material.

Table 4.1: Cenospheres elemental oxide analysis (%)

Silicon Di-oxide (SiO ₂)	50.71
Aluminium Oxide (Al ₂ O ₃)	23.85
Iron Oxide (Fe ₂ O ₃)	3.54
Calcium Oxide (CaO)	15.50
Sodium Oxide (Na ₂ O)	0.86
Potassium Oxide (K ₂ O)	2.25
Magnesium Oxide (MgO)	0.58
Manganese di Oxide (MnO ₂)	0.10
Titanium Di-oxide (TiO ₂)	1.84
Sulphur tri Oxide (SO ₃)	0.39
Phosphorous Pentoxide (P ₂ O ₅)	0.38

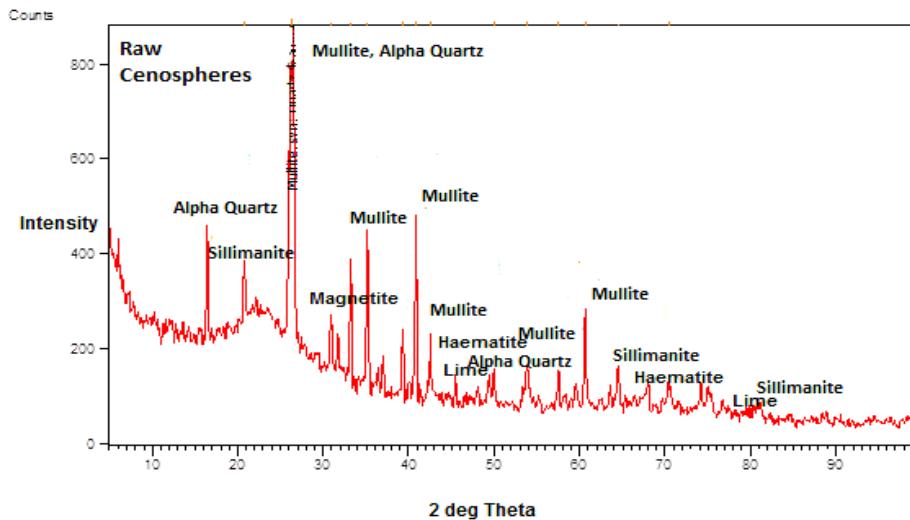


Fig. 4.1: X-ray Diffraction (XRD) pattern of Cenospheres

From the comparison of the mineralogical data from the XRD graph at Fig: 4.1, it can be seen from the analysis that the raw fly ash cenospheres sample could be distinguished into two major matrices: the amorphous constituent of glassy aluminosilicates and crystalline constituent as represented in terms of mullite, quartz, calcite, hematite, magnetite and lime. The mineralogy is revealed in Table 4.2.

Table 4.2: Major mineral phases in Cenospheres

XRD Phases present in Cenospheres	Content (%)
Amorphous phase (glassy) (Alumino-silicates)	68.33
Crystalline phases	31.67
Mullite	10.08
Quartz	14.88
Calcite	2.99
Hematite	1.04
Magnetite	1.52
Lime	1.16

The amorphous phase which comprises of alumino-silicate glass is present to an extent of about 68.3% and the crystalline phases of about 31.7% which is evident from sharp crystalline peaks. It is also evident that the predominant compounds present in crystalline phases of the cenospheres are mullite (alumino-silicate) up to 10.1 %, quartz of about 14.9%, calcite 3.0 %, haematite 1.0 % magnetite content of about 1.52 and lime of about 1.2%.

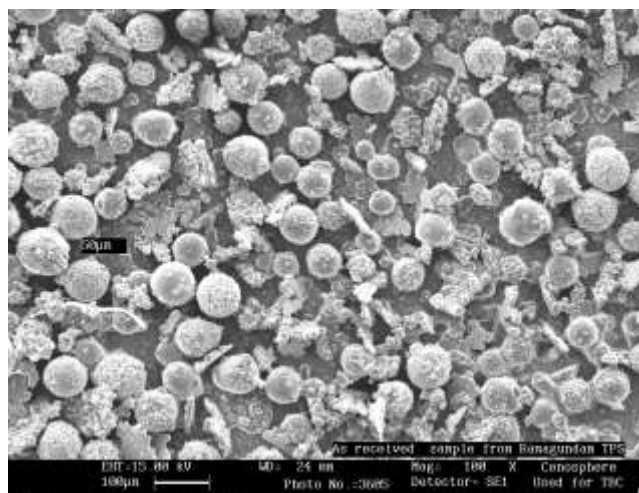


Fig. 4.2: Cenospheres particles

4.2 Morphological Analysis of Cenospheres

The ‘as received’ fly ash cenospheres particles as seen under a scanning microscope picture is shown in Fig. 4.2. The section of an individual cenospheres particle of the

cenospheres particle is shown in Fig. 4.3. The SEM micrograph depicts morphology of cenospheres particles as collected from the ash pond of the power plant which shows the measured thickness of the ruptured cenospheres wall ranging from 2.6 to 2.8 μm thick

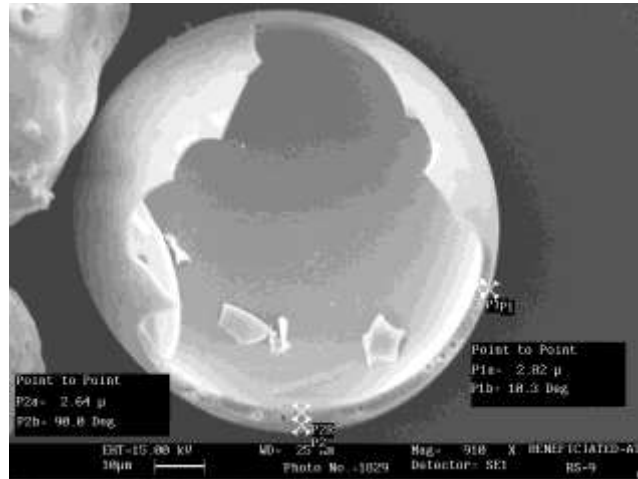


Fig. 4.3: Individual Hollow Cenospheres particle

4.3 Particle Size Distribution Analysis of Cenospheres

The particle size distribution of fly ash cenospheres was carried out using Malvern Laser Beam Particle Size Analyzer by wet sieve analysis method which showed the results tabulated in Table 4.3. The particle size of cenospheres varies from <45 microns to 400 microns with majority of the particles in the size range of 45-250 microns.

Table 4.3: Particle size distribution of cenospheres

Particle Size (Passing through)	%	Particle Size (Retained on)	%
400μm	98.6	250μm	10.9
300μm	90.3	180μm	24.4
150μm	27.6	106μm	44.8
100μm	5.6	90μm	5.7
50μm	3.9	75μm	8.6
20μm	0.02	45 μm	4.3

4.4 Fusion Temperature (AFT) determination of cenospheres

The measured cenospheres fusion temperatures are tabulated below in Table 4.4 and the results show that the initial deformation temperature of the cenospheres is 1260⁰C, which indicates that the cenospheres is refractory.

Table 4.4: Fusion Temperature of Cenospheres

Ash Fusion Temperature (⁰ C)			
Initial Deformation Temperature	Softening Temperature	Hemi-spherical Temperature	Fluid Temperature
1260	1260	1290	1360

4.5 Discussions on the study

The chemical constituents and the phase analysis of the cenospheres reveal that the presence of alumino-silicates make up to 75 wt. % which contributes for higher melting point of cenospheres which is about 1200-1350⁰C and lower coefficient of thermal expansion ($6.1 \times 10^{-6} / ^{\circ}\text{C}$), both of which are of paramount importance for applications as a refractory material [P K Rohatgi 2006]. This gives an indication that the fly-ash cenospheres can be used at relatively high temperatures before reaching its melting point. Therefore cenospheres was considered as the main ingredient of the body compositions for the development lightweight composite product. The mullite crystals are largely attributed to kaolinite and illite minerals in the coal which contributes towards the glass and cenospheres formation during combustion in the boiler at high temperatures[Joseph Biernacki et al 2008].

Mullite is an extremely valuable mineralogical phase required for producing products that need to withstand high temperatures, corrosive environments, or other adverse conditions. It has a low coefficient of thermal expansion, good thermal and electrical insulation capacity and has outstanding hot load-bearing properties. It is, in short, the key ingredient for developing refractory and ceramic products. The major chemical constituents of cenospheres are made up of metallic oxides like Silica (SiO₂), Iron

(Fe₂O₃), Alumina (Al₂O₃) and Calcia (CaO) which forms the bulk chemical composition [Ananda Kumar et al 2014].

The chemical constituents of the ash and their concentration decide the ash fusion temperature characteristics [Ananda Kumar et al 2014]. The ash having high alkali oxide concentration will fuse at a lower temperature while the ash containing higher proportion of the refractory oxides will fuse at high temperatures. The mullite and sillimanite phases which are aluminosilicate phase forms the major constituent of the cenospheres taken for the study and it is an extremely valuable mineralogical phase that withstand high temperatures and hence these phases are responsible for the refractory behavior of the cenospheres and the fusion temperature of the ash cenospheres is 1360⁰C and this also depends primarily on the concentration of these refractory constituents [Ananda Kumar et al 2014].

The combinations of various particle sizes of cenospheres contribute for improving the packing factor and effective packing density of the composites fabricated through powder metallurgy routes.

CHAPTER 5

RESULTS AND DISCUSSIONS ON INITIAL STUDY ON HIGH TEMPERATURE SINTERING BEHAVIOR OF ALUMINIUM CENOSPHERES MIX

5.1 Results and Discussions of high temperature conventionally sintered aluminium cenospheres mix

5.1.1 Microstructural and Phase Analysis of mix sintered conventionally sintered at 650⁰C

In the conventional sintering initially, the aluminium- cenospheres mix was heated at 650⁰C. The corresponding microstructure and XRD graph is shown in Fig. 5.1. The SEM micrograph shows the aluminium-cenospheres mix after sintering conventionally at 650⁰C. It can be seen that the sphericity of the cenospheres is intact with pores appearing on the cenospheres surface due to escape of gaseous component from the cenospheres through the surface. The aluminium powder is appearing as plate like structure which is surrounding the cenospheres. From the XRD graph, it is evident that the predominant compounds present in cenospheres are silicon, aluminium and sillimanite without much change in the phases and these phases were present in the raw mix prior to sintering also.

5.1.2 Microstructural and Phase Analysis of mix sintered conventionally sintered at 750⁰C

The next higher temperature at which the aluminium-cenospheres mix was heated was at 750⁰C. The corresponding microstructure and XRD graph is shown in Fig. 5.2. The SEM micrograph shows the aluminium-cenospheres mix after sintered at conventionally 750⁰C. It can be seen that the spherical shape of the cenospheres is still intact exists without crumbling of the shape or laminations on the cenospheres surface. The increase in the temperature has not affected the cenospheres surface. The XRD graph shows aluminum, silicon and sillimanite which is an alumino-silicate as the predominant phases. The aluminium phase still exists at this temperature. No shifts in the 2 θ values in the corresponding XRD peak observed in the XRD.

5.1.3 Microstructural and Phase Analysis of mix sintered conventionally sintered at 850⁰C

The aluminum-cenospheres mix was further heated to the next high temperature at 850⁰C. The corresponding microstructure and XRD graphs are shown in Fig. 5.3. The SEM micrograph shows the aluminium-cenospheres mix after sintering conventionally at 850⁰C. It can be seen that crumbling in the spherical shape has begun to occur in the cenospheres particle. The increase in the temperature has further diminished the cenospheres surface with pores getting enlarged and opening to the surface. The aluminium and cenospheres mix appear to be fused together without showing their distinctive features as observed at lower temperatures. The XRD graph shows the presence of alumina and cristobalite which are high temperature phases of aluminum oxide and silica as the major phases. There is a shift in the 2 θ values with more refinement in the corresponding XRD peak which is observed through the XRD graph.

5.1.4 Microstructural and Phase Analysis of mix sintered conventionally sintered at 950⁰C

Further, the aluminum-cenospheres mix was heated at the next higher temperature at 950⁰C. The corresponding microstructure and XRD graphs are shown below in Fig. 5.4. The SEM micrograph shows the aluminium-cenospheres mix after sintering conventionally at 950⁰C. It can be seen that the shape of the cenospheres particle appearing to be transforming into porous mass from spherical shape at this temperature. The increase in the temperature has started to affect the sphericity of the cenospheres. The XRD graph shows the formation of alumina and silicon as the predominant phases. There is further shift in the 2 θ values from 38-2 θ degrees to 27-2 θ values. More crystalline peaks are observed predominantly throughout the XRD pattern.

5.1.5 Microstructural and Phase Analysis of mix sintered conventionally sintered at 1050⁰C

The aluminum-cenospheres pellet was sintered at the next higher temperature of 1050⁰C and the corresponding microstructure and XRD graphs are shown below in

Fig. 5.5. The SEM micrograph shows the aluminium-cenospheres mix after sintering conventionally at 1050⁰C. It can be seen that the shape of the cenospheres particle occurring as chunks and is further reduced to fragments with complex shapes whereby the cenospheres shape is further disintegrated and scattered. The XRD graph now shows the formation of high temperature alumina, silicon and sillimanite phases as predominant. There is refinement of peaks with reduction in many crystalline peaks are observed predominantly throughout the XRD pattern.

5.1.6 Microstructural and Phase Analysis of mix sintered conventionally sintered at 1150⁰C

The aluminum-cenospheres mix was now sintered at the highest temperature of 1150⁰C and the corresponding microstructure and XRD graphs are shown in Fig. 5.6. The SEM micrograph shows the aluminium-cenospheres mix after sintering conventionally at 1150⁰C. It can be seen that only sintered fragments/ chunks seen as residual mass. The mix is now complex chunk of highly porous and sintered mass which is not distinguishable with that of the features of initial material in terms of its morphology. The XRD graph now shows the mullite, alumina and silicon as the major high temperature phases that exist at this point of time. The sintered material is highly crystalline as can be seen from the peaks throughout the XRD pattern. The XRD patterns for the peaks obtained at different sintering temperatures are appended in Fig. 5.8.

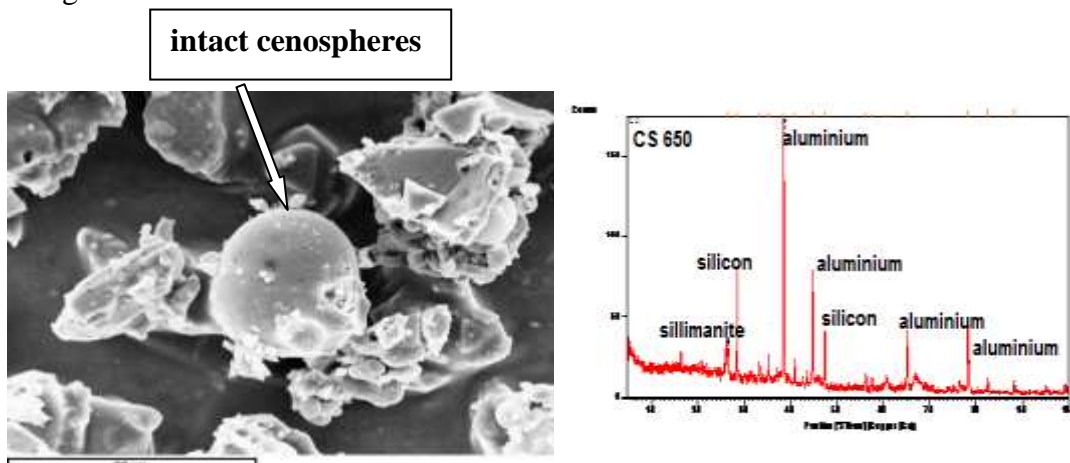


Fig.5.1: Microstructure and XRD of conventionally sintered mix at 650⁰C

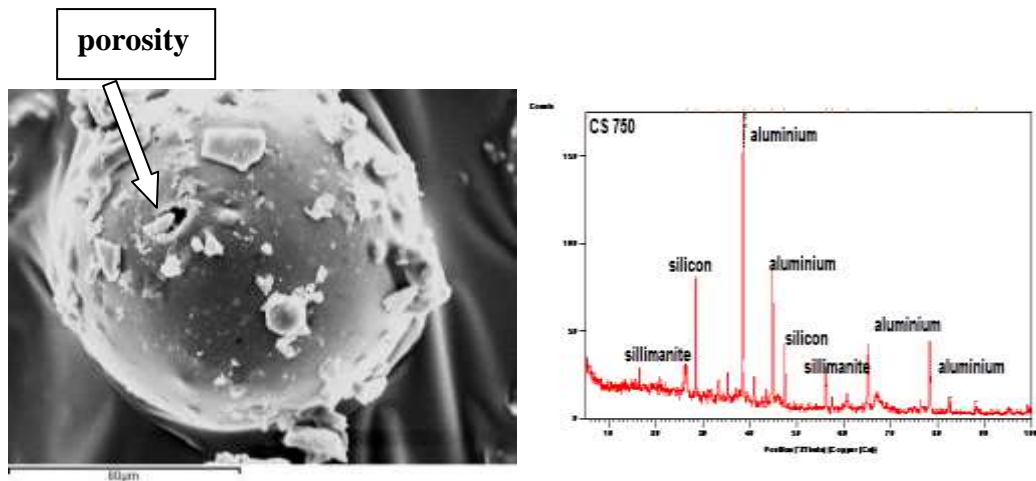


Fig.5.2: Microstructure and XRD of conventionally sintered mix at 750⁰C

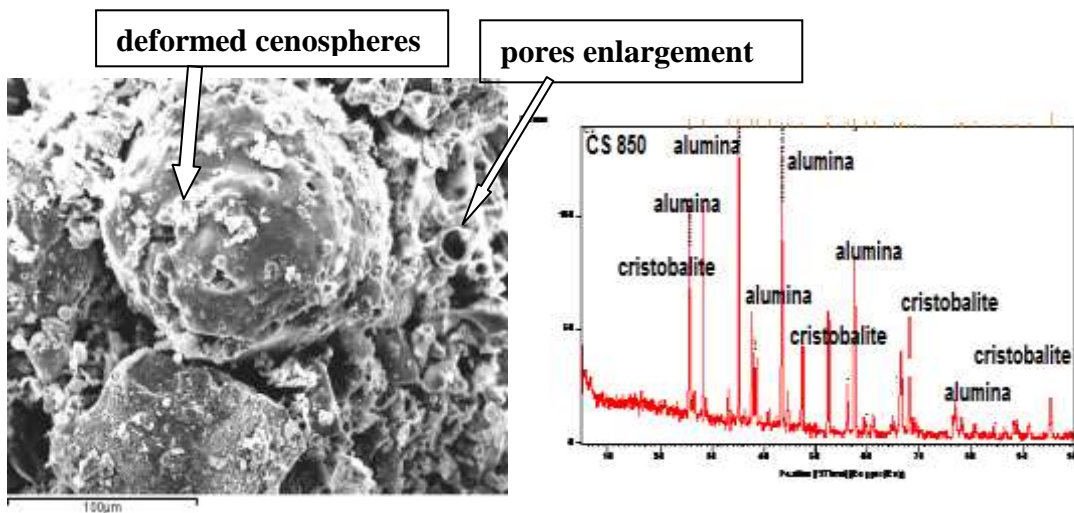


Fig.5.3: Microstructure and XRD of conventionally sintered mix at 850⁰C

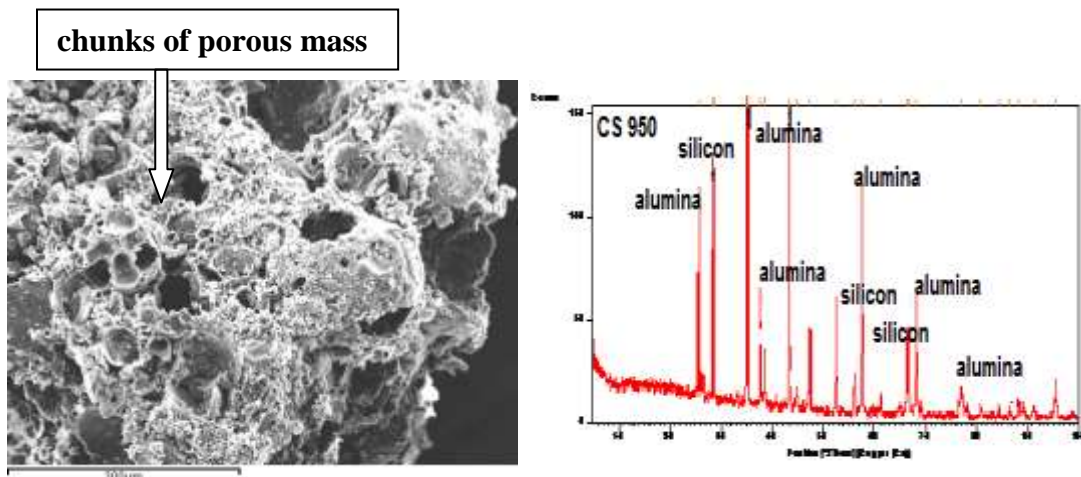


Fig.5.4: Microstructure and XRD of conventionally sintered mix at 950⁰C

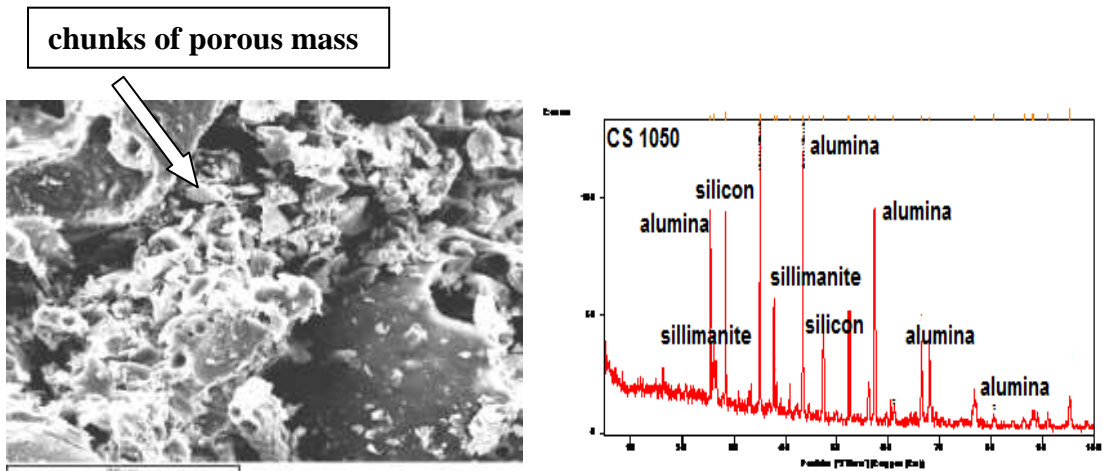


Fig.5.5: Microstructure and XRD of conventionally sintered mix at 1050⁰C

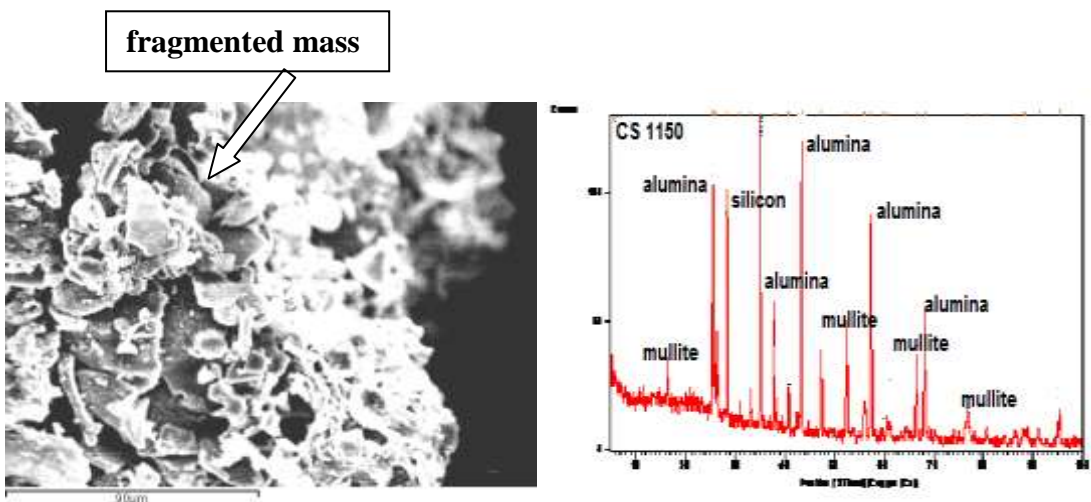


Fig.5.6: Microstructure and XRD of conventionally sintered mix at 1150⁰C

5.2 Results and Discussions of Microwave sintered Aluminium Cenospheres mix

5.2.1 Microstructural and Phase Analysis of mix sintered in microwave at 650⁰C

The initial temperature at which the aluminium cenospheres mix was sintered in microwave was at 650⁰C. The corresponding microstructure and XRD graph is shown in Fig. 5.7. The SEM micrograph shows the aluminium-cenospheres mix after sintering in microwave at 650⁰C. It can be seen that the sphericity of the cenospheres is intact with pores appearing on the cenospheres surface as could be seen in the conventionally sintered mix at this temperature. This is due to escape of gaseous component from the cenospheres through the surface. From the XRD graph it is evident that the predominant compounds present in cenospheres are aluminium and

mullite without much change in the phases and these phases were present in the raw mix prior to sintering also.

5.2.2 Microstructural and Phase Analysis of mix sintered in microwave at 750⁰C

The next temperature at which the aluminium cenospheres mix was sintered in microwave was at 750⁰C. The corresponding microstructure and XRD graph is shown below in Fig. 5.8. The SEM micrograph shows the aluminium-cenospheres mix after sintering in microwave at 750⁰C. It can be seen that the spherical shape of the cenospheres ceases to exist with crumbling of the shape with laminations observed on the cenospheres surface and due to increase in the temperature the pore has diminished from the cenospheres surface. The XRD graph shows the formation of alumina, silicon and corundum as the predominant phases. The aluminium phase exist owing to the melting temperature of aluminum at above 650⁰C and the aluminum- cenospheres mix forming corundum as the phase which has alumina and silica as the major components. There is a shift in the 2 θ values and corresponding XRD peak also which is observed through the XRD graph.

5.2.3 Microstructural and Phase Analysis of mix sintered in microwave at 850⁰C

The aluminum-cenospheres mix was further heated in microwave at the next high temperature i.e at 850⁰C and the corresponding microstructure and XRD graphs are shown below in Fig. 5.9. The SEM micrograph shows the aluminium-cenospheres mix after sintering at 850⁰C in microwave. It can be seen that further crumbling in the shape of the cenospheres particle occurs with more laminations observed on the cenospheres particle. The increase in the temperature has further diminished the cenospheres sphericity. The XRD graph shows the transformation of into alumina and silicon as the predominant phases. The mullite and corundum phase ceases to exist at this temperature of about this temperature of 850⁰C with precipitation of silicon as one of the major phases. There is a shift in the 2 θ values with more refinement in the corresponding XRD peak which is observed in the XRD graph.

5.2.4 Microstructural and Phase Analysis of mix sintered in microwave at 950⁰C

The aluminum-cenospheres mix was next sintered in microwave at a temperature of 950⁰C and the corresponding microstructure and XRD graphs are shown below in Fig. 5.10. From the SEM micrograph of the aluminium-cenospheres mix after sintering at 950⁰C in microwave, it can be seen that the shape of the cenospheres particle occurs as chunks of porous mass. The increase in the temperature has further diminished totally transformed the spherical shape of the cenospheres into a light weight crumbled mass with increase in the volume. The XRD graph shows the formation of silicon, alumina and corundum as the predominant phases. There is further shift in the 2θ values from 38- 2θ degrees to 18- 2θ values. More crystalline peaks are observed predominantly throughout the XRD pattern.

5.2.5 Microstructural and Phase Analysis of mix sintered in microwave at 1050⁰C

The aluminum-cenospheres mix was further sintered at a temperature of 1050⁰C in microwave and the corresponding microstructure and XRD graphs are shown below in Fig. 5.11. The SEM micrograph shows the aluminium-cenospheres mix after sintering in microwave at 1050⁰C and it can be seen that the shape of the cenospheres particle occurring as chunks of porous mass is further reduced to fragments. The XRD graph shows the formation of silicon and corundum phases. There is refinement of peaks with reduction in many crystalline peaks are observed predominantly throughout the XRD pattern.

5.2.6 Microstructural and Phase Analysis of mix sintered in microwave at 1150⁰C

Finally the aluminum-cenospheres mix was sintered at 1150⁰C and the corresponding microstructure and XRD graphs are shown below in Fig. 5.12. The SEM micrograph shows the aluminium-cenospheres mix after sintering in microwave at 1150⁰C and it can be seen that only fragments of the chunks of porous mass exist at this stage of sintering. The XRD graph now shows the precipitation of mullite which is an alumino-silicate and alumina as the major high temperature phases that exist. The sintered material is highly crystalline as can be seen from the peaks throughout the XRD pattern.

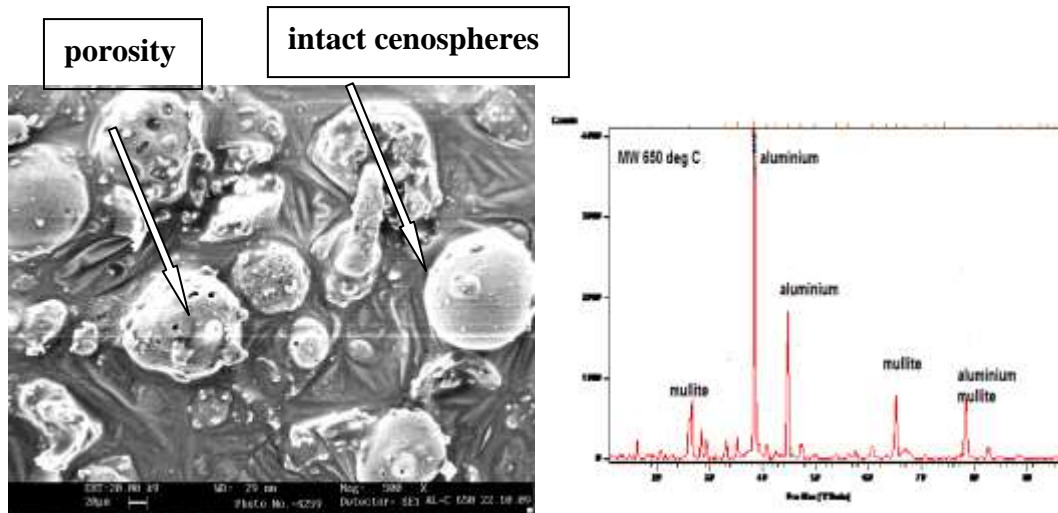


Fig.5.7: Microstructure and XRD of microwave sintered mix at 650°C

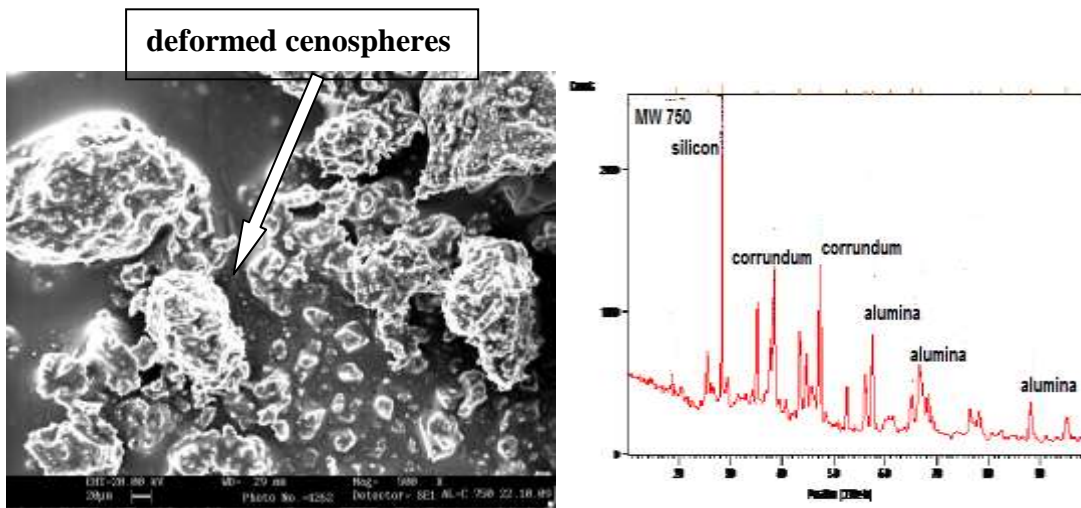


Fig.5.8: Microstructure and XRD of microwave sintered mix at 750°C

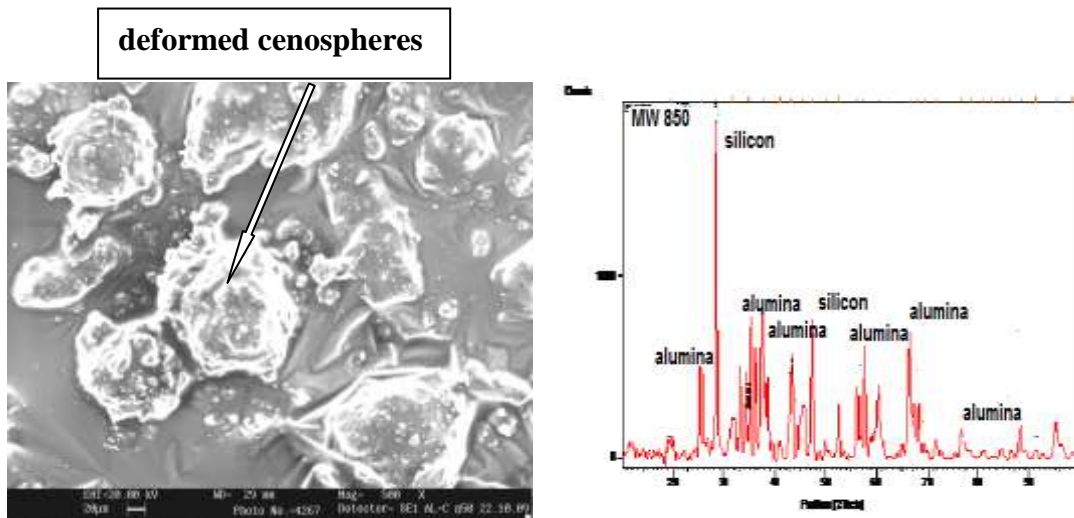


Fig.5.9: Microstructure and XRD of microwave sintered mix at 850°C

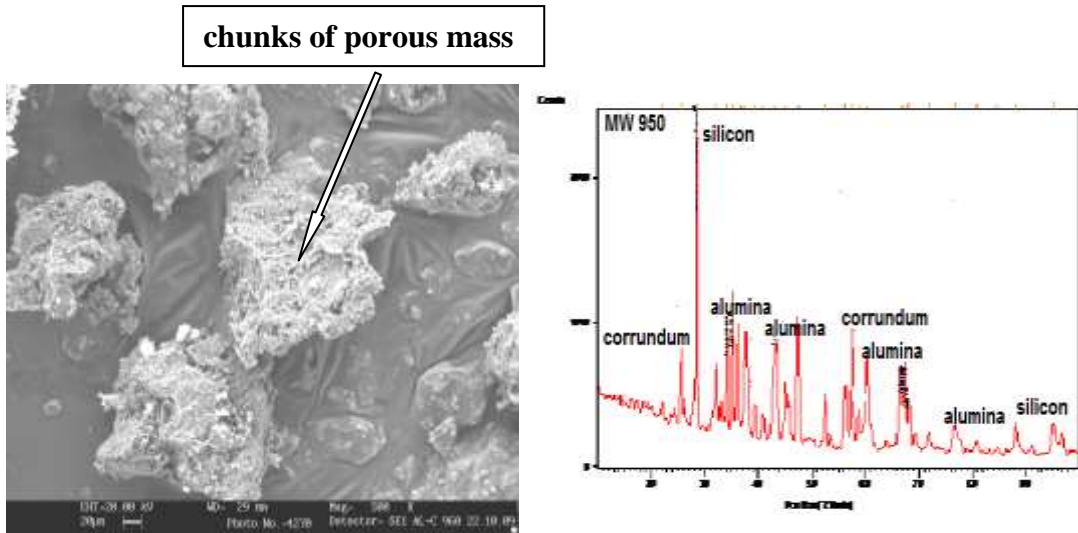


Fig.5.10: Microstructure and XRD of microwave sintered mix at 950⁰C

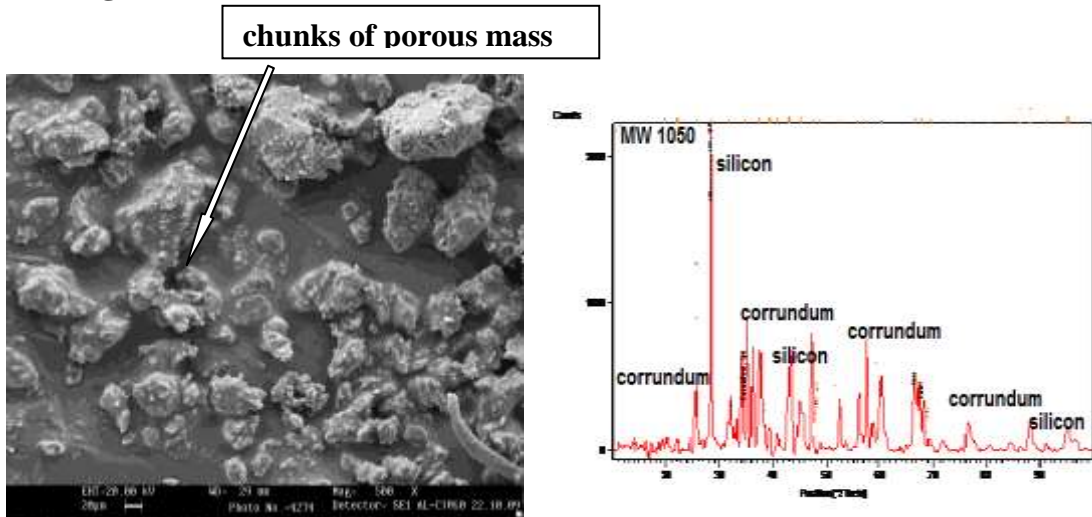


Fig.5.11: Microstructure and XRD of microwave sintered mix at 1050⁰C

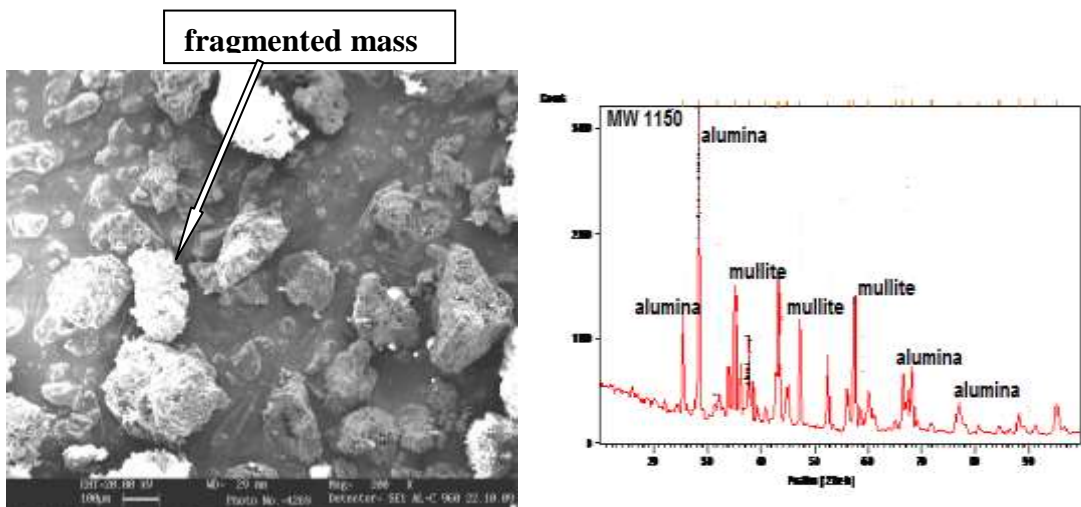


Fig.5.12: Microstructure and XRD of microwave sintered mix at 1150⁰C

Table No. 5.1 Phases of Aluminium Cenospheres mix at various temperatures

Temperature (°C)	Phases at various temperatures	
	Conventionally sintered	Microwave sintered
650	Aluminium, Silicon, Sillimanite	Aluminium, Mullite
750	Aluminium, Silicon, Sillimanite	Alumina, Corundum, Silicon
850	Alumina, Cristobalite	Alumina, Silicon
950	Alumina, Silicon,	Alumina, Silicon, Corundum
1050	Alumina, Silicon, Sillimanite	Silicon Corundum
1150	Alumina, Mullite, Silicon	Alumina, Mullite

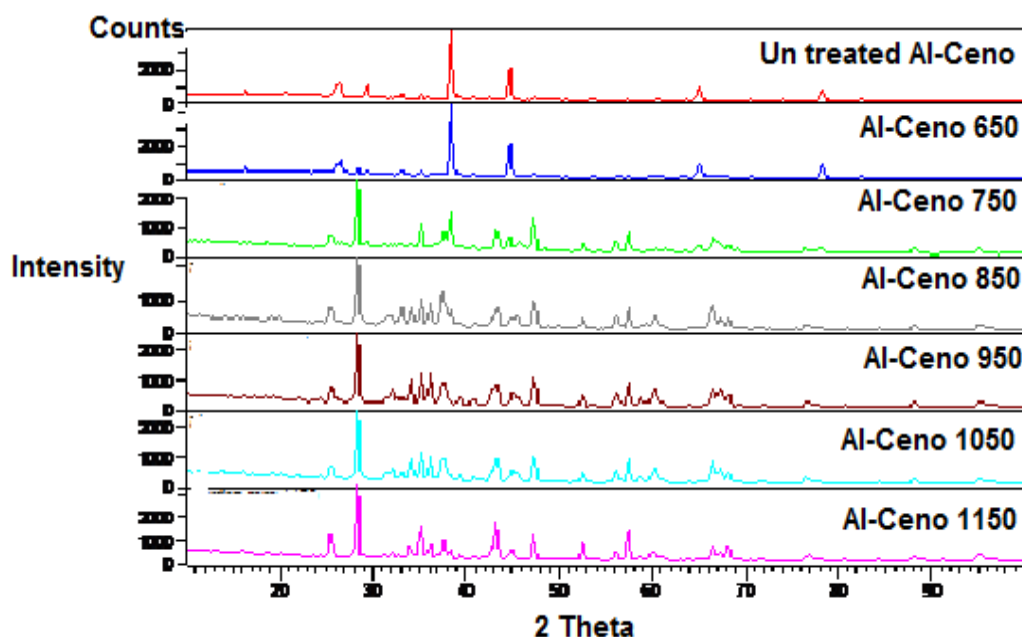


Fig.5.13: XRD graphs of Un-sintered and microwave sintered mix at various temperatures

Table 5.2 Comparison of properties of Microwave and Conventional sintered composites samples at various temperatures from 650 to 1050°C.

Temperature of sintering [°C]	Conventionally sintered mix			Microwave sintered mix		
	Water Absorption (%)	Brinell Hardness Number	Bulk Density [g/cc]	Water Absorption (%)	Brinell Hardness Number	Bulk Density [g/cc]
650	38.0	12	1.01	27.2	23	1.03
750	37.6	30	1.10	26.8	39	1.16
850	36.4	32	1.22	25.8	41	1.37
950	31.3	35	1.28	24.8	44	1.39
1050	24.8	39	1.39	19.9	47	1.47
1150	24.1	41	1.41	19.2	48	1.49

Table 5.3 Comparison of properties of Microwave and Conventional sintered composites samples at 650°C only.

Temperature [°C]	Water absorption (%)	Brinell Hardness Number [HB]	Bulk Density [g/cc]
Conventionally sintered composites			
650	38.0	12	1.01
Microwave sintered composites			
650	27.2	23	1.13

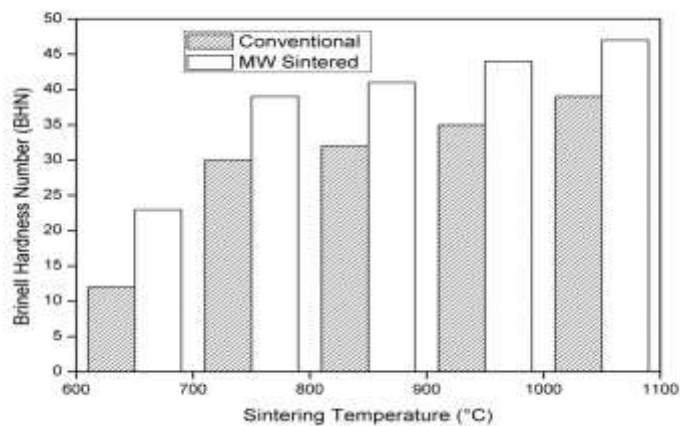


Fig. 5.14: Sintering Temperature versus BHN for Conventional and Microwave Sintered Composites

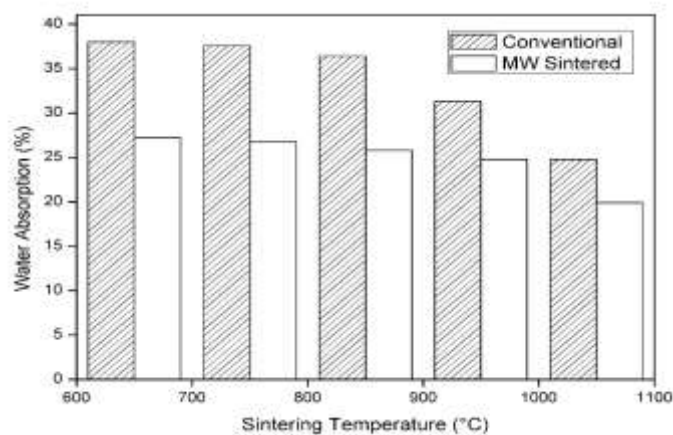


Fig. 5.15: Sintering Temperature versus Water Absorption for Conventional and Microwave Sintered Composites

5.3 Discussions on the study

The properties of a given material are also determined by its microstructure. The critical issue in micro structural development is the densification of the material and coarsening. The micro structural development depends on the parameters such as optimized temperature, sintering time, heating rate and the pressure. The morphology and the mineralogy of the aluminium cenospheres change rapidly with change in temperature. The chemical constituents in the cenospheres as well as the eutectics that form at various temperatures are responsible for the morphological features too. Lower melting compounds formed which fuse at different temperatures tries to change the morphology and structure of the initial material. These type of observations are seen both for the conventionally sintered and microwave sintered samples.

For the conventionally sintered mix, from the microstructure at 650⁰C, it can be seen that the sphericity of the cenospheres is intact with pores appearing on the cenospheres surface due to escape of gaseous component from the cenospheres through the surface. The aluminium powder is appearing as plate like structure which is surrounding the cenospheres. Further increase in temperature to 750⁰C it can be seen that the spherical shape of the cenospheres is still intact exists without crumbling of the shape or laminations on the cenospheres surface. The increase in the temperature has not affected the cenospheres surface. At 850⁰C it can be seen that crumbling in the spherical shape has begun to occur in the cenospheres particle. The increase in the temperature has further diminished the cenospheres surface with pores getting enlarged and opening to the surface. The aluminium and cenospheres mix appear to be fused together without showing their distinctive features as observed at lower temperatures. At 950⁰C, it is seen that the shape of the cenospheres particle appearing to be transforming into porous mass from spherical shape at this temperature. The increase in the temperature has started to affect the sphericity of the cenospheres. Further sintering the mix at 1050⁰C, it is seen that the shape of the cenospheres particle occurring as chunks and is further reduced to fragments with complex shapes whereby the cenospheres shape is further disintegrated and scattered

and finally at 1150⁰C only sintered fragments/ chunks seen as residual mass. The mix is now complex chunk of highly porous and sintered mass which is not distinguishable with that of the features of initial material in terms of its morphology. The sintered material is highly crystalline as can be seen from the peaks throughout the XRD pattern.

For the microwave sintered mix at 650⁰C, from the SEM micrograph it can be seen that the sphericity of the cenospheres is intact with pores appearing on the cenospheres surface as could be seen in the conventionally sintered mix at this temperature. This is due to escape of gaseous component from the cenospheres through the surface. When sintering the mix at 750⁰C, microstructure shows the spherical shape of the cenospheres which ceases to exist with crumbling of the shape with laminations observed on the cenospheres surface and due to increase in the temperature and the pore has diminished from the cenospheres surface. At 850⁰C micrograph it can be seen that further crumbling in the shape of the cenospheres particle occurs with more laminations observed on the cenospheres particle. The increase in the temperature has further diminished the cenospheres sphericity. At 950⁰C sintering it can be seen that the shape of the cenospheres particle occurs as chunks of porous mass. The increase in the temperature has further diminished the spherical shape of the cenospheres and transformed the same into a light weight crumbled mass with increase in the volume. Further at 1050⁰C it can be seen that the shape of the cenospheres particle occurring as chunks of porous mass is further reduced to fragments. And finally at 1150⁰C and it can be seen that only fragments of the chunks of porous mass exist at this stage of sintering. Here too the sintered material is highly crystalline as can be seen from the peaks throughout the XRD pattern.

The Table no. 5.1 shows the comparison of the phases that are present in conventional and microwave sintered samples at various temperatures. It is seen at 650⁰C that metallic aluminium and silicon phases along with sillimanite phase are seen in conventionally sintered samples whereas metallic aluminium and mullite phases are seen in microwave sintered sample. At 750⁰C sintering, the conventionally

sintered sample has aluminium, silicon and sillimanite phases whereas alumina, corundum and silicon phases are seen in microwave sintered ones. At 850⁰C sintering temperature the conventionally sintered sample has alumina and cristobalite, which is a high temperature phase of silica, whereas microwave sintered sample has alumina and silicon phase. At 950⁰C temperature the conventionally sintered sample has alumina and silicon and microwave sintered sample has alumina, silicon and corundum phases. At 1050⁰C temperature the conventionally sintered sample has alumina, silicon and sillimanite phases and the microwave sintered sample alumina, silicon and corundum phases and finally at 1150⁰C temperature the conventionally sintered sample has alumina, mullite and silicon phases and the microwave sintered sample has alumina and mullite phases.

The phases of alumino silicates present is different in conventionally samples compared to microwave sintered sample though the chemical constituents of the compound is the same. The formation of a particular phase at a particular temperature and sintering process is attributed to the reaction kinetics of the material at that instance. The other factors that govern the formation of a particular phase are the atomic diffusivity, nucleation, grain growth and precipitation coupled with thermodynamic conditions which are prevailing at the time of formation of the phase. The above conditions are different for conventional sintering as well as microwave sintering. The silica present in the cenospheres thermodynamically has a tendency to react with aluminium melt at temperatures beyond 650⁰C and the reactions are both oxidation and reduction reactions. A portion of the silica from cenospheres react with aluminium in the molten state forming alumino-silicates which is an oxidation reaction, and at the same time there is also reduction reaction in which portion of silica reduces to silicon. [P K Rohatgi et al 2009].

From the Fig.5.13 which depicts the XRD graphs of mix sintered at various temperatures in microwave, it can be seen that the aluminium and cenospheres mix did not show much change in the phase distribution till 650⁰C. The aluminium remained in the metallic state with silicon while the alumino-silicates remained in the form of sillimanite and mullite phases. As the temperature increased beyond 650⁰C,

the metallic phases of aluminium and silicon begin to convert into their respective oxide phases like sillimanite, mullite, alumina, spinel and others. Even after the sintering temperature was increased up to 1150⁰C, the changes was found to be negligible, but there was some variation in the concentration of the oxide phase with formation of multi oxide phases based on aluminium, silicon with other chemical constituents present in the cenospheres.

Sudharshan et al [2008] have also observed that at higher temperatures of sintering, there is both oxidation and reduction reactions occurring but formation of complex oxides due to oxidation reaction is predominant in the composite when sintering at higher temperatures beyond 650⁰C. The thermodynamic analysis of the aluminum cenospheres composite indicate a possibility of chemical reaction between the aluminium melt and cenospheres particles leading to reduction of alumina, silica and iron oxide to their respective metallic state during their contact with the melt and some oxidation of the same taking place. For example in the reduction reaction, the elemental Si formed by the reduction reaction would alloy with the matrix and that the Gibbs free energy and the heats of reaction of this reaction are highly exothermic in nature. As a result greater amount of eutectic silicon is seen in the composite and the chemical reaction indicates the increase in silicon level in the matrix. This may be possible since the XRD graphs of this study also indicate the presence of silicon and alumina peaks in the high temperature sintered samples. The increased oxidation reactions severely alter properties of the composite such as bulk density, hardness, water absorption etc.

The Tables 5.2 and 5.3 and Fig. 5.14 and 5.15 describe the properties of the aluminium cenospheres mix sintered at various temperatures both through conventional and microwave sintering, were measured for Brinell Hardness, Water Absorption (%) and Bulk Density (g/cc) and the comparison of the same have been appended in Table 5.2. The properties of composite mix pellets sintered only at temperature at 650⁰C both through conventional and microwave sintering were measured for Brinell Hardness Number (BHN), Water Absorption (%) and Bulk Density (g/cc) and the comparison of the same have been appended below in Table

5.3. It is observed from the tables that as the temperature of sintering increases, the physical properties of the composite mix also undergo numerous changes. As the temperature of sintering was increased, there was increase in bulk density and Hardness Number (BHN) and reduction in water absorption characteristic in both conventionally and microwave sintered samples. The water absorption (%) values of microwave sintered composites is seen lower compared to conventionally sintered composites by about 24.5%. The BHN and bulk density values of microwave sintered composites are higher compared to conventionally sintered composites by about 24.2% and 6.1% respectively. The above are average of all values measured for samples sintered from 650⁰C to 1150⁰C for both types of sintering modes.

At higher temperatures, the sintering temperature and the process adopted highly influence the properties of the composite such as bulk density, mechanical strength, thermal stability, porosity and shrinkage of the samples [Mahnicka L et al 2012]. The development of physical and mechanical properties is related to the phases formed due to reaction sintering between alumina and alumino- silicates in the composite and formation of compact microstructure [Nath S K et al]. Material density is an important characteristic for predicting mechanical properties and permeability. As the density increases (and porosity decreases), the mechanical properties also increase with decrease in permeability [ASM Handbook Vol.7 1998].

The rapid heating rate is the key to produce products with a high sintered density for a given microstructure and grain size compared to slow heating for the same sintered density. Conventional sintering has definite disadvantages accompanied with difficulties since conventional sintered product have differential sintering that give rise to differential densification leading to inconsistent properties which can be seen from the values from the above tables and figures. In this context, microwave sintering is an alternative sintering technique to overcome these problems of conventional sintering. Since microwave sintering is a non-contact sintering technique in which heat gets transferred to the product through electromagnetic radiation. By microwave sintering large amount of heat can be transferred to the material's interior which reduces differential sintering to a large extent. The microwave sintered

products also have finer micro-structural development, with average grain size and higher density which result in enhanced properties such as water absorption, BHN and bulk density as compared to the conventionally sintered ones.

By microwave sintering all the properties of the given material are enhanced by its micro structural development in which the densification of the material and coarsening occurs rapidly and effectively throughout the bulk of the material. The rapid heating rate achieved by microwave heating is the key to produce products with a high sintered density for a given microstructure and grain size compared to slow heating for the same sintered density by conventional heating. Since microwave sintering is a non-contact sintering technique, the heat gets transferred to the product through electromagnetic radiation. By microwave sintering large amount of heat can be transferred to the material's interior which reduces differential sintering to a large extent. Hence the microwave sintered products have finer micro-structural development, with average grain size and higher density which result in enhanced properties as compared to the conventionally sintered ones.

Morteza Oghbaei et al has reported that microwave sintering effectively assist the forward diffusion of ions which accelerates the sintering. This results in matrix densification by grain growth process. Sintering process aids re-crystallization, grain growth and densification at high temperatures in the body that is being sintered. This densification mechanism is strongly dependent on diffusion of ions between the same sample particles. The mechanism of grain growth rate is assisted by the grain boundary diffusion process. It has been found that intense microwave field concentration is active around the particles of the sample while sintering. The power of this microwave field between the particles of the sample in the bulk of the material is about 30 times higher than the external field and this is sufficient to ionize the sample particles at its surface. This accelerates ionic diffusion which promotes rapid densification of the material is promoted under microwave sintering.

Apart from the microwave radiation, the surrounding electromagnetic field also effectively enhances the ionic diffusion kinetics near the grain boundaries. The

kinetic energy of the ions at the grain boundary increases which thereby decrease the activation energy required for the forward ion jump and in the process increases the barrier height for the reverse jump. This mechanism promotes forward diffusion of the inter grain ions which accelerates the grain growth during sintering. This leads to an uniform grain growth and grain size distribution, which leads to effective densification of the product thereby leading to enhanced engineering properties.

David Raja Selvam et al [2013] have reported that the hardness of the AMC's linearly increases with increase in reinforcement. As the reinforcement which is ceramic in nature increases the surface area of the matrix and the matrix grain size gets reduced. The present of ceramic phase also reduces the ductility of the matrix due to reduction in the ductile metal content. This statement is well supported in our study from the Fig.5.14.

The microwave sintering has also shown that the sintering takes place uniformly throughout the mass to be sintered with better microstructure and properties. The sintering process is rapid, with reduced processing times, uniform temperature and has minimal thermal gradients. It also has substantial energy savings with high efficiency coupled with novel and improved properties, finer microstructures and environmental friendly process. Certain changes in the process need to be adopted such as change in sintering atmosphere from oxidizing environment to reducing environment. From the above study it is concluded that:

1. Aluminum metal matrix composites can be fabricated at a temperature of about 650°C. The matrix formed is that of pure aluminum metal without undergoing oxide formation. The filler cenospheres are also evenly dispersed throughout the matrix with its shape intact. It was observed that the aluminium metal powder reacts with cenospheres to form alumino-silicates and alumina (Al_2O_3) at temperatures beyond 650°C and above, in the oxidizing atmosphere. Beyond this temperature the cenospheres has undergone self-sintering to become complex oxides the matrix also seizes to be metallic.
2. At very high temperatures beyond 650° in conventional sintering, the matrix is

transformed into a complex mixture of various alumino-silicates and high temperature oxides. Microwave sintering can be an adoptive & effective rapid sintering method for development of aluminium- cenospheres composites fabricated through powder metallurgy route at lower temperatures without undergoing oxidation.

3. The microwave sintered Aluminum Cenospheres metal matrix composite samples showed better physical and morphological properties when compared with the conventionally sintered ones.
4. The Microwave sintered samples showed decrease in Apparent Porosity by 44%, increase in Hardness by 17%, and increase in Bulk Density by about 30% compared to the conventionally sintered samples. The microwave sintering has also shown that the sintering takes place uniformly throughout the bulk of the material. The sintering process is rapid, has high heating rates, reduced processing times, uniform temperature throughout with minimal thermal gradients.

It is also concluded from the study that the sintering temperature of composite needs to be restricted to a temperature which is nearer to 665°C which is the melting temperature of pure aluminium, to obtain a pure metallic matrix composed of only aluminium without undergoing oxidation. The XRD also substantiates the finding that the matrix is of pure aluminium when sintered at the temperature of 665°C as done during experimentation. The morphology in terms of sphericity of the cenospheres is also intact and the shape is well retained at this temperature as seen from the SEM image. The physical properties measured on the composites sintered at this temperature also supports the finding that the properties are better and these properties ably contribute for the development of aluminium matrix composites embedded with cenospheres for use in engineering applications.

CHAPTER 6

RESULTS AND DISCUSSIONS ON PHYSICAL, MORPHOLOGICAL AND MICROSTRUCTURAL PROPERTIES

The aluminium-cenospheres pellets sintered in microwave and conventionally sintered at 665⁰C temperature have been evaluated for the phases by XRD analysis, morphological analysis by SEM and physical properties such as bulk density, water absorption and hardness (BHN).

6.1 Results and discussions on morphological and micro-structural analysis

The XRD pattern of the pure aluminium powder only taken for the matrix confirmed the presence of aluminium as can be seen from XRD peaks in Fig 6.1 and 6.2 when sintered at temperature of 665⁰C both in conventional and microwave sintering. The graphs showed the presence of aluminium confirming the metallic matrix and the composite has not undergone oxidation or presence of any oxide phase is seen. Even the process change has not brought about any new oxide formation or new phase formation.

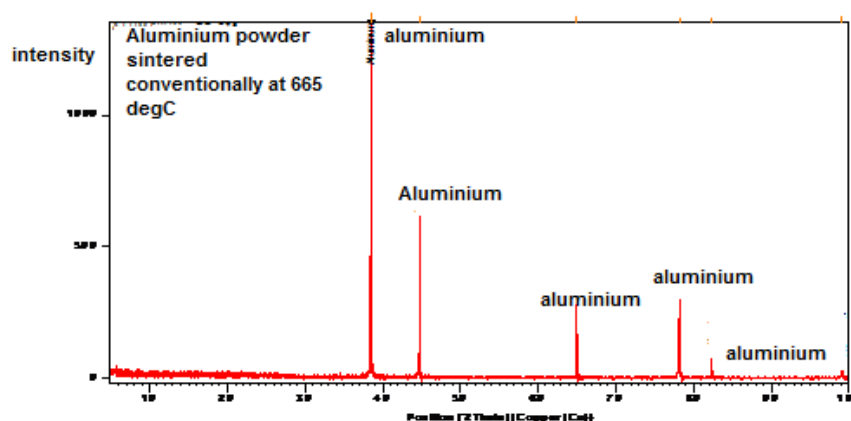


Fig.6.1: XRD of conventionally sintered aluminium powder at 665⁰C

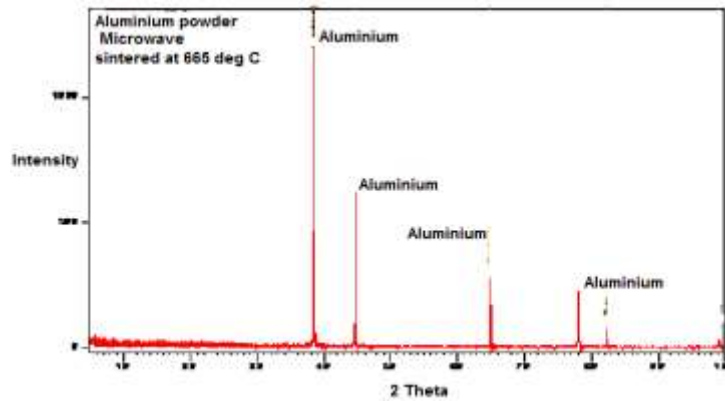


Fig.6.2: XRD of microwave sintered aluminium powder at 665⁰C

From the mineralogical data obtained from the XRD patterns shown at Fig.6.3 and 6.4. for the composites with cenospheres sintered at 665⁰C both in conventional and microwave sintering, it was seen that composites have more crystalline phases such as mullite and silicon along with metallic aluminium due to long and clear distinctive peaks in XRD.

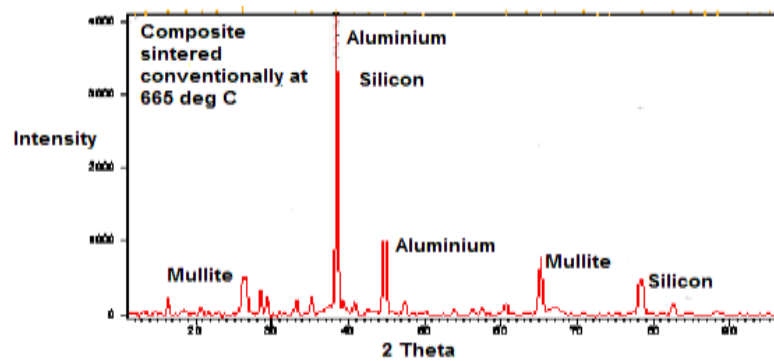


Fig.6.3: XRD of conventionally sintered composite at 665⁰C

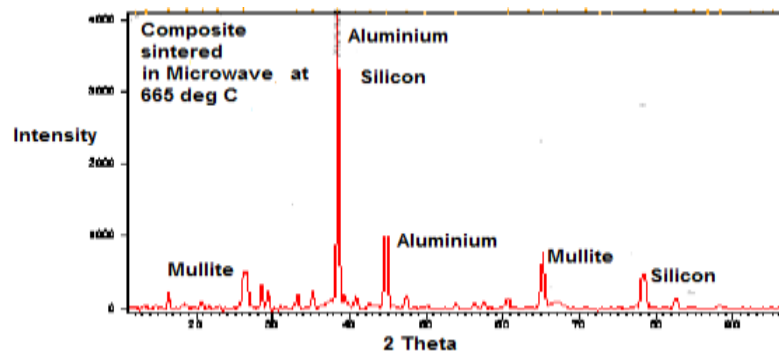
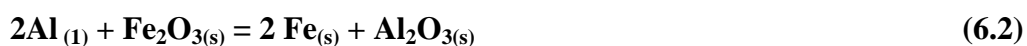
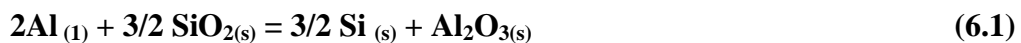


Fig.6.4: XRD of microwave sintered composite at 665⁰C

These crystalline phases mainly comprising of mullite is contributed from cenospheres. Cenospheres have these crystalline phases present in them inherently are seen present along with aluminium and silicon in the matrix as seen from the XRD graphs at Fig. 6.3 and 6.4.. The above phases were present in the raw cenospheres prior to sintering also.

Mullite is an extremely valuable mineralogical phase in cenospheres that withstands high temperatures, corrosive environments, or other adverse conditions. It has low coefficient of thermal expansion, good thermal and electrical insulation capacity and has outstanding load-bearing properties at high temperatures and aids development of refractory and ceramic products. The aluminium in the matrix remained in metallic form without the formation of aluminium oxide at this temperature of 665⁰C. These results are encouraging since the aim of this study was to retain the metallic structure of the aluminium in the matrix without giving room for the formation of aluminium oxide [Mahnicka L 2012]. But it is observed that as the cenospheres content was incorporated into the composite matrix, the intensity of the aluminium peak is also getting reduced as evident from the XRD patterns.

Sudharshan et al. [2008] has reported that there is a possibility of chemical reaction between aluminum melt and fly ash cenospheres particles. As cenospheres consists of predominantly silica, alumina and iron oxide, a chemical reduction reaction is taking place with these oxides when they come in contact with the melt. The silicon and iron diffuses into the pure aluminium melt and react to form Al-Si eutectic and Al₅FeSi phase which precipitates during solidification of the melt. The reactions are as follows:



The Gibb's Free Energy change (ΔG^0) and Heat (ΔH^0) for the above chemical reaction for the molten aluminium and SiO₂ is -312 683 J mol⁻¹ and -372 260 J mol⁻¹ and aluminium and Fe₂O₃ are -797 295 J mol⁻¹ and -857 678 J mol⁻¹ respectively at

700⁰C. [Guo R Q et al 1998]. The matrix continues to be aluminum with eutectic aluminum silicon phase formed by reduction reaction alloying with the matrix.

The microstructure at Fig.6.5 depicts a single cenospheres revealing the morphological change that has occurred when it is sintered at 665⁰C. At the interface of cenospheres and aluminium it is observed that there is an interfacial reaction both oxidation and reduction reactions occurring, thereby leading to formation of eutectics which melt at a lower temperature. This reaction not only has changed the morphology of the cenospheres but also has contributed to porosity and segregation. However at some portions clusters of aluminum melt with ruptured cenospheres is also observed with pores open to the surface, thereby contributing to increase in porosity.

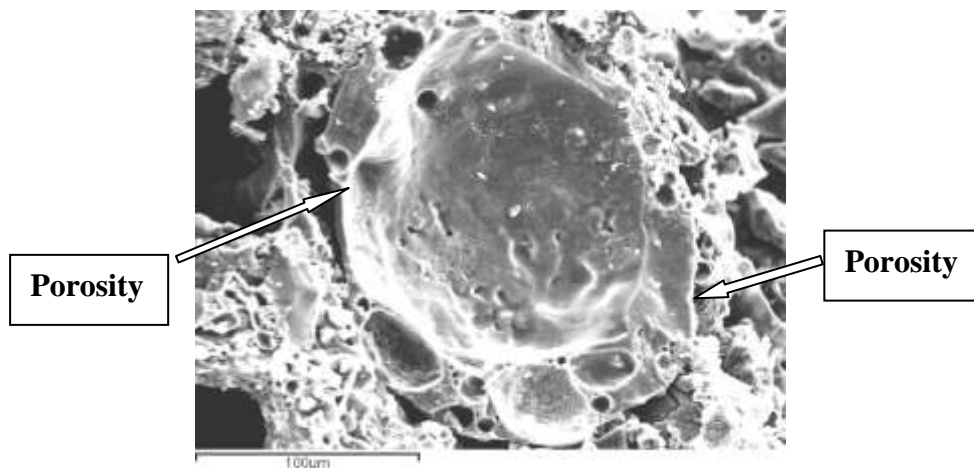


Fig.6.5: Microstructure of aluminium cenospheres interface at 665⁰C

The microstructure at Fig.6.6 of the sintered composite reveals uniform dispersion of cenospheres in the aluminum matrix. There is no segregation of the cenospheres in the matrix and dispersion is achieved from homogeneously mixing the composition material. Controlled temperature also aids homogeneity in the mix since if the fluidity of the aluminium melt is high, there is a possibility of segregation of the liquid phase which is the aluminium at that temperature and the solid phase being the cenospheres, both have different densities thereby leading to segregation and random dispersion of the solid phase which alters the properties of the final product in terms of mechanical, tribological, thermal properties etc., However at some portions clusters of aluminum melt with ruptured cenospheres is observed with pores open to the

surface, which is also one of the factors contributing to increased porosity in the composite.

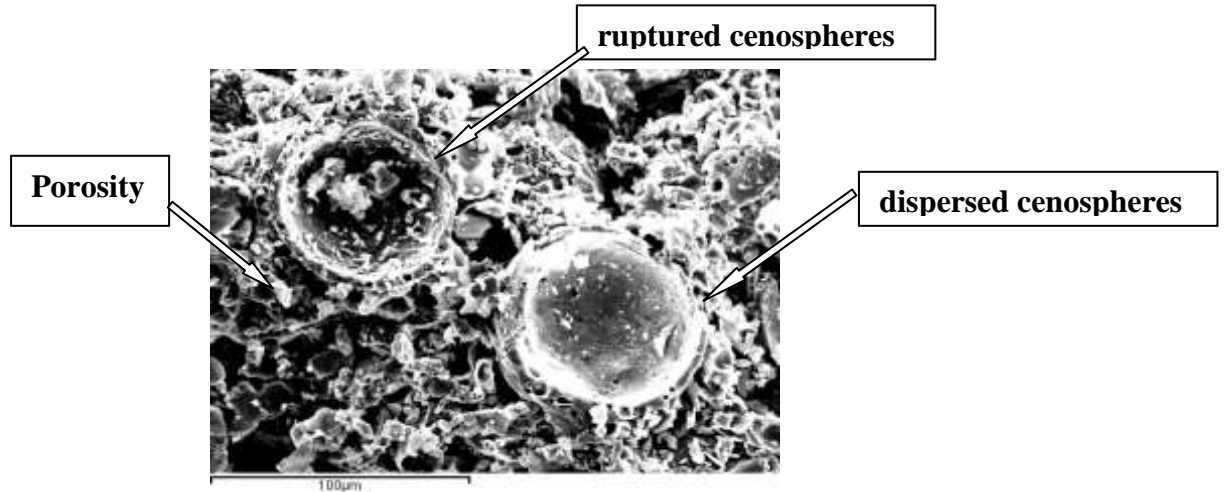


Fig.6.6: Dispersed cenospheres seen in aluminium matrix in microwave sintered composite at 665^oC

6.2 Physical Properties evaluation

The samples have been evaluated for physical properties for bulk density, water absorption and porosity using Archimedes principle.

6.2.1 Bulk Density measurements

It can be seen from the Table 6.1 that bulk density value for the pure aluminium composites without cenospheres addition was 2.15 and 2.2 g/cc for the conventional (C) and microwave sintered (M) samples designated as 1C and 1M respectively. Microwave sintered samples show bulk density value higher by about 2.3 % compared to conventionally sintered one.

As the cenospheres content was increased from 0 to 10, 20, 30, 40 and 50 vol. %, the bulk density of the composites decreased proportionally. But the bulk density value was on the higher side for all the microwave sintered samples compared conventionally sintered ones which varies from 2.1 to 2.7 %..

The decreasing trend in the bulk density values proportionally to the increase in cenospheres content can be seen in the Fig.6.7. The microwave sintered samples

exhibiting increased values in the bulk density compared to conventionally sintered samples which can also be seen from the figure.

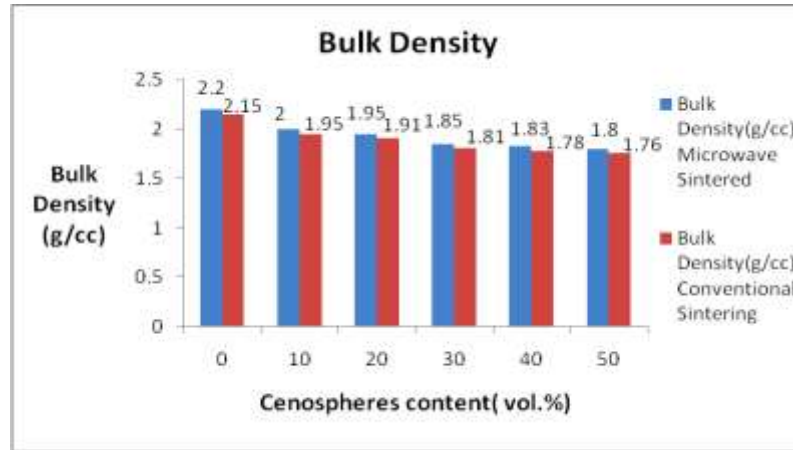


Fig. 6.7: Bulk Density (g/cc) graph of samples

6.2.2 Water Absorption evaluation

It can be seen from the Table 6.2 that water absorption (%) value for the pure aluminium composites without cenospheres addition were 17.48 and 14.78 % for the 1C and 1M samples respectively. Microwave sintered samples showed lesser water absorption value by about 18.2 % compared to conventionally sintered one.

As the cenospheres content was increased from 0 to 10, 20, 30, 40 and 50 vol. %, the water absorption of the composites increased proportionally. But the water absorption values were on the lower side for all the microwave sintered samples compared conventionally sintered ones, which varied from 12.2 to 13.6%..

The increasing trend in the water absorption values proportionally to the increase in cenospheres content can be seen in the Fig.6.8. The microwave sintered samples exhibiting decreased values in the water absorption compared to conventionally sintered samples which can also be seen from the figure.

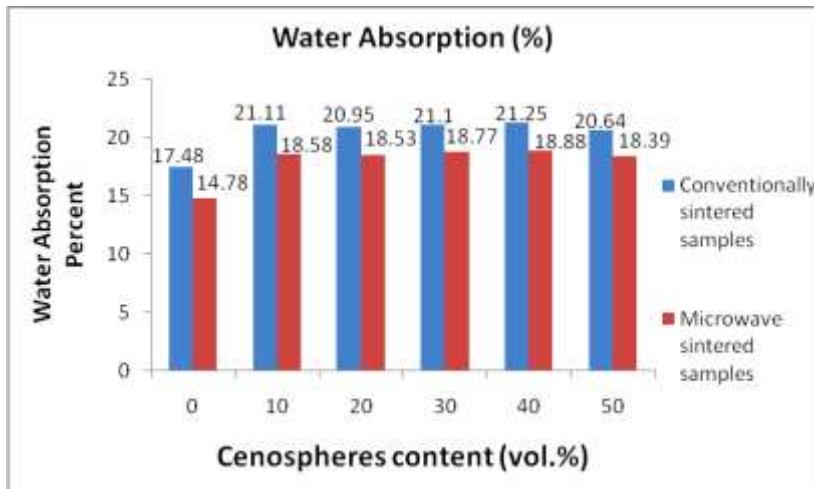


Fig. 6.8: Water Absorption (%) values of samples

6.2.3 Porosity evaluation

It can be seen from the Table 6.3 that Porosity (%) value for the pure aluminium composites without cenospheres addition were 30.49 and 26.38 % for the 1C and 1M designated samples respectively. Microwave sintered samples showed lesser porosity value by about 15.6 % compared to conventionally sintered one.

As the cenospheres content was increased from 0 to 10, 20, 30, 40 and 50 vol. %, the porosity value of the composites increased proportionally. But the porosity values were on the lower side for all the microwave sintered samples compared conventionally sintered ones which varied from 18.6 to 23.1%.

The increasing trend in the porosity (%) values proportionally to the increase in cenospheres content can be seen in the Fig.5.3. The microwave sintered samples exhibiting decreased values in the porosity (%) compared to conventionally sintered samples which can also be seen from the Fig. 6.9.

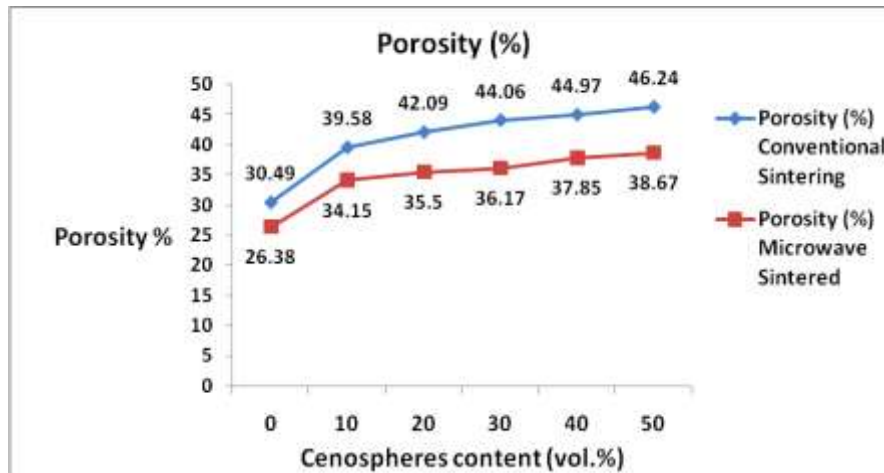


Fig. 6.9: Porosity (%) values of samples

The porosity of the composites seems to increase with the increase in volume % of cenospheres. The physical properties such as bulk density, water absorption and porosity of the composites decide the other properties of such as mechanical strength, thermal insulation, electrical properties and tribological characteristics.

6.3 Discussions on physical morphological and micro-structural properties

It is observed from the experimental results that as the cenospheres content increased in the composites, the porosity increased, bulk density decreased and water absorption increased. With the increase in cenospheres content which is hollow and porous, more hollow space is getting introduced in the reinforcement and also in the bulk of the material. Increasing the hollow space area in the bulk of the material increased the hollow space volume, subsequently altering the properties of the composite in terms of density, water absorption and hardness. The cenospheres size fraction is comparatively more compared to the aluminium particle size. The increased cenospheres content also decreased the surface contact area in between the particles of the matrix material and the reinforcement due to its hollow and empty space [M Kok 2005].

The cenospheres primarily contains alumino-silicate phases and are not subjected to any phase transformation up to 900⁰C. Hence these are suitable for making cenospheres filled aluminum SF. It is further noted that the cenospheres are almost

spherical in nature and some of the cenospheres are associated with tiny cenospheres on their surfaces. The shells of the cenospheres are porous in nature. The porosity level in the cenospheres shell is around 10%. The cenospheres retain their shape and size during mechanical stirring and thus effectively could be used for making cenospheres filled aluminum SF using stir-casting technique. [D.P. Mondal et al 2009]

In the present study liquid phase sintering has been employed in which the aluminium having melting point of 662°C is in the liquid form at the temperature of 665°C in which all composites have been sintered in the present study. The essential requirement during sintering is the wetting of the reinforcement i.e. cenospheres by the aluminium in the liquid phase. At higher concentration of aluminium matrix material and lower concentrations of cenospheres reinforcement in the composite in terms of vol. % as seen in 2C and 2M composites, the aluminium metal in liquid state is quite sufficient to hold the cenospheres in the matrix and impart good properties in terms of increased bulk density, hardness, lower porosity and water absorption properties in addition to decreased wear and erosion behavior accompanied by good flexural and compressive strengths. As the cenospheres content started to increase in compositions 3C and 3M samples onwards up to 6C and 6M samples, the aluminium melt is not sufficient to hold the cenospheres in the matrix and properties of the composites are altered.

High melting point, ionic or covalent bonded materials such as cenospheres which are ceramic in nature have a high concentration of metallic oxides in the bulk of its composition and they are generally poorly wetted by liquid metals, except at high temperatures. It is therefore apparent that these cenospheres act as barrier to aluminium wetting during sintering. At high concentrations of cenospheres in the composite, this phenomenon is still more pronounced. Even aluminium metal also has a very thin layer of oxide on its surface which is a barrier and needs to be disrupted or removed. For aluminium at 600°C , a $\text{PO}_2 < 10^{-50}$ atmospheres is required to reduce aluminium into oxide.

G B Schaffer opines that based on an understanding of fundamental liquid phase sintering phenomena it is possible to define certain ideal phase diagram characteristics. The key features of an ideal liquid phase sintering system report that:

- A) The reinforcement should have a lower melting point than the matrix base or an alternative is a low melting point eutectic formation during sintering, which is less advantageous because liquid formation does not occur spontaneously on heating.

Observation: In the present study undertaken, the cenospheres reinforcement used has high melting point up to 1500°C compared to the matrix aluminium which is 662°C . There are no indications of lower melting eutectic formation at the sintering temperature of 665°C when the sintered composite was examined for phases by XRD. The phases observed by XRD are sillimanite, mullite and alumina which are the major phases have high melting points and the concentration of the same increases with increase in the cenospheres vol %. Since the system under study does not satisfy the point A of an ideal phase diagram characteristic, the composite structure is a poor structure leading to decrease in the certain properties such a hardness, wear and erosion properties and mechanical strength of the composites when there is an increasing in the loading of cenospheres from 10 to 50 % in the compositions that were studied.

- B) The solubility of the reinforcement in the base should be low because this ensures that the reinforcement remains segregated to particle boundaries and maximizes the liquid volume.

Observation In the present study from the SEM image it is seen that the solubility of cenospheres reinforcement is very low in the matrix since cenospheres are seen well dispersed in the matrix and no segregation of the same to particle boundary is observed. The liquid volume of aluminium metal is high in composition having lower cenospheres content, but as the concentration of cenospheres vol. % is increased, the wetting of the same by

aluminium melt is not effective. This again leads to the poor structure leading to decrease in the certain properties such a hardness, wear and erosion properties and mechanical strength of the composites when cenospheres are loaded from 10 to 50 % in the compositions.

- C) While the matrix should be soluble in the liquid, it is not necessary for the matrix to be soluble in the solid reinforcement. Completely miscible liquids ensure that mass transport is not constrained.

Observation In the present study it is seen that the matrix is in the liquid state at the time of sintering. The matrix being soluble in the solid reinforcement is not observed from the microstructure. There is no complete miscibility between the aluminium liquid matrix and the solid cenospheres reinforcement. The mass transport is constrained at the higher concentrations of cenospheres again leading to the poor structure and decreased properties such a hardness, wear and erosion properties and mechanical strength of the composites when cenospheres are loaded from 10 to 50 % in the compositions.

- D) In addition, the base matrix should also have a high diffusivity in the liquid. This ensures high rates of mass transport and therefore rapid sintering.

Observation In the present study it is seen that the matrix has limited diffusivity state at the time of sintering. This is confirmed by the SEM image which shows the cenospheres well dispersed in the matrix. High rates of mass transport and rapid sintering is possible in microwave sintered samples rather than the conventionally sintered ones as can be seen from the improved properties in the microwave sintered ones even in compositions having cenospheres loaded from 10 to 50 vol.%.

The cenospheres which are also inert create a hydrostatic tensile stress in the matrix which opposes the sintering stress. In the aluminium matrix, cenospheres act as rigid inclusions and these inclusions move towards each other. Each inclusion therefore

experiences a force due to the presence of the other inclusions and closer the particles, the greater the force. The matrix between the inclusions is therefore under compression and faster than average densification occurs between particles which are separated by a gap smaller than the average, i.e. there is a critical separation distance which is equal to the average separation distance. When a summation is carried out over many particles, the composite will densify at a slower rate than an unreinforced matrix. The regions between closely spaced inclusions, which densify at a rate greater than the average, increase in strength relative to the un-sintered regions. A tensile stress therefore develops in the remaining porous regions, which are also constrained from sintering by the newly sintered regions. This causes de-sintering and crack-like void formation which is the cause in the conventionally sintered samples to exhibit properties that are inferior than the microwave sintered samples [Maksim Antonov 2006].

Morteza Oghbaei et al [2010] has reported that microwave sintering effectively assist the forward diffusion of ions which accelerates the sintering. This results in matrix densification by grain growth process. Sintering process aids re-crystallization, grain growth and densification at high temperatures in the body that is being sintered. This densification mechanism is strongly dependent on diffusion of ions between the same sample particles. The mechanism of grain growth rate is assisted by the grain boundary diffusion process. It has been found that intense microwave field concentration is active around the particles of the sample while sintering. The power of this microwave field between the particles of the sample in the bulk of the material is about 30 times higher than the external field and this is sufficient to ionize the sample particles at its surface. This accelerates ionic diffusion which promotes rapid densification of the material is promoted under microwave sintering.

Apart from the microwave radiation, the surrounding electromagnetic field also effectively enhances the ionic diffusion kinetics near the grain boundaries. The kinetic energy of the ions at the grain boundary increases which thereby decrease the activation energy required for the forward ion jump and in the process increases the

barrier height for the reverse jump. This mechanism promotes forward diffusion of the inter grain ions which accelerates the grain growth during sintering.

By microwave sintering all the properties of a given material are enhanced by its microstructural development in which the densification of the material and coarsening occurs rapidly and effectively throughout the bulk of the material. The micro structural development depends on the parameters such as optimized temperature, sintering time, heating rate and the pressure. The rapid heating rate achieved by microwave heating is the key to produce products with a high sintered density for a given microstructure and grain size compared to slow heating for the same sintered density by conventional heating. Since microwave sintering is a non-contact sintering technique, the heat gets transferred to the product through electromagnetic radiation. By microwave sintering large amount of heat can be transferred to the material's interior which reduces differential sintering to a large extent. Hence the microwave sintered products have finer micro-structural development, with uniform grain growth and grain size distribution coupled with higher densification of the product thereby leading to enhanced engineering properties.

Hence it is concluded from this study that the composites exhibit good properties only at a certain vol. % of cenospheres are present in the matrix. Most of the physical and mechanical properties decrease proportionally to increase in the cenospheres content. The mix design needs to be properly selected to fabricate composites with required properties for use in applications.

CHAPTER 7

RESULTS AND DISCUSSIONS ON THE TRIBOLOGICAL PROPERTIES

7.1. Jet Erosion Study

The sintered samples were subjected to particle Jet Erosion test to assess the erosion resistance properties of the composites as per ASTM G76-04 standard using silica particles impingement using gas jets. The erosion tests were conducted at angles of 30, 45, 60 and 90 deg for 15 minute duration each. The photographs of the eroded samples of various compositions that were conventionally sintered is shown in Fig. 7.1 and the microwave sintered samples are shown in Fig.7.2.



Fig. 7.1: Erosion test samples of conventionally sintered samples



Fig. 7.2: Erosion test samples of microwave sintered samples

It is seen from the photographs at Fig.7.1 and 7.2 that the erosion loss of the samples increases with increase in cenospheres content both in microwave (1M to 6M) as well conventionally sintered samples (1C to 6C). The erosion loss of microwave sintered

samples is much less at all impact angles compared to conventionally sintered samples. Among M1 to M6 samples, M1 has exhibited lower erosion loss compared to M6. Similarly, for the conventionally sintered samples C1 to C6, it is observed that C1 shows the least erosion loss compared to C6.

7.1.1 Jet Erosion Study of 1C and 1M composite samples

The graph at Fig.7.3 depicts the erosion loss of the samples pertaining to only aluminium samples 1C and 1M carried out at angles of 30°, 45°, 60° and 90°. The erosion loss is almost in the same level at all the angles of erosion to which the sample has been subjected. The conventionally sintered 1C sample showed more erosion loss compared to the microwave sintered 1M sample. The erosion loss is slightly lower at the angle of 90° for both the samples. The erosion loss varied from high as 0.01g to low as 0.009g for the conventionally sintered sample and high as 0.0085g to low as 0.0074g for the microwave sintered samples.

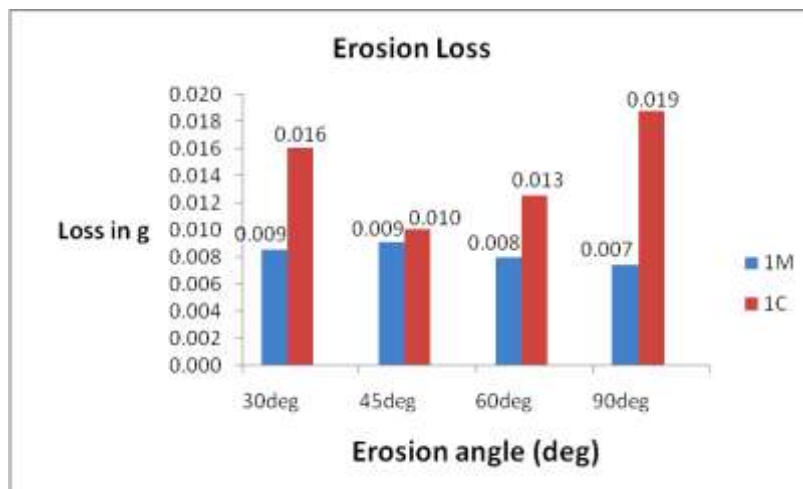


Fig. 7.3: Erosion loss comparison of 1C and 1M samples

7.1.2 Jet Erosion Study of 2C and 2M composite samples

The graph at Fig.7.4 depicts the erosion loss of the samples pertaining to aluminium cenospheres samples 2C and 2M carried out at angles of 30°, 45°, 60° and 90°. The erosion loss is high at the angle of 30° and low at the angle of 60° for both the samples. The conventionally sintered 2C sample showed more erosion loss as compared to the microwave sintered 2M sample. The erosion loss varied from high as 0.1095g to low

as 0.0443g for the conventionally sintered sample and 0.0806g to 0.0356g for the microwave sintered samples.

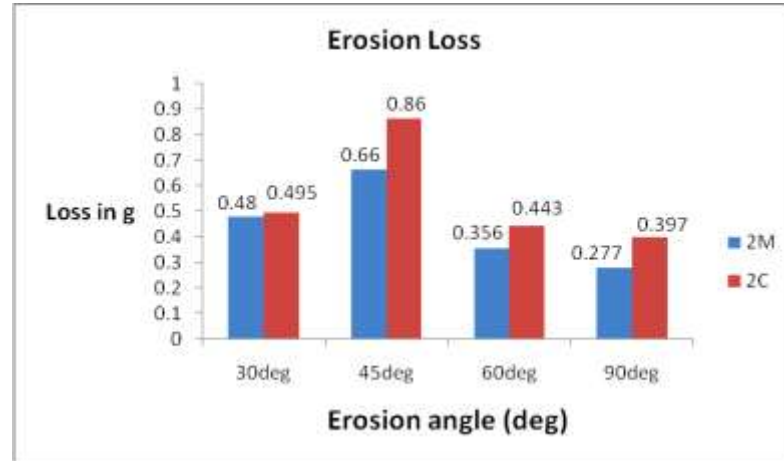


Fig. 7.4: Erosion loss comparison of 2C and 2M samples

7.1.3 Jet Erosion Study of 3C and 3M composite samples

The graph at Fig.7.5 depicts the erosion loss of the samples pertaining to aluminium cenospheres samples 3C and 3M carried out at angles of 30°, 45°, 60° and 90°. The erosion loss is high at the angle of 30° and low at the angle of 90° for both the samples. The conventionally sintered 3C sample showed more erosion loss as compared to the microwave sintered 3M sample. The erosion loss varied from high as 0.116g to low as 0.126g for the conventionally sintered sample and 0.151g to 0.0504g for the microwave sintered samples.

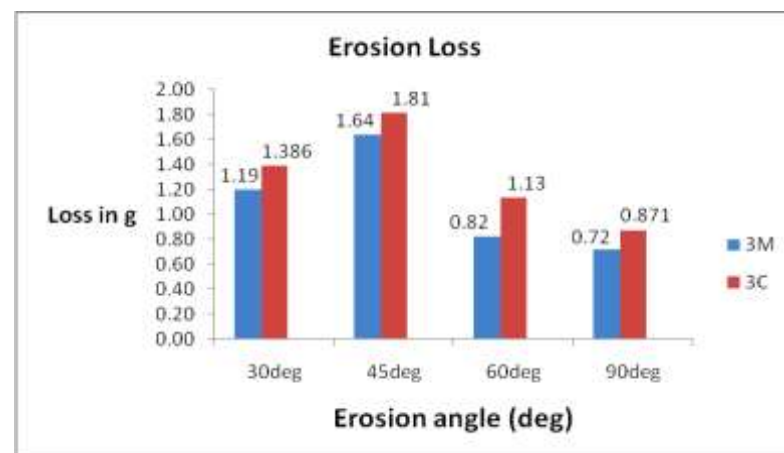


Fig. 7.5: Erosion loss comparison of 3C and 3M samples

7.1.4 Jet Erosion Study of 4C and 4M composite samples

The graph at Fig.7.6 depicts the erosion loss of the samples pertaining to aluminium cenospheres samples 4C and 4M carried out at angles of 30°, 45°, 60° and 90°. The erosion loss is high at the angle of 30° and low at the angle of 90° for both the samples. The conventionally sintered 4C sample showed more erosion loss as compared to the microwave sintered 4M sample. The erosion loss varied from high as 0.4g to low as 0.28g for the conventionally sintered sample and 0.4032g to 0.28g for the microwave sintered samples.

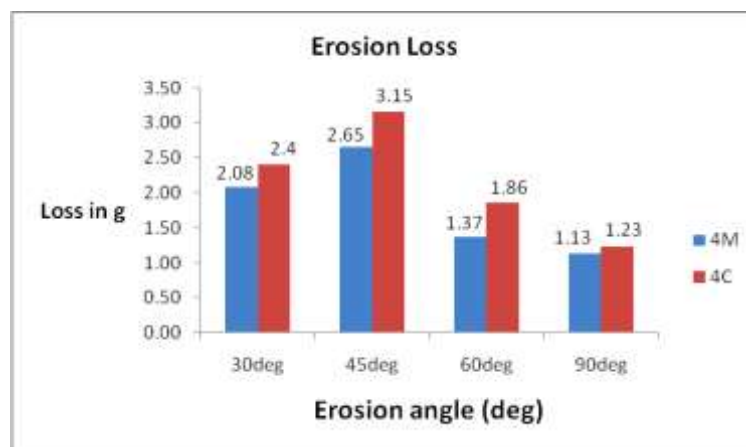


Fig. 7.6: Erosion loss comparison of 4C and 4M samples

7.1.5 Jet Erosion Study of 5C and 5M composite samples

The graph at Fig.7.7 depicts the erosion loss of the samples pertaining to aluminium cenospheres samples 5C and 5M carried out at angles of 30°, 45°, 60° and 90°. The erosion loss is high at the angle of 30° and low at the angle of 90° for both the samples. The conventionally sintered 5C sample showed more erosion loss as compared to the microwave sintered 5M sample. The erosion loss varied from high as 0.4783g to low as 0.1121g for the conventionally sintered sample and 0.4032g to 0.28g for the microwave sintered samples.

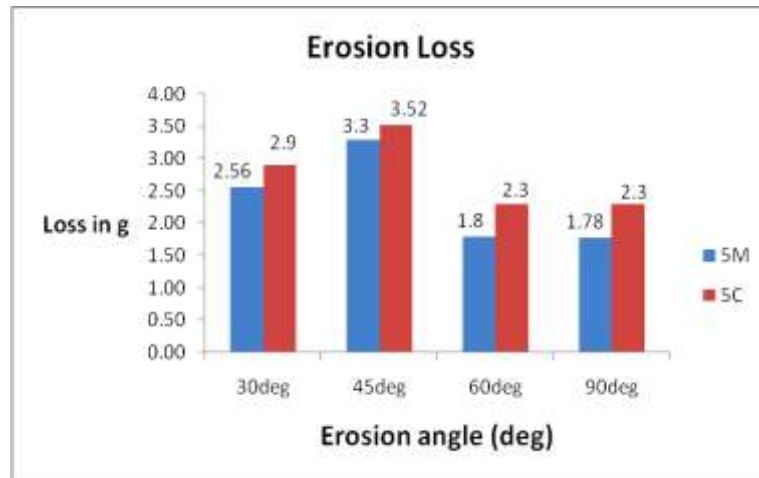


Fig. 7.7: Erosion loss comparison of 5C and 5M samples

7.1.6 Jet Erosion Study of 6C and 6M composite samples

The graph at Fig.7.8 depicts the erosion loss of the samples pertaining to aluminium cenospheres samples 6C and 6M carried out at angles of 30°, 45°, 60° and 90°. The erosion loss is high at the angle of 60° and low at the angle of 30° for both the samples. The conventionally sintered 6C sample showed more erosion loss as compared to the microwave sintered 6M sample. The erosion loss varied from high as 1.72g to low as 1.54g for the conventionally sintered sample and 0.4032g to 0.28g for the microwave sintered samples.

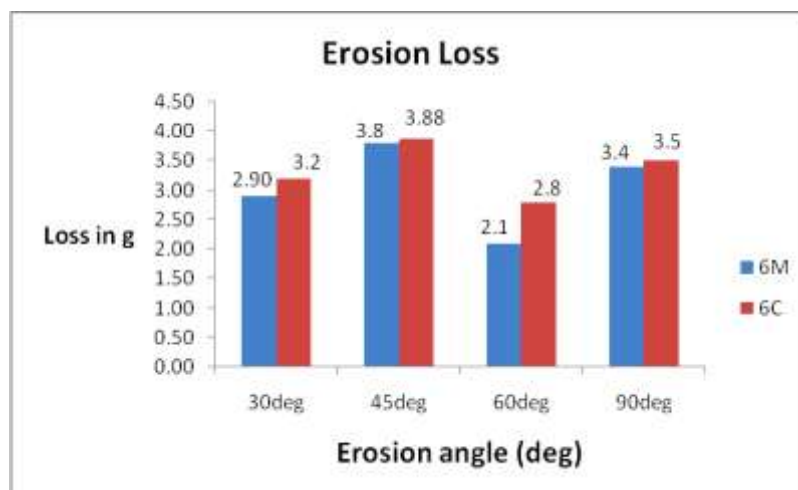


Fig. 7.8: Erosion loss comparison of 6C and 6M samples

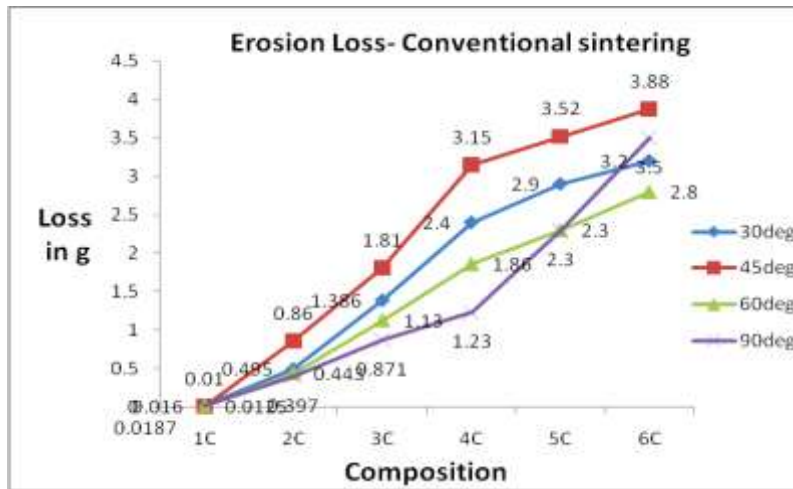


Fig. 7.9: Erosion Loss of conventionally sintered samples at 30°, 45°, 60° and 90° angles

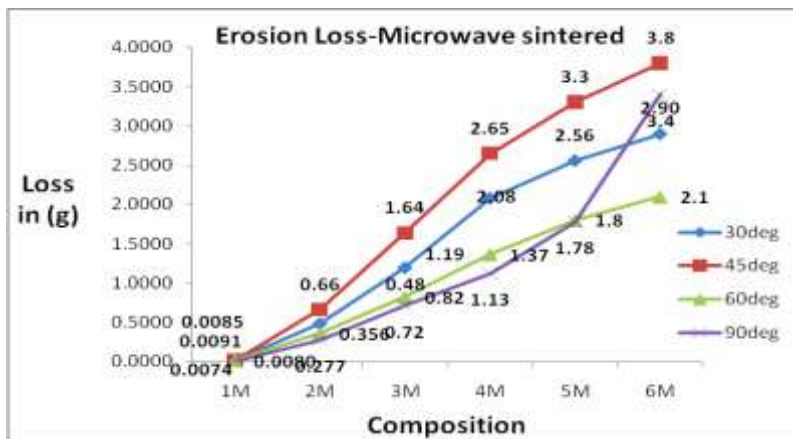


Fig. 7.10: Erosion Loss of microwave sintered samples at 30°, 45°, 60° and 90° Angles

7.2 Dry Sliding Wear behavior

The composite samples were subjected to wear behavior test using pin on disc machine against 62 HRC hardened alloy steel having surface roughness of 10 μm, for a sliding distance of 6000m with varying loads of 1, 2 and 3kg and the weight losses were recorded. The scanning electron microscopy technique was employed for microscopic examination of the worn surfaces and subsurface sections of wear surfaces to assess the type of wear mechanism prevailing in the worn samples. The SEM micrograph for the samples tested at 3kg load only and which had higher amount of wear loss was chosen for study to assess the wear behavior for the samples of all compositions sintered in both the sintering modes.

The slide wear data have been obtained for the conventionally sintered (1C to 6C) and microwave sintered samples (1M to 6M) and the slide wear data for each composition has been evaluated at loads of 1, 2 and 3kg.

7.2.1 Dry Sliding Wear behavior study of 1C and 1M composite samples

The graph at Fig 7.11 shows the wear loss behavior of the 1C and 1M samples which are composed of pure aluminium and without cenospheres addition and the samples sintered in conventional and microwave sintering routes respectively. It can be seen from the figure that weight loss of both the samples are low at 1 kg load and which progressively increases when the load is also increased to 2 kg and maximum wear loss occurs at 3 kg loading. The conventionally sintered samples showed higher wear loss than the microwave sintered samples. The wear loss for the conventionally sintered sample was 0.02g at 1 kg load, 0.03g at 2 kg load and 0.19g at 3 kg loading whereas the microwave sintered sample exhibited wear loss of 0.01g at 1 kg load, 0.02g at 2 kg load and 0.14g at 3kg load which is comparatively less than the conventionally sintered sample which is about 50 % less at 1 kg, 33.3% less at 2 kg and 26.3% less at 3 kg load respectively.

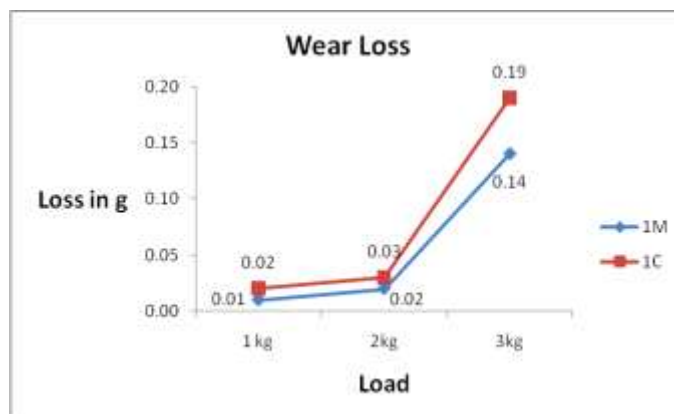


Fig. 7.11: Wear loss comparison of 1C and 1M samples at 1, 2 and 3kg load

The wear surface shown at Fig.7.12 and 7.13 is that of 1C and 1M composites which are comprised of pure aluminium only without cenospheres and the sample sintered conventionally and in microwave respectively. The wear surface shown is that of samples tested for sliding wear at 3 kg load. The samples surface shows striations

which are a series of ridges and linear marks on the worn out surface when seen at a magnification of 100 X.

The worn out surface of the material reveals material flow in the direction of rotation of the disc on to which the sample was in contact during the test. The aluminium metal matrix has plastically deformed and the wear debris is seen accumulated on the banks of the striations. The striations or wear tracks are seen running parallel to each other in the direction of disc rotation. The wear type appears to be ‘adhesive wear’ which has been caused by the sample and the disc both moving in relative motion to each other, which has caused plastic deformation of the matrix and the debris of the material are pulled out from the bulk and transferred on to the surface. The amount of debris flow is very much pronounced for the conventionally sintered samples compared to microwave sintered samples as seen from the microstructures.

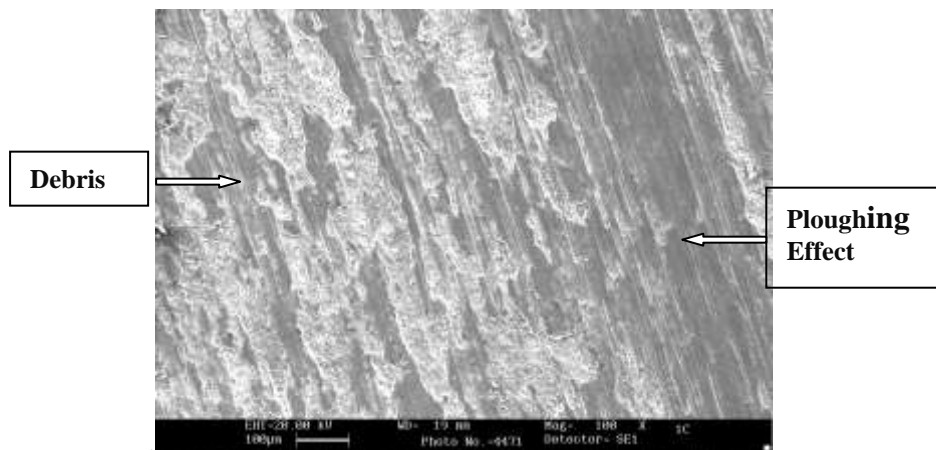


Fig. 7.12: Wear surface of conventionally sintered 1C at 3kg load (100X)

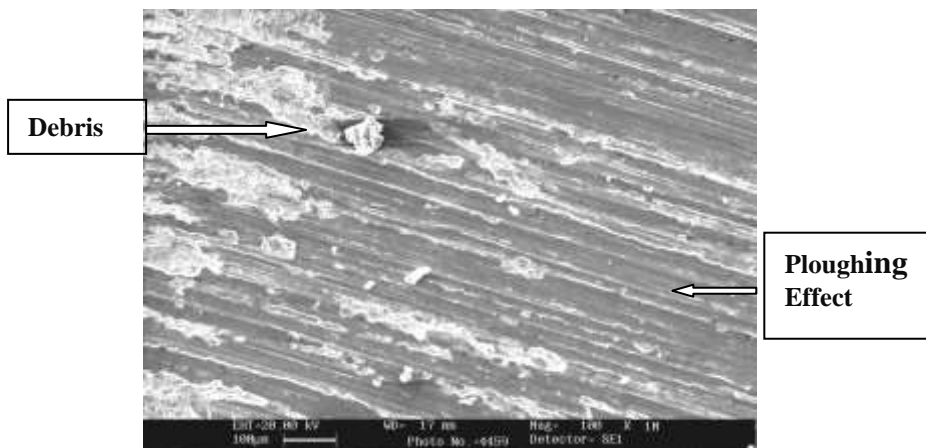


Fig. 7.13: Wear surface of microwave sintered 1M sample at 3kg load (100X)

7.2.2 Dry Sliding Wear behavior study of 2C and 2M composite samples

The graph at Fig.7.14 shows the wear loss behavior of the 2C and 2M samples which are composed of 90% aluminium and with 10% cenospheres and the samples have been sintered in conventional and microwave sintering routes respectively. It can be seen from the figure that weight loss of both the samples are low at 1 kg load and progressively increases when the load is also increased to 2 kg and maximum wear loss occurring at 3 kg load. The conventionally sintered samples showed higher wear loss than the microwave sintered samples for this composition too. The wear loss for the conventionally sintered sample was 0.17g at 1 kg load, 0.26g at 2 kg load and 0.52g at 3 kg loading whereas the microwave sintered sample exhibited wear loss of 0.08g at 1 kg load, 0.14g at 2 kg load and 0.32g at 3kg load which is less than the conventionally sintered sample which is less by about 52.9 % at 1 kg, 46.2 % at 2 kg and 38.5% less at 3 kg load respectively.

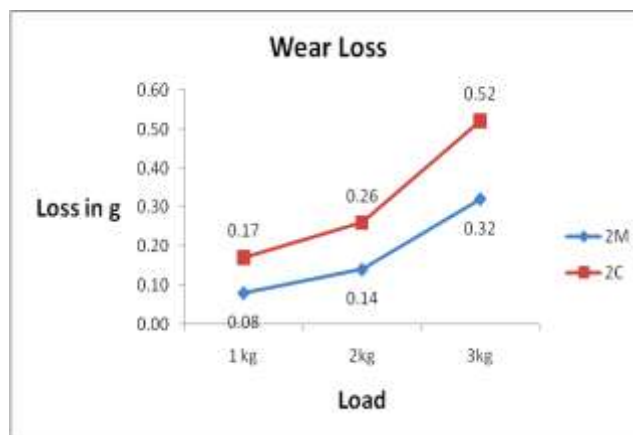


Fig. 7.14: Wear loss comparison of 2C and 2M samples at 1, 2 and 3kg load

The wear surface shown at Fig.7.15 and Fig. 7.16 shows surfaces of 2C and 2M composites which are comprised of 90 vol.% of aluminium and 10 vol.% of cenospheres and the samples sintered conventionally and in microwave respectively. Both the microstructures show series of ridges and linear marks on the worn out sample surface seen at a magnification of 100 X. The worn out surface of the material reveals material flow in the direction of rotation of the disc on to which the sample was in contact during the test. Here too the aluminium metal matrix has

plastically deformed and the wear debris is seen accumulated on either sides of the striations. The striations marks are seen running parallel to each other in the direction of disc rotation and the wear type also appears to be ‘adhesive wear’ caused by the sample and the disc both moving in relative motion to each other. The matrix has also plastically deformed indicating metallic matrix and the debris of the material are pulled out from the bulk and deposited on to the surface. The amount of debris flow is more pronounced in the conventionally sintered samples compared to microwave sintered samples as seen from the microstructures.

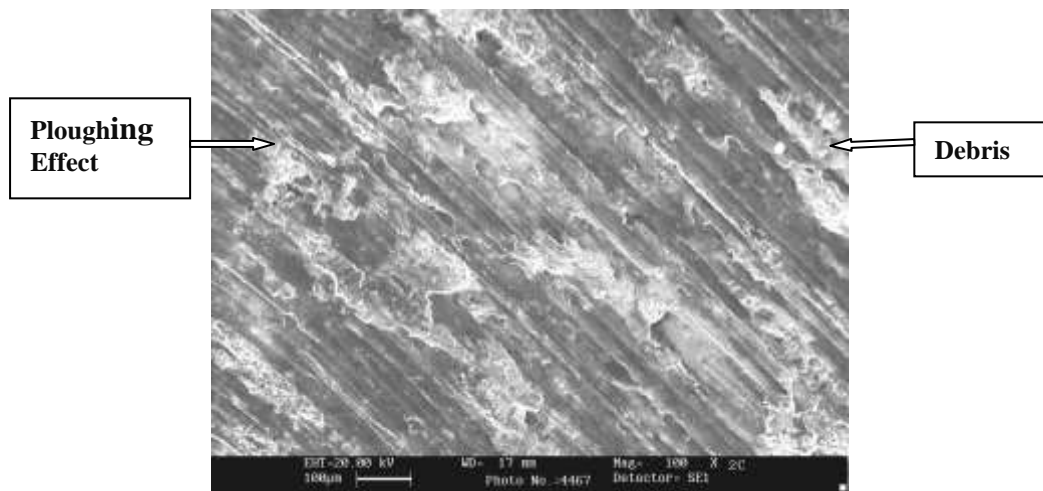


Fig. 7.15: Wear surface of 2C (10 vol.% cenospheres) sample at 100X

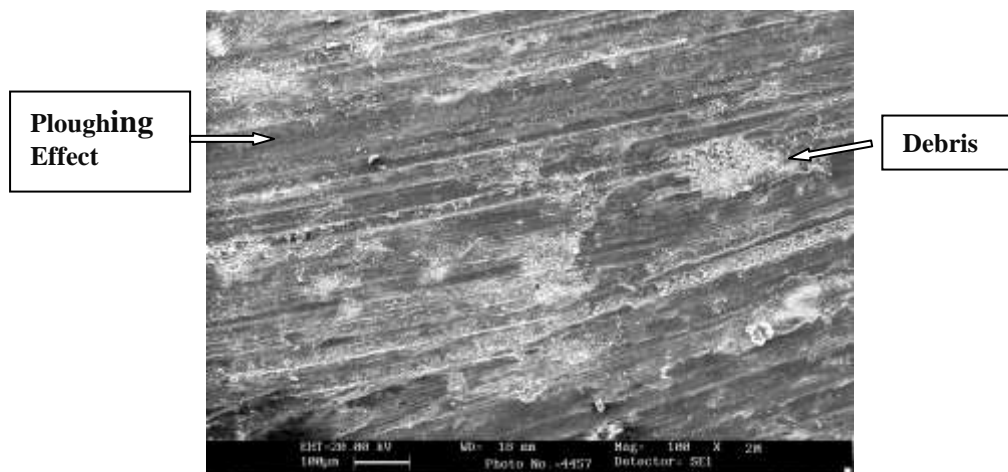


Fig. 7.16: Wear surface of 2M (10 vol.% cenospheres) sample at 100X

7.2.3 Dry Sliding Wear behavior study of 3C and 3M composite samples

The graph at Fig 7.17 depicts the wear loss behavior of the 3C and 3M samples which are composed of 80% aluminium and with 20% cenospheres and samples sintered in

conventional and microwave routes respectively. It can be seen that weight loss of both the samples are low at 1 kg load and are high at 2 kg and maximum at 3 kg load. The microwave sintered samples have lower wear rates for this composition too. The wear loss was 0.34g, 0.58g and 0.72g at 1, 2 and 3 kg loading respectively for the microwave sintered samples whereas the conventionally sintered sample exhibited wear loss of 0.42g at 1 kg load, 0.68g at 2 kg load and 0.98g at 3kg load which is higher than the microwave sintered sample by about 19.0 % at 1 kg, 14.7 % at 2 kg and 26.5% less at 3 kg load respectively.

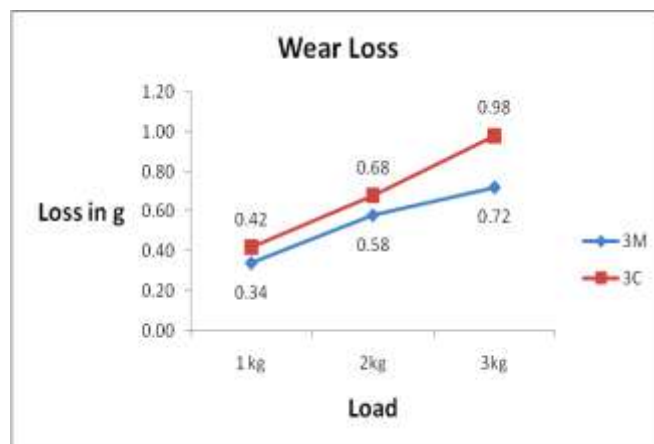


Fig. 7.17: Wear loss comparison of 3C and 3M samples at 1, 2 and 3kg load

7.2.4 Dry Sliding Wear behavior study of 4C and 4M composite samples

The wear loss behavior for the 4C and 4M samples are depicted in graphs at Fig 6.18 which are composed of 70% aluminium and with 30% cenospheres composites that are conventionally and microwave routes sintered respectively. The weight loss of both the samples is low at 1 kg load and maximum at 3 kg load. The wear loss was 0.55g, 0.81g and 1.3g at 1, 2 and 3 kg loading respectively for the microwave sintered samples which is less by about 23.6 % at 1 kg, 37.7 % at 2 kg and 27.8 % less at 3 kg load respectively compared to the conventionally sintered sample which exhibited wear loss of 0.72g at 1 kg load, 1.30g at 2 kg load and 1.8g at 3kg load.

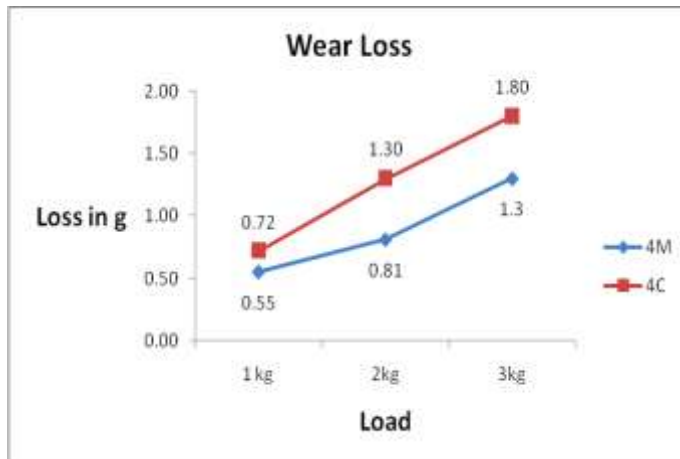


Fig. 7.18: Wear loss comparison of 4C and 4M samples at 1, 2 and 3kg load

The wear surface shown at Fig.7.19 and Fig. 7.20 pertains to the worn out surfaces of 4C and 4M composites which are comprised of 70 vol.% of aluminium and 30 vol.% of cenospheres and the samples sintered conventionally and in microwave respectively. Both the microstructures do not show ridges or linear marks on the worn out sample surface when seen at a magnification of 100 X.

The worn out surface of the material is quite different with surface appearing to have a combination of plastic and brittle nature of fracture. The wear surface shown reveals ruptured cenospheres pulled out from the matrix along with the matrix material. Here too the aluminium metal matrix has plastically deformed. The striations marks are less seen and the wear type also appears to be having a combination of both ‘adhesive’ wear and ‘abrasive’ type of wear. As more and more cenospheres gets loaded into the matrix, the material is becoming more ceramic in nature than metallic one. The structure is a combination of both metallic and ceramic phase. The matrix has plastically deformed and there appears to be metal flow caused due to localized heating due to wear action thereby indicating adhesive wear at the areas having more metallic phase and abrasive type of wear near the interface of metal and cenospheres. There are no indications of the debris of the material being pulled out from the bulk and deposited on the surface as in the case of pure metallic matrix. The microstructure in both the samples appear to be similar and have the same type of features.

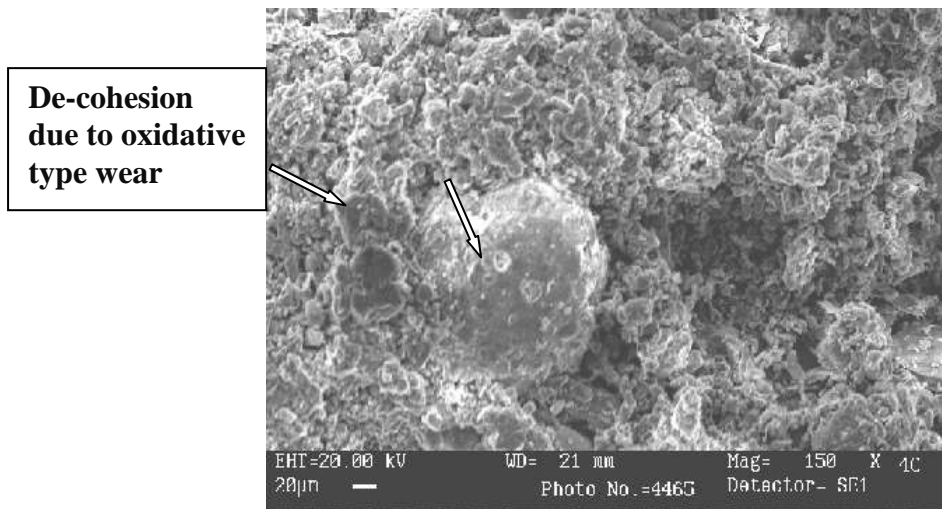


Fig. 7.19: Wear surface of 4C (30 vol.% cenospheres) sample at 150X

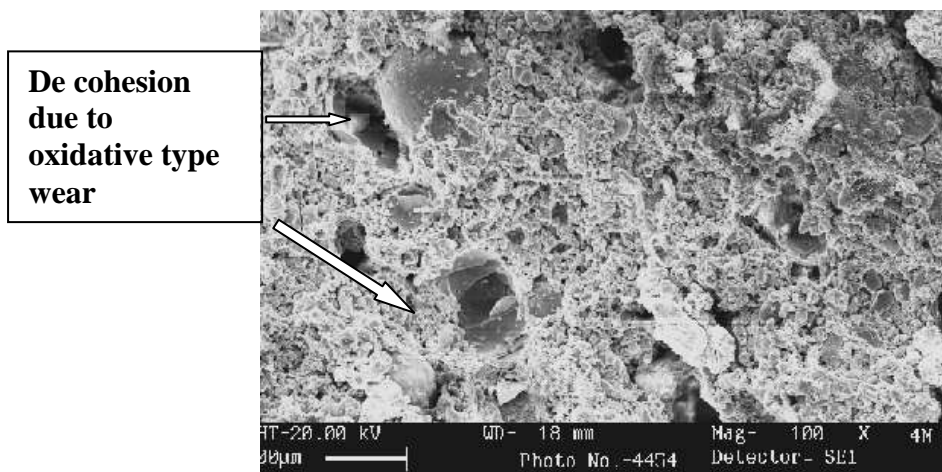


Fig. 7.20: Wear surface of 4M (30 vol.% cenospheres) sample at 100X

7.2.5 Dry Sliding Wear behavior study of 5C and 5M composite samples

The wear loss behavior for the 5C conventionally sintered sample and 5M microwave sintered sample are depicted in graphs in Fig 7.21 which are composed of 60% aluminium and with 40% cenospheres. The wear loss was 0.95g, 1.6g and 2.2g at 1, 2 and 3 kg loading respectively for the microwave sintered samples which is less by about 22.8 % at 1 kg, 15.8 % at 2 kg and 15.4 % less at 3 kg load respectively compared to the conventionally sintered sample which exhibited wear loss of 1.23 at 1 kg load, 1.90g at 2 kg load and 2.6 at 3kg load. The weight loss also seems to be

increasing proportionately in the samples with increase in volume percent of cenospheres content in the composites.

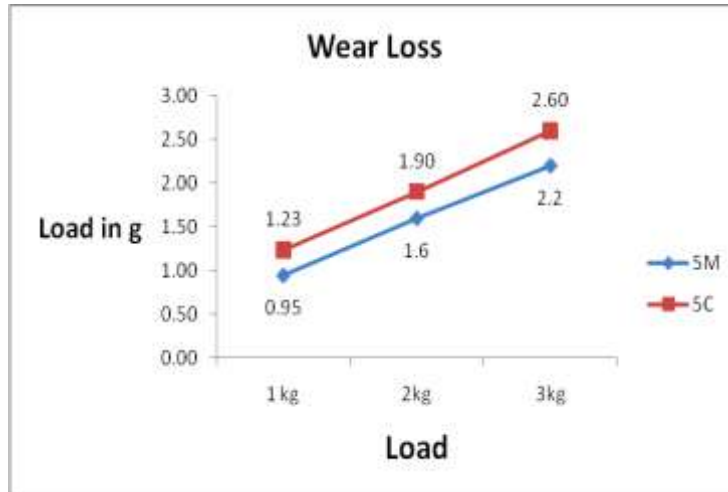


Fig. 7.21: Wear loss comparison of 5C and 5M samples at 1, 2 and 3kg load

The wear surface shown at Fig.7.22 and Fig. 7.23 is of the worn out surfaces of 5C and 5M composites which are comprised of 60 vol.% of aluminium and 40 vol.% of cenospheres and the samples sintered conventionally and in microwave respectively. Both the wear surface does not show any signs of ridges and or linear marks on the worn out sample surface seen at a magnification of 100 X.

The worn out surface of the material is appearing to have a combination of plastic and brittle nature of fracture but predominantly brittle fracture owing to increase cenospheres content. The wear surface also reveals ruptured cenospheres pulled out from the matrix. The aluminium metal matrix has plastically deformed and no striations marks are seen and the wear type also appears to be having a combination of both adhesive and abrasive type of wear. As more and more cenospheres is getting loaded into the matrix, the material is becoming more ceramic in nature but retaining the metallic matrix. The structure is a combination of both metallic and ceramic phase. The matrix has plastically deformed near the areas having more metallic phase showing adhesive wear and abrasive type of wear near the interface of metal and cenospheres. There are no indications of the debris of the material being pulled out from the bulk and deposited on the surface as in the case of pure metallic matrix. The

wear surface in both the samples appears to be similar and have the same type of features.

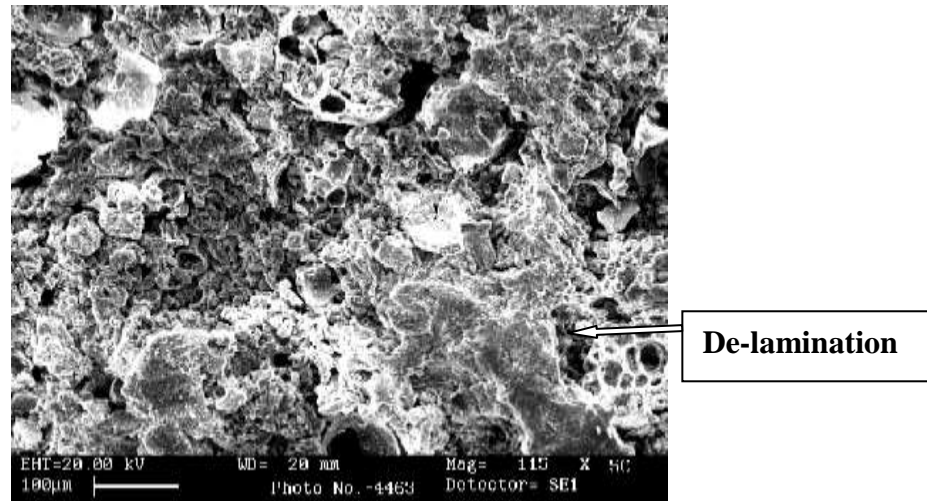


Fig. 7.22: Wear surface of 5C (40 vol.% cenospheres) sample at 115X

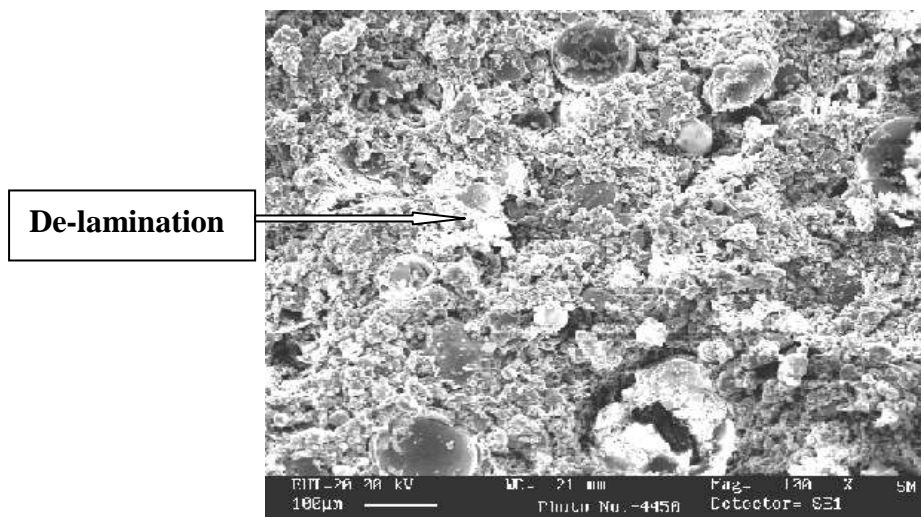


Fig. 7.23: Wear surface of 5M (40 vol.% cenospheres) sample at 100X

7.2.6 Dry Sliding Wear behavior study of 6C and 6M composite samples

The wear loss behavior for the 6C conventionally sintered sample and 6M microwave sintered sample are depicted in graphs at Fig 7.24 and the samples are composed of 50% aluminium and with 50% cenospheres. The wear loss was 1.15g, 2.3g and 2.9g at 1, 2 and 3 kg loading respectively for the microwave sintered samples which is less by about 45.5, 17.9 % and 12.1% less at 1, 2 and 3 kg load respectively compared to the conventionally sintered sample which exhibited higher wear loss of 2.11 at 1 kg, 2.8 at 2 kg and 3.3 g at 1, 2 and 3kg loads respectively. Here too the weight loss

seems to be increasing proportionately to the increase in volume percent cenospheres content in the composites.

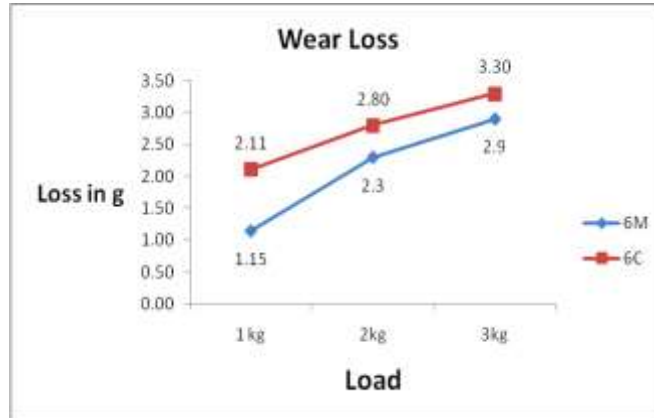


Fig. 7.24: Wear loss comparison of 6C and 6M samples at 1, 2 and 3kg load

7.2.7 Dry Sliding Wear behavior study of conventional and microwave sintered composite samples

The wear loss behavior of the conventionally sintered sample labeled 1C to 6C tested at loads of 1 kg, 2 kg and 3 kg is compared in the graph at Fig 6.25. It is observed from the graph that the wear loss is high for 6C sample at 3 kg load whereas the 6C samples tested at 1 kg load showed the least weight loss. The weight loss in g for the 1C, 2C, 3C, 4C, 5C and 6C samples was 0.02, 0.17, 0.42, 0.72, 1.23 and 2.11 g respectively for the test conducted at 1 kg load. The weight loss were 0.03, 0.26, 0.68, 1.30, 1.90 and 2.80 for the composites tested at 2 kg load and the weight loss were 0.19, 0.52, 0.98, 1.80, 2.60 and 3.30 g for the samples tested at 3 kg load respectively.

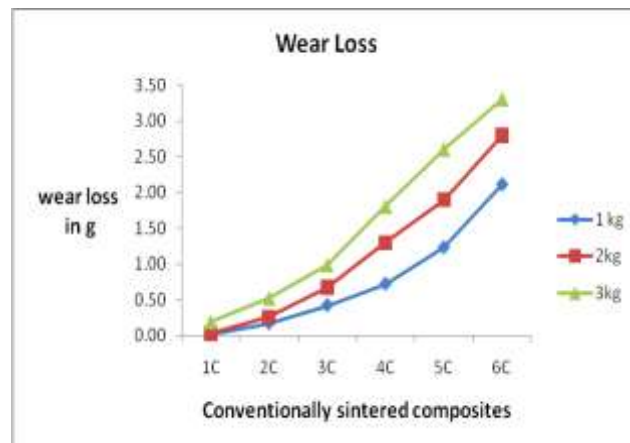


Fig. 7.25: Wear Loss of conventionally sintered sample at 1, 2 and 3 kg load

The wear loss behavior of the microwave sintered sample labeled 1M to 6M tested at loads of 1 kg, 2 kg and 3 kg is compared in the graph at Fig 7.26. It is observed from the graph that the wear loss is high for 6M sample at 3 kg load whereas the 6M samples tested at 1 kg load showed comparatively less wear loss. The wear loss in terms of weight in g for the 1M, 2M, 3M, 4M, 5M and 6M samples was 0.01, 0.08, 0.34, 0.55, 0.95 and 1.15 g respectively for the test conducted at 1 kg load. The weight loss was 0.02, 0.14, 0.58, 0.81, 1.60 and 2.30 for the composites tested at 2 kg load and the weight loss were 0.14, 0.32, 0.72, 1.30, 2.20 and 2.90 g for the samples tested at 3 kg load respectively.

A progressive increase in weight loss is observed for the both the conventionally and microwave sintered samples as the volume percent of cenospheres increased from 0 to 50. The sample appears to be more brittle than metallic with the increase in the ceramic phase by addition of cenospheres in both types of samples.

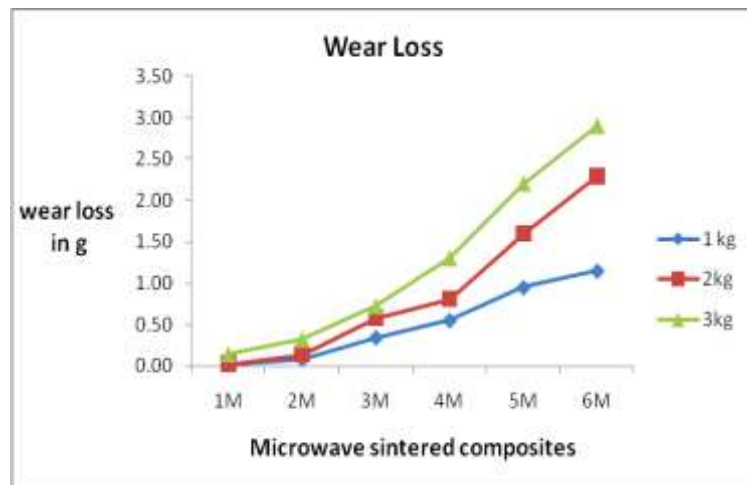


Fig. 7.26: Wear Loss of microwave sintered sample at 1, 2 and 3 kg load

7.3 Discussions on Jet Erosion Study

It is observed that the erosion resistance properties of the composite samples show encouraging results up to 30 vol. % loading of cenospheres in the composites. The samples also exhibited sufficient ductility at this vol. % of cenospheres. Thereafter, as the percentage of cenospheres increased beyond 30% and aluminum content

decreased, the erosion loss of the samples increased with decrease in erosion resistance characteristic. The ductility has also sufficiently reduced and the material had mixed behavior exhibiting partly ductile and partly brittle nature. The erosion loss seems to be more pronounced at acute erosion angle of 30° for all the samples and the loss was comparatively less at impingement angles between 60 to 90° deg for the conventionally sintered samples. The erosion loss was between 3.0-13.9 % lower for the microwave sintered samples at 30° , 2.1 to 43.8 % at 45° , 19.6 to 33.3% at 60° and 6.2 to 62.6% wear loss at 60° angles. The graphs at Fig 7.9 support this observation. The samples showed craters with high erosion rates in the composite loaded with cenospheres beyond 30 vol. % as can be observed in the photographs at Fig 7.1 & 7.2.

The microwave sintered samples showed better performance in terms of erosion loss of 12.5% which is less than the conventionally sintered ones as can be seen from Fig 7.10. The high erosion rate samples showed craters in the composite containing cenospheres beyond 30 vol. %. The reasons are attributed to the fact that as the grain/filler size increases beyond a certain level, both the strength and the hardness decrease with increased porosity of the composite which is contributed by cenospheres addition [Sudharshan et al 2008]. The reduction in hardness and density of the samples at Fig.6.7 and Fig. 6.10 also supports this finding. The development of finer microstructure in the microwave sintered samples leads to better erosion loss resistance.

Wilson S Ball has reported that ductility of the MMCs gets significantly lowered by the addition of ceramic reinforcements. This renders MMCs to lower its capacity to absorb strain which results in greater plastic constraint for impact loads which creates micro fractures in the material there by facilitating material removal. It is reported that MMCs has a lower erosion resistance compared to that of its matrix alloy.

The wear rates are pronounced at the acute angles of impact which is a characteristic of erosion modes found in ductile materials. This is supported by Fig 7.10 wherein it is indicated that the erosion losses are high for all the compositions for both

conventional and microwave sintered samples at angles of 30°, 45° and 60° because during erosion by abrasive particle, most of the impact energy is consumed for cutting rather than plastic deformation and work hardening.

Morteza Oghbaei et al [2010] has reported that microwave sintering effectively assist the forward diffusion of ions which accelerates the sintering. This results in matrix densification by grain growth process. Sintering process aids re-crystallization, grain growth and densification at high temperatures in the body that is being sintered. This densification mechanism is strongly dependent on diffusion of ions between the same sample particles. The mechanism of grain growth rate is assisted by the grain boundary diffusion process. It has been found that intense microwave field concentration is active around the particles of the sample while sintering. The power of this microwave field between the particles of the sample in the bulk of the material is about 30 times higher than the external field and this is sufficient to ionize the sample particles at its surface. This accelerates ionic diffusion which promotes rapid densification of the material is promoted under microwave sintering.

Apart from the microwave radiation, the surrounding electromagnetic field also effectively enhances the ionic diffusion kinetics near the grain boundaries. The kinetic energy of the ions at the grain boundary increases which thereby decrease the activation energy required for the forward ion jump and in the process increases the barrier height for the reverse jump. This mechanism promotes forward diffusion of the inter grain ions which accelerates the grain growth during sintering.

By microwave sintering all the properties of a given material are enhanced by its microstructural development in which the densification of the material and coarsening occurs rapidly and effectively throughout the bulk of the material. The microstructural development depends on the parameters such as optimized temperature, sintering time, heating rate and the pressure. The rapid heating rate achieved by microwave heating is the key to produce products with a high sintered density for a given microstructure and grain size compared to slow heating for the same sintered density by conventional heating. Since microwave sintering is a non-contact sintering

technique, the heat gets transferred to the product through electromagnetic radiation. By microwave sintering large amount of heat can be transferred to the material's interior which reduces differential sintering to a large extent. Hence the microwave sintered products have finer micro-structural development, with uniform grain growth and grain size distribution coupled with higher densification of the product thereby leading to enhanced engineering properties.

Hence it is concluded from this study that the composites exhibit good properties only at a certain vol. % of cenospheres are present in the matrix. Most of the physical and mechanical properties decrease proportionally to increase in the cenospheres content. The mix design needs to be properly selected to fabricate composites with required properties for use in applications.

7.4 Discussions on Dry Sliding Wear Behaviour

It is seen from Fig.7.25 and 7.26 that the dry sliding wear loss increases as the cenospheres content increases in the composites and the wear rate also remarkably increases as the load increases. The wear loss is high at 3 kg loading of the sample. The wear loss in conventionally sintered composites is more pronounced than the microwave sintered samples. The wear loss is mild at lower cenospheres content and tends to become severe as the cenospheres content gets increased. The dry sliding wear loss was between 19 to 53.0 % lower for the microwave sintered samples at 1 kg load, 14.7 to 46.2 % at 2 kg load and 12.1 to 38.5% at 3 kg load compared to the conventionally sintered samples.

In the wear loss study it is observed that all the four types of wear mechanisms viz. Adhesive type, Abrasive type, Oxidative type and De-lamination type are prevalent depending on the matrix filler proportions. [Shuvendu Tripathy 2009]. Adhesive type of wear is observed at lower volume content of cenospheres high aluminium content composites viz 1C and 1M samples. It is seen from the SEM micrographs of the wear surfaces at Fig. 7.12, 7.13, 7.15 and 7.16, that plastic flow and curl ups are observed in the composites having high aluminum content and at higher loads the

amount of curling phenomena is increased, due to ploughing action of steel disc against soft aluminum.

In Fig.7.19 and Fig.7.20, the SEM micrographs shows broken cenospheres in the wear debris due to abrasive action of the cenospheres and the wear type termed as Abrasive wear. As the cenospheres content increases the wear mechanism is more abrasive in nature. At higher loads in the samples having higher cenospheres content, the curling effect, material flow and the ploughing effect are not observed as the ductility is reduced. The cenospheres are exposed due to the wear of matrix owing to the combined effect of higher loads and the abrasive type of wear, which also contributes to the increased wear loss [Sudharshan et al 2008].

During the sliding process, the material is made to move back and forth several times along with the applied loads and this action, in the process produces wear debris. When the load that is applied leads to higher stresses than the fracture stress that of cenospheres, they lose their ability to support loads and consequently the aluminium matrix comes into direct contact with the abrading face and we see large grooves in the form of striations on the surface. This creates a severed localized deformation which give rises to stress concentrators like cracks. The phenomenon of de-cohesion of the reinforcement that is cenospheres from the matrix leads to debris formation which is substantial. The debris morphology shows the particle to be flake like as well as particulate type.

The volume of the wear debris increases as the normal load is also increased proportionately to the applied loads. The shape and morphology of the debris also varies with the applied load. Grooves were less severe for lower loads. These features are a characteristic of abrasion wear in the hard steel surface when hard particles come in between the contacting surfaces, which then plough or cut the pin shaped sample which causes wear by removal at the surface of the material. During ploughing action the material is displaced on either side of the groove in the samples which had more cenospheres content. The debris has the presence of the dislodged cenospheres. The abrasion is extensive in aluminium cenospheres composites due to

the presence of dislodged and fractured cenospheres that are trapped at the sliding interface which gets embedded in the counter face, contributing to abrasive wear. In addition, fractured cenospheres particles trapped between the sliding surfaces would also cause abrasion of the steel disc, as would work hardened fragments of matrix alloy and steel [Shuvendu Tripathy 2009, Nikhil Gupta et al 2015].

In the compositions having higher cenospheres content the predominant wear mechanism is the oxidation and de-lamination type of wear. This is evident from the Fig 7.19 & 7.20. Here the dark surfaces are found to be covered extensively by a thin layer of fine particles with large amounts of fine powder also seen in the wear debris. These are the oxidative type of wear that is indicative characteristics of frictional heating during sliding which has caused oxidation of the surface, with wear occurring through the removal of oxide fragments. On continuous sliding, oxide wear debris completely fills out the grooves on the sample surface, and gets compacted into a protective layer preventing metallic contact and wear rate of the composite drops.

De-lamination wear mechanism as seen from Fig.7.22 and 7.23 has been linked to the process of fatigue related wear mechanism in which repeated sliding induces subsurface cracks that gradually grow and eventually shear to the surface, forming long thin wear sheets. De-lamination is observed to be more extensive under the higher load. [Shuvendu Tripathy 2009, Nikhil Gupta et al 2015].

The reduction in hardness and density also contributes to increased wear in samples which have high volume of cenospheres. The conventionally sintered samples have more wear loss of about 86 % compared to the microwave sintered samples. This is due to finer micro structure formation and improved properties in the composites sintered in microwave.

The scanning electron microscopy technique was employed for microscopic examination of the worn surfaces and subsurface sections of wear surfaces for all the samples, to assess the type of wear mechanism prevailing in the worn samples. Here the fly ash cenospheres are exposed to slide wear by way of fragmented particles

resulting in higher wear loss. The amount of debris increases with increase in load and abrasive action.

In the composition where the concentration of aluminium is high as in 1C, 1M and 2C and 2M, during the pin on disc test, the surface of the counter face reacts to form ferrous oxide (Fe_3O_4) along with aluminum oxide (Al_2O_3) forming what is called the mix layer between the composite pin and the counter face. The work hardening of the aluminium also occurs during this sliding action with formation of iron oxide film on the surface which enhances the wear resistance with minimal wear loss.

At higher cenospheres concentration and lower aluminium content as in samples above 3C and 3M up to 6C and 6M and with increased load, it can be seen that oxide layer gets smashed out during the sliding action resulting in higher wear loss. It was also observed that the wear rate of the aluminium cenospheres composites increases as the load increases. This is in line with the findings reported by other researchers. It was observed that wear loss was found to be increasing with increase in cenospheres content in the composites. This increase in wear loss of the composite is due to the reason the reinforcement material is getting eroded from the matrix due to the sliding action and the load acting upon it. Cenospheres are hollow and highly porous structured material and its strength depends on the relative wall thickness. For the same reinforcement vol. fraction, the higher wall thickness/radius ratio and the size of the particle also significantly alter the wear properties of the resultant composite.

Worn out surface of the composite with 20 vol. % and above cenospheres was characterized by many pull-out and exposures of the cenospheres particles and more wear debris was observed which indicated the poor interfacial strength between the aluminium matrix and cenospheres reinforcement. Large grooves and scratches appeared on the worn surfaces as shown in Fig.7.19, 7.20, 7.22 and 7.23 and there was no indication of plastic deformation. This increase in wear loss can also be attributed to a poor interfacial bonding between aluminium and cenospheres particles. As the cenospheres content increases beyond 20 vol. % the wear loss increased with

increasing the load. This may be due to clustering of cenospheres particles and poor interfacial bonding between aluminium matrix and cenospheres particles [Shanmuga Sundaram et al 2011]. It is reported that when two surfaces are in sliding motion relative to each other and the surfaces are in sliding contact, wear mechanisms such as surface abrasion, oxidation, de-lamination and adhesion may happen either separately or in combination. The SEM morphology of the worn out surface of the composites indicate the following.

- a. At lower loads and lower cenospheres content the aluminium matrix supports the load and prevents wear loss due to the work hardening of the aluminium surface, which also forms a layer of oxide which is wear resistant. This prevents the damages caused due to sliding action and abrasion wear mechanism becomes dominant under this condition.
- b. In compositions with increased cenospheres content and higher applied load the resultant stresses exceed the fracture stress of the cenospheres particle. The hollow, porous and thin walled cenospheres particles are exposed to the surface during wear process, wherein they lose their capacity to sustain the load and finally rupture and are detached from the matrix. In addition, the worn out particles of cenospheres also act as third body abrasive which initiate friction and penetrate the opposing surface at the contact point thereby leading to ploughing action at the interface.

It follows from the above observations that the main wear mechanism at higher loads in the composites containing higher vol.% of cenospheres is delaminating wear causing excessive fracture of the reinforcement and the matrix, resulting in deterioration of the wear resistance of the composites. When the composite is subjected to the higher load, cracks on the surface propagates in the subsurface which causes material loss on the surface in the form of flakes or thin sheets. De-lamination was observed to be more extensive under the higher loads. [Shanmuga Sundaram et al 2011].

Hence it is concluded from this study that the composites exhibit good properties only at a certain vol. % of cenospheres are present in the matrix. Most of the physical and mechanical properties decrease proportionally to increase in the cenospheres content. The mix design needs to be properly selected to fabricate composites with required properties for use in applications.

Microwave sintering of process seems to be very effective route in enhancing the tribological behavior of the composites. In tribological performances, the slide wear loss is reduced for the microwave sintered samples and the erosion loss is also observed to be lower compared to conventionally sintered ones. The SEM picture corroborates the slide wear data in terms of grain morphology. The dispersion of cenospheres seems to be quite uniform and well distributed in the metal matrix. The densification is quite effective in microwave sintered samples as they show less voids and defects with good morphological features compared to conventionally sintered ones. This is well supported by density values.

CHAPTER 8

RESULTS AND DISCUSSIONS ON THERMAL PROPERTIES

The conventionally and microwave sintered aluminium cenospheres composite samples have been studied for thermal properties such as thermal shock resistance test and linear coefficient of thermal expansion tests. The thermal shock resistance test was intended to find out the resistance of the composites to thermal shocks and thereafter to know the decrease in mechanical strength especially compression strength in particular. The compression test was performed in Enkay make UTM machine of capacity 100T.

The compressive yield strength (σ_{CYS}) of both types of sintered samples were first evaluated prior to the thermal shock resistance test. The procedure for the thermal shock resistance test comprised of heating the composite samples to a temperature of 500⁰C and holding the samples at this temperature for 15 minutes. The heated samples were then immediately quenched in water bath which was held at ambient temperature. This constitutes 1 cycle. The conventionally sintered 1C to 6C samples and microwave sintered sample 1M to 6M samples were only studied for the test. The samples were subjected to thermal shock resistance tests comprising of 5, 10 and 25 cycles. The compression strength of the samples after completion of 5, 10 and 25 thermal cycles were measured.

8.1 Compressive Yield Strength (MPa) of conventionally sintered samples before and after thermal shock cycles

It can be seen from Fig.8.1 that for the conventionally sintered samples, the compressive yield strength of 1C sample which is comprised of only pure aluminium showed 125.0 MPa prior to thermal shock test. The strength decreased to 123.8 MPa which is 1.0 % after 5 cycles, 121.7 MPa which is 4.9 % decrease in the strength after 10 cycles and 120.1 MPa which is 5.4% reduction in the compression strength after

25 cycles. It can be seen that for the microwave sintered samples, the compressive yield strength of the sample 140.3 MPa prior to thermal shock test. The strength decreased to 138.8 MPa which is 0.9 % after 5 cycles, 133.7 MPa which is 4.7 % reduction in strength after 10 cycles and 131.1 MPa which is 5.1% reduction in compression strength after 25 thermal shock cycles.

The 2C sample showed compressive yield strength of 76.5 MPa prior to thermal shock cycles and the strength decreased by 5.1 % after 5 cycles, 11.9 % after 10 cycles and 44.3 % after 25 cycles. The 3C sample showed compressive yield strength of 71.2 MPa prior to thermal shock cycles and the strength decreased by 5.5 % after 5 cycles, 11.1 % after 10 cycles and 44.0 % after 25 cycles. The 4C sample showed compressive yield strength of 67.1 MPa prior to thermal shock cycles and the strength decreased by 8.2 % after 5 cycles, 12.5 % after 10 cycles and 49.3 % after 25 cycles. The 5C sample showed compressive yield strength of 63.8 MPa prior to thermal shock cycles and the strength decreased by 9.6 % after 5 cycles, 13.9 % after 10 cycles and 49.8 % after 25 cycles. The 6C sample showed compressive yield strength of 62.5 MPa prior to thermal shock cycles and the strength decreased by 22.9 % after 5 cycles, 39.0 % after 10 cycles and 49.4 % after 25 cycles.

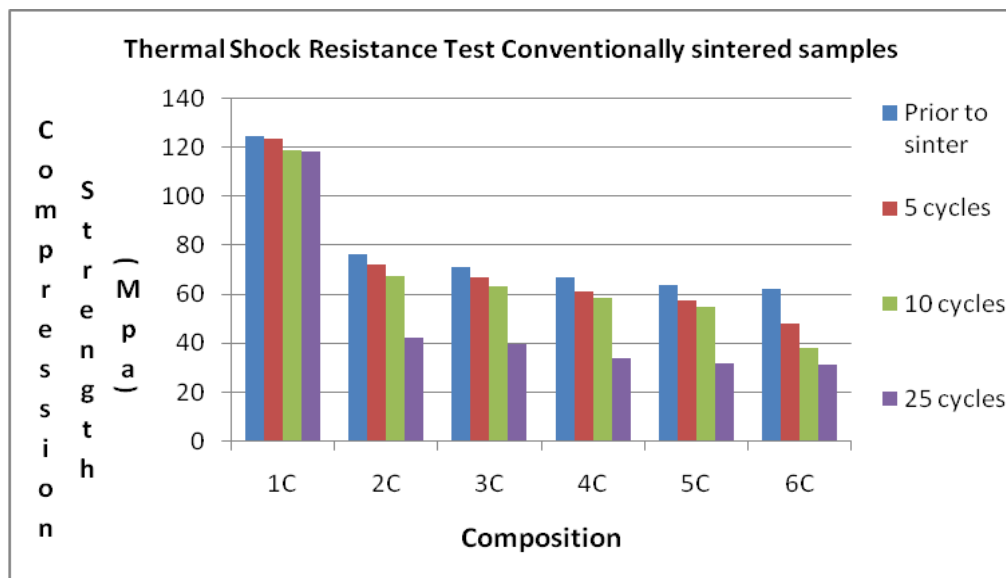


Fig. 8.1: Thermal Shock Resistance of Conventionally sintered samples

8.2 Compressive Yield Strength (MPa) of Microwave sintered samples before and after thermal shock cycles

It can be seen from Fig.8.2 that for the microwave sintered samples, the compressive yield strength of 1M sample which is comprised of only pure aluminium showed 140.3 MPa prior to thermal shock test. The strength decreased by 0.9 % after 5 cycles, 4.7 % after 10 cycles and 5.1% after 25 cycles. The 2M sample showed compressive yield strength of 97.6 MPa prior to thermal shock cycles and the strength decreased by 4.6 % after 5 cycles, 11.6 % after 10 cycles and 30.9 % after 25 cycles. The 3M sample showed compressive yield strength of 89.3 MPa prior to thermal shock cycles and the strength decreased by 4.6 % after 5 cycles, 9.0 % after 10 cycles and 34.3 % after 25 cycles. The 4M sample showed compressive yield strength of 86.2 MPa prior to thermal shock cycles and the strength decreased by 8.0 % after 5 cycles, 9.9 % after 10 cycles and 35.8 % after 25 cycles. The 5M sample showed compressive yield strength of 76.6 MPa prior to thermal shock cycles and the strength decreased by 9.1 % after 5 cycles, 18.1 % after 10 cycles and 39.2 % after 25 cycles. The 6M sample showed compressive yield strength of 71.7 MPa prior to thermal shock cycles and the strength decreased by 20.9 % after 5 cycles, 33.9 % after 10 cycles and 47.6 % after 25 cycles.

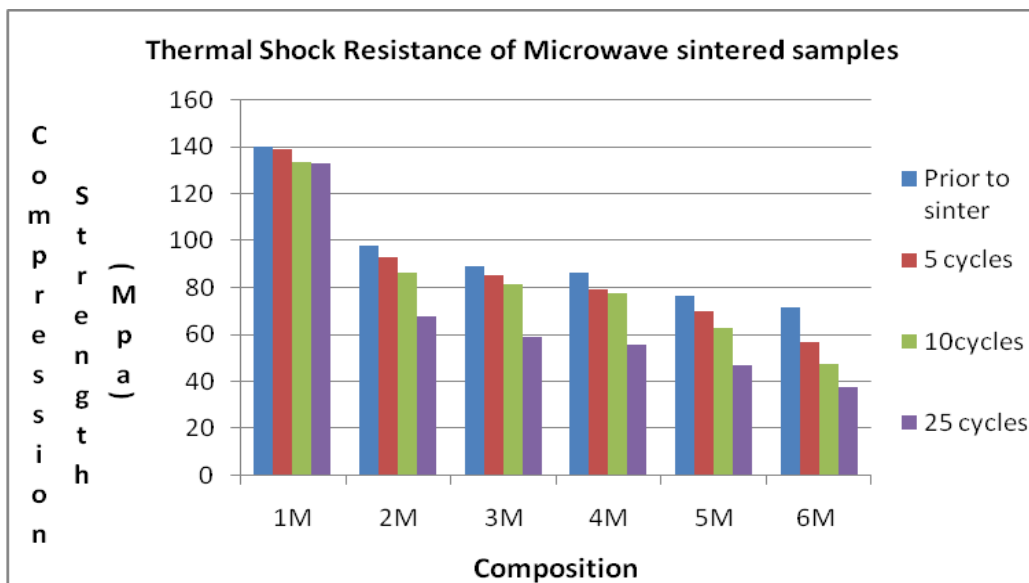


Fig. 8.2: Thermal Shock Resistance of Microwave sintered samples

8.3 Linear Co-efficient of Thermal Expansion (α)

The Linear Coefficient of Thermal Expansion (CTE) of the composites for pure aluminium powder samples showed value of $25.6 \times 10^{-6}/^{\circ}\text{C}$ which is near the theoretical value of pure aluminium. The CTE of the composites decreased as the cenospheres content increased from 10 vol. % to 50 vol. % i.e. from 20.6 to $7.3 \times 10^{-6}/^{\circ}\text{C}$ for the conventionally sintered samples as shown in Fig. 8.3. For the microwave sintered samples, the CTE of the composites decreased as the cenospheres content from 16.3 to $3.6 \times 10^{-6}/^{\circ}\text{C}$ which is much lower than the conventionally sintered samples. The microwave sintered showed less co-efficient of thermal expansion compared to conventionally sintered ones which were on the higher side by 20.9 to 50.7 %.

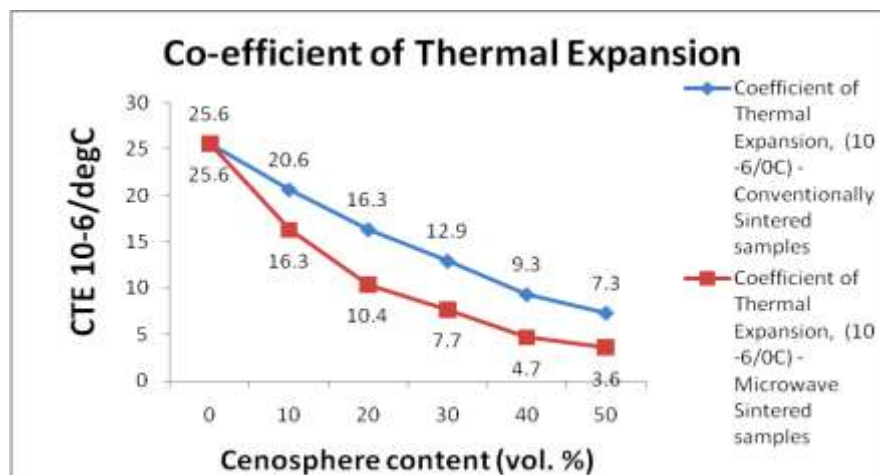


Fig. 8.3: Comparison of Co-efficient of Thermal Expansion of composites

8.4 Discussions on thermal properties

At higher temperatures of sintering, pores become more closed because micro pores vanish during the sintering process of the material. The sintering temperature and the process influence the bulk density, mechanical strength, thermal stability, porosity and shrinkage of the samples [Morteza Oghbaei et al 2010]. The development of physical and mechanical properties is related to the phases formed due to reaction sintering between alumina and alumino-silicates and formation of compact microstructure [Satapathy et al 2012]. Material density is an important characteristic for predicting mechanical properties and permeability. As the density increases (and

porosity decreases), the mechanical properties also increase with decrease in permeability [Ananda Kumar et al 2014].

Shanmuga Sundaram et al [2011] have observed that the aluminum composite's density and strength decrease with increasing vol. per cent of fly ash cenospheres in the composite. Rohatgi et al [1997] has reported that cenospheres are ceramic in nature, and that the ceramic particles will have low coefficient of thermal expansion when compared to metallic samples and therefore the incorporation of cenospheres, a ceramic material as filler in the metal matrix composite will reduce the CTE of the resulting composite. Since cenospheres is also an alumino-silicate, this also reduces the CTE in aluminium matrix. This is evident from the CTE values depicted in Table 8.3, which shows that as the cenospheres content is increased from 10 to 50 %, the CTE is also reduced in both the conventionally and microwave sintered samples. Microwave sintered samples still showed lower CTE compared to conventional sintered samples. Guo et al [1997] have also reported that a ceramic phase is formed at the interface between cenospheres and aluminium due to reaction of Al with Si present in cenospheres. This ceramic phase formation is also one of the reasons for reduction in CTE of the composite containing cenospheres.

Sintering of aluminium- cenospheres powders composites through microwave appears promising. It is observed that the aluminium metal powder remains in metallic state at temperature range of 665⁰C. The matrix formed is metallic rather than oxide as observed in the previous experiments conducted beyond 750⁰C. In the reported studies it is noted that aluminium cenospheres syntactic foams have a significantly lower CTE compared to the matrix material. A lower CTE value in the pure aluminium matrix syntactic foam containing fly ash cenospheres was observed. The metallic oxides in cenospheres such as alumina, silica, and iron oxides etc., being ceramic in nature also reduces the CTE of the aluminum from $25.3 \times 10^{-6} \text{ }^{\circ}\text{C}^{-1}$ to $3.6 \times 10^{-6} \text{ }^{\circ}\text{C}^{-1}$. Some of the researchers also observed that increase in the particle reinforcement also decreased the CTE of particulate MMCs. It is also reported that the CTE of the composite is dependent on a range of mechanisms from plastic

yielding to volume fraction of the fractured and broken particles [James Cox et al 2014].

P K Rohatgi et al [2005] have opined that CTE of the aluminium matrix and cenospheres reinforcement are different and this can lead to micro voids or cracks with entrapped air at the interface of the particle and the matrix which has a bearing on the CTE. Sudharshan et al. [2008] has reported that there is a possibility of chemical reaction between aluminum melt and fly ash cenospheres particles. As cenospheres consists of predominantly silica, alumina and iron oxide, a chemical reduction reaction is taking place with these oxides when they come in contact with the melt. The silicon and iron diffuses into the pure aluminium melt and react to form Al-Si eutectic and Al₅FeSi phase which precipitates during solidification of the melt. These oxide phases are responsible for the decreased CTE in the samples.

Morteza Oghbaei et al [2010] has reported that microwave sintering effectively assist the forward diffusion of ions which accelerates the sintering. This results in matrix densification by grain growth process. Sintering process aids re-crystallization, grain growth and densification at high temperatures in the body that is being sintered. This densification mechanism is strongly dependent on diffusion of ions between the same sample particles. The mechanism of grain growth rate is assisted by the grain boundary diffusion process. It has been found that intense microwave field concentration is active around the particles of the sample while sintering. The power of this microwave field between the particles of the sample in the bulk of the material is about 30 times higher than the external field and this is sufficient to ionize the sample particles at its surface. This accelerates ionic diffusion which promotes rapid densification of the material is promoted under microwave sintering.

Apart from the microwave radiation, the surrounding electromagnetic field also effectively enhances the ionic diffusion kinetics near the grain boundaries. The kinetic energy of the ions at the grain boundary increases which thereby decrease the activation energy required for the forward ion jump and in the process increases the

barrier height for the reverse jump. This mechanism promotes forward diffusion of the inter grain ions which accelerates the grain growth during sintering.

By microwave sintering all the properties of a given material are enhanced by its microstructural development in which the densification of the material and coarsening occurs rapidly and effectively throughout the bulk of the material. The micro structural development depends on the parameters such as optimized temperature, sintering time, heating rate and the pressure. The rapid heating rate achieved by microwave heating is the key to produce products with a high sintered density for a given microstructure and grain size compared to slow heating for the same sintered density by conventional heating. Since microwave sintering is a non-contact sintering technique, the heat gets transferred to the product through electromagnetic radiation. By microwave sintering large amount of heat can be transferred to the material's interior which reduces differential sintering to a large extent. Hence the microwave sintered products have finer micro-structural development, with uniform grain growth and grain size distribution coupled with higher densification of the product thereby leading to enhanced engineering properties.

Hence it is concluded from this study that the composites exhibit good properties only at a certain vol. % of cenospheres are present in the matrix. Most of the physical and mechanical properties decrease proportionally to increase in the cenospheres content. The mix design needs to be properly selected to fabricate composites with required properties for use in applications.

CHAPTER 9

RESULTS AND DISCUSSIONS ON MECHANICAL PROPERTIES

9.1 Compressive strength

The Fig. 9.1 illustrates the comparison in the compression strength behavior of the conventionally sintered samples 1C to 6C and microwave sintered sample 1M to 6M. It is seen that the compression strength of the conventionally sintered samples 1C which comprises of pure aluminium powder is 125.0 kg/cm^2 . The compression strength reduced to 76.5 kg/cm^2 when the cenospheres content was incorporated in the 2C sample to a tune of 10 vol. %. This shows a reduction of the compression strength by 38.8%. When the cenospheres content was increased to 20 vol. % in the 3C sample the compression strength reduced to 71.2 kg/cm^2 which is 43.0 % decrease in the strength compared to pure aluminium sample. When the cenospheres content was increased to 30 vol. % in the 4C sample the compression strength reduced to 67.1 kg/cm^2 which is 46.3% decrease in the strength compared to pure aluminium 1C sample. The cenospheres content further when increased to 40 vol. % in the 5C sample the compression strength reduced to 63.8 kg/cm^2 which is 49.0% decrease in the strength compared to pure aluminium 1C sample. Further when the cenospheres content was increased to 50 vol. % in the 6C sample the compression strength further reduced to 62.5 kg/cm^2 which is 50.0% decrease in the strength compared to pure aluminium 1C sample.

It is seen that the compression strength of the microwave sintered samples 1M which comprises of pure aluminium powder is 140.3 kg/cm^2 . The compression strength reduced to 97.6 kg/cm^2 when the cenospheres content was incorporated in the 2M sample to a tune of 10 vol. %. This shows a reduction of the compression strength by 30.43%. When the cenospheres content was increased to 20 vol. % in the 3M sample the compression strength reduced to 89.3 kg/cm^2 which is 36.4% decrease in the strength compared to pure aluminium sample. When the cenospheres content was increased to 30 vol. % in the 4M sample the compression strength reduced to 86.2

kg/cm² which is 38.6 % decrease in the strength compared to pure aluminium 1M sample. The cenospheres content further when increased to 40 vol. % in the 5M sample the compression strength reduced to 76.6 kg/cm² which is 45.4% decrease in the strength compared to pure aluminium 1M sample. Further when the cenospheres content was increased to 50 vol. % in the 6M sample the compression strength further reduced to 71.7 kg/cm² which is 48.9 % decrease in the strength compared to pure aluminium 1M sample

A progressive decrease in compression strength is observed for the both the conventionally and microwave sintered samples as the volume percent of cenospheres increased from 0 to 50. The sample appears to be more brittle than metallic with the increase in the ceramic phase by addition of cenospheres in both types of samples. Microwave sintered samples showed compression strength higher by about 1.1% compared to its counterpart, the conventionally sintered ones.

The microwave sintered samples had a higher compressive strength by about 10.9%, 21.6%, 20.3%, 22.1%, 16.7 % and 12.8 % for 0, 10, 20, 30, 40 and 50 vol. % cenospheres content respectively compared to the conventionally sintered ones. Microwave sintered samples had a overall higher compressive strength of about 26.8% compared to its counterpart, the conventionally sintered ones.

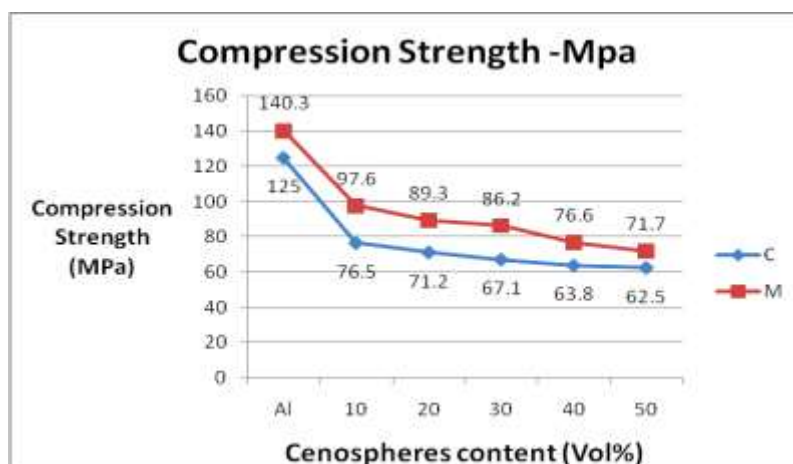


Fig. 9.1: Comparison of Compression Strength of composites

9.1.1 Finite Element Method Analysis of conventionally sintered samples

The results of the conventionally and microwave sintered composites samples tested for. compression strength was validated through FEM. The results of the same are discussed. The samples were analyzed for the Stress vs. Displacement behavior of both the types of samples sintered differently.

9.1.1.1 FEA Stress vs. Displacement analysis of 1C sample

The Fig.9.2 indicate the stress vs. displacement plots analyzed for the 1C samples comprising of pure aluminium which has been sintered conventionally. It is observed from the plots that the maximum stress that the sample withstood was 135.6 MPa and the displacement observed to be 0.574 mm. The maximum stress concentration is observed to be at the periphery at the top edge of the sample. The displacement also appears to be maximum at the periphery, both in the Y axis. The FEM analysis indicates that the compressive stress is higher by about 7.8 % compared to tested samples.

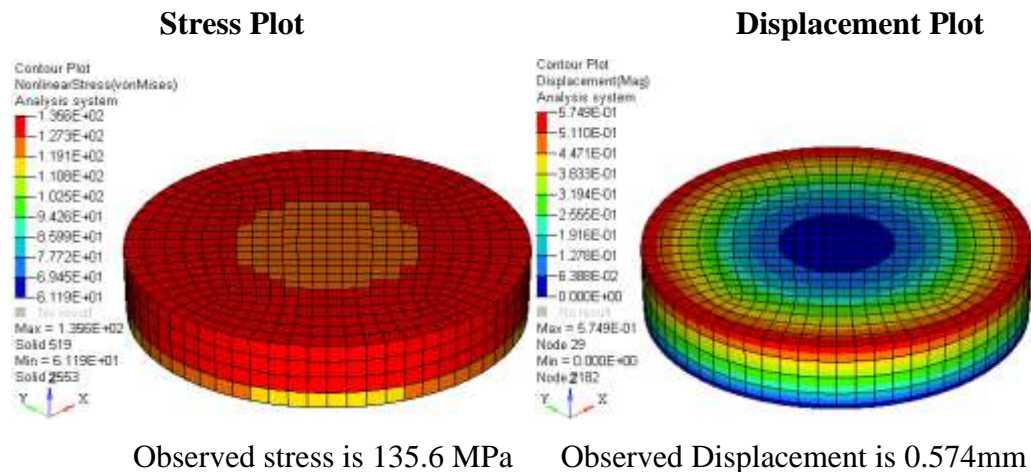


Fig. 9.2: FEA of Stress vs. Displacement of 1C sample

9.1.1.2 FEA Stress vs. Displacement analysis of 2C sample

The Fig.9.3 indicate the stress vs. displacement plots analyzed for the 2C samples comprising of aluminium with 10 vol. % cenospheres sintered conventionally. It is observed from the plots that the maximum stress that the sample withstood was 84.57MPa and the displacement observed to be 0.0193 mm. The maximum stress

concentration is observed to be at the outer top edges of the sample. The displacement value is maximum at the periphery, both in the Y axis. The FEM analysis indicates that the compressive stress has decreased by about 37.6 % compared to 1C sample with increase in cenospheres content, but the compressive stress value by FEA are higher by about 9.50 % compared to tested samples.

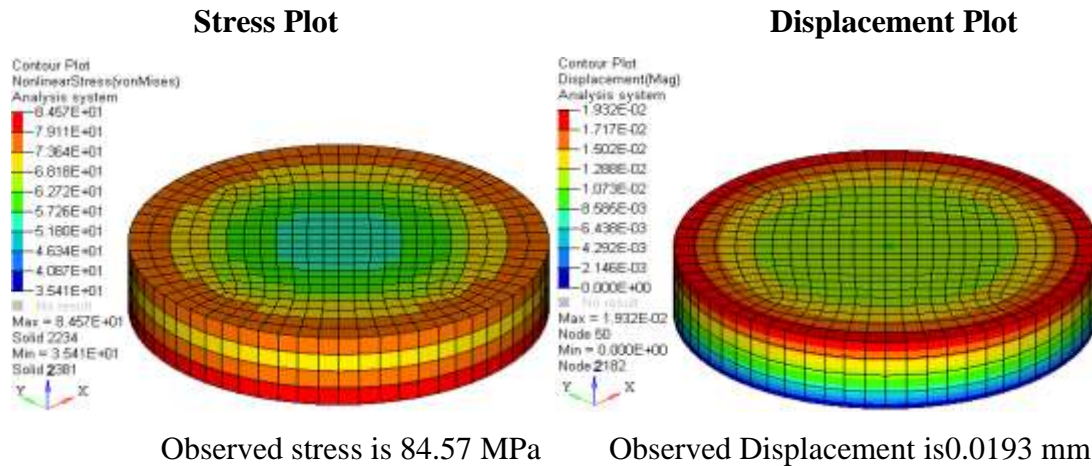


Fig. 9.3: FEA of Stress vs. Displacement of 2C sample

9.1.1.3 FEA Stress vs. Displacement analysis of 3C sample

The Fig. 9.4 indicate the stress vs. displacement plots analyzed for the 3C samples comprising of aluminium with 20 vol. % cenospheres sintered conventionally. It is observed from the plots that the maximum stress that the sample withstood was 78.71MPa and the displacement observed to be 0.0183 mm. The maximum stress concentration is observed to be at the outer bottom edges of the sample. The displacement value is maximum at the outer top edge at the periphery, both in the Y axis. The FEM analysis indicates that the compressive stress has decreased by about 41.9 % compared to 1C sample with increase in cenospheres content, but the compressive stress value of FEA are higher by about 9.51 % compared to tested samples.

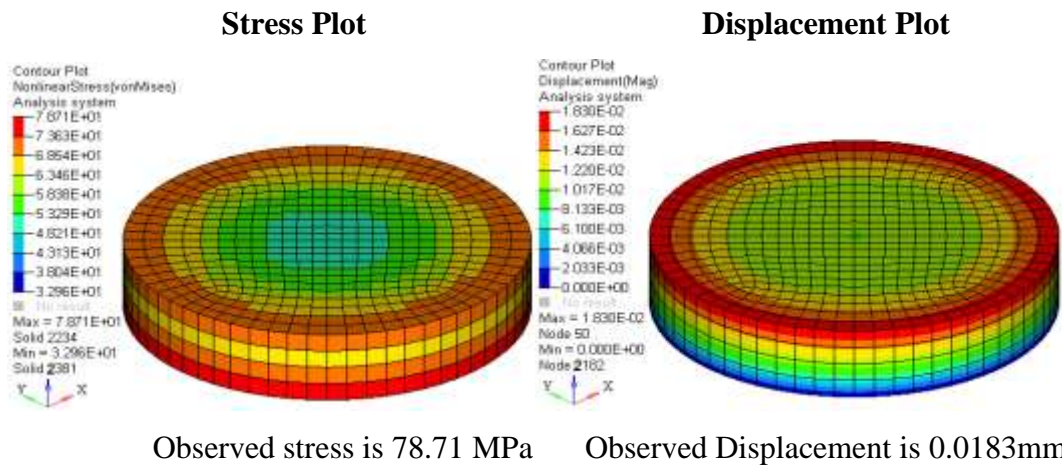


Fig. 9.4: FEA of Stress vs. Displacement of 3C sample

9.1.1.4 FEA Stress vs. Displacement analysis of 4C sample

The Fig. 9.5 indicate the stress vs. displacement plots analyzed for the 4C samples comprising of aluminium with 30 vol. % cenospheres sintered conventionally. It is observed from the plots that the maximum stress that the sample withstood was 74.18 MPa and the displacement observed to be 0.0172 mm. The maximum stress concentration is observed distributed at the outer bottom edge of the sample. The displacement value is maximum at the top edge at the periphery, both in the Y axis. The FEM analysis indicates that the compressive stress has decreased by about 45.3 % compared to 1C sample with increase in cenospheres content, but the compressive stress value calculated through FEA is higher by about 9.54 % compared to tested samples.

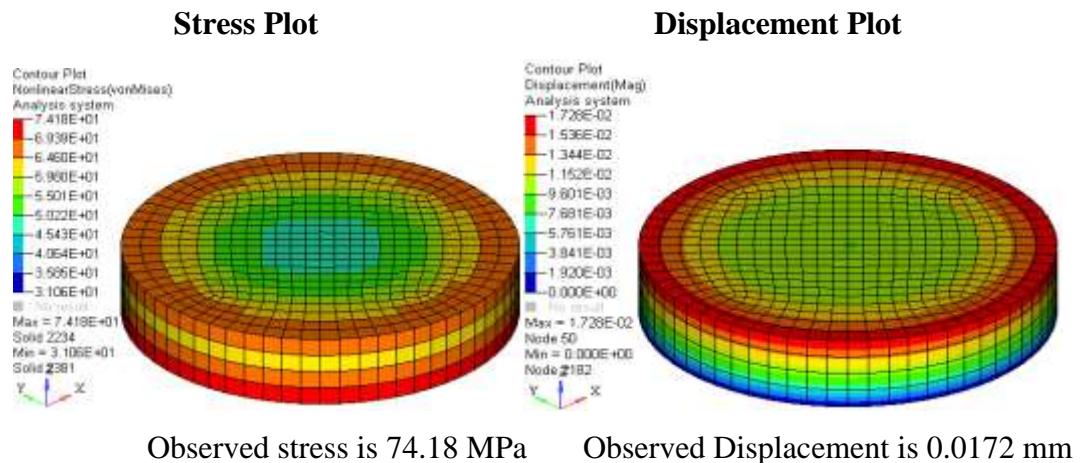
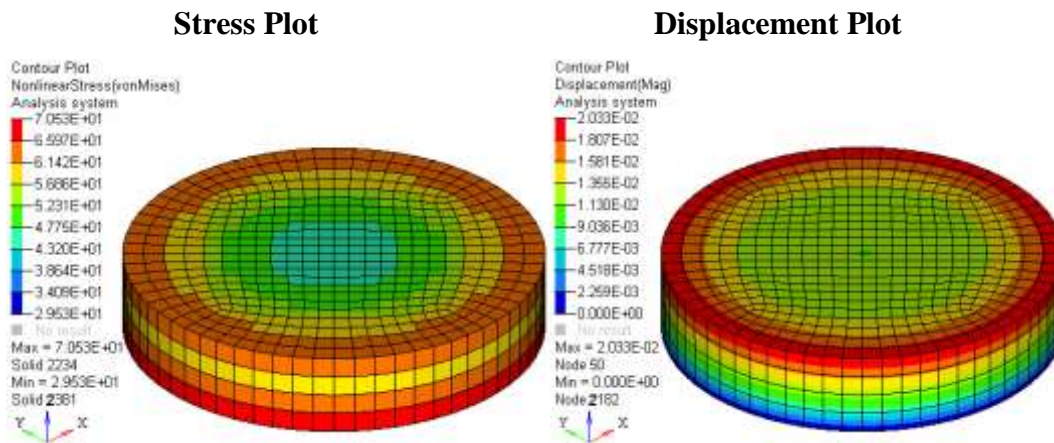


Fig. 9.5: FEA of Stress vs. Displacement of 4C sample

9.1.1.5 FEA Stress vs. Displacement analysis of 5C sample

The Fig. 9.6 indicate the stress vs. displacement plots analyzed for the 5C samples comprising of aluminium with 40 vol. % cenospheres sintered conventionally. It is observed from the plots that the maximum stress that the sample withstood was 70.53 MPa and the displacement observed to be 0.0230 mm. The maximum stress concentration is observed distributed at the outer bottom edges of the sample. The displacement value is also maximum at the top edge at the periphery, both in the Y axis. The FEM analysis indicates that the compressive stress has further decreased by about 48.0 % compared to 1C sample with increase in cenospheres content. The stress value calculated is higher by about 9.52 % compared to tested samples.



Observed stress is 70.53 MPa Observed Displacement is 0.0230mm

Fig. 9.6: FEA of Stress vs. Displacement of 5C sample

9.1.1.6 FEA Stress vs. Displacement analysis of 6C sample

The Fig. 9.7 indicate the stress vs. displacement plots analyzed for the 6C samples comprising of aluminium with 50 vol. % cenospheres sintered conventionally. It is observed from the plots that the maximum stress that the sample withstood was 70.53 MPa and the displacement observed to be 0.0230 mm.

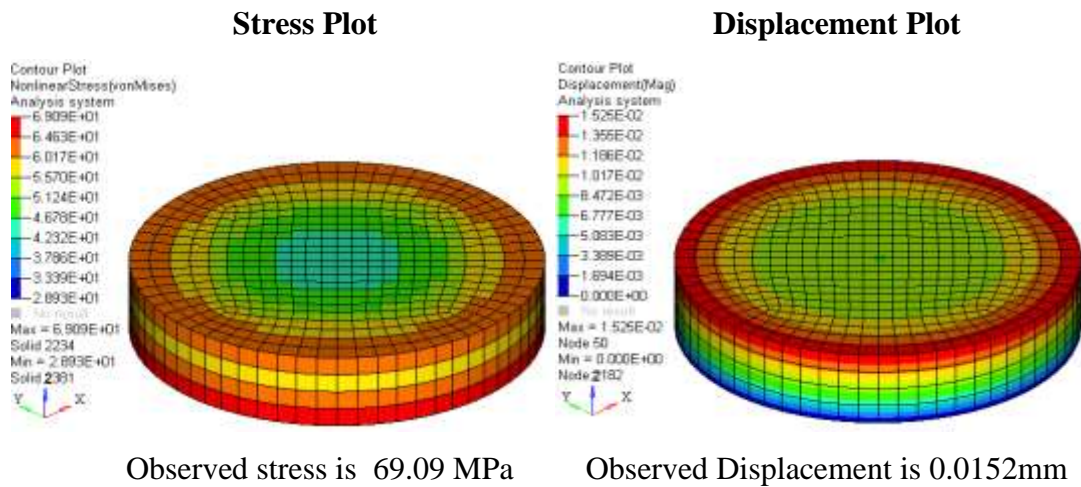


Fig. 9.7: FEA of Stress vs. Displacement of 6C sample

The maximum stress and displacement is observed to be distributed at the outer bottom edges of the sample and outer top edge of the sample in the Y axis respectively. The FEM analysis indicates that the compressive stress has further decreased by about 48.0 % compared to 1C sample with increase in cenospheres content, but the compressive stress values calculated through FEA is higher by about 9.54 % compared to tested samples.

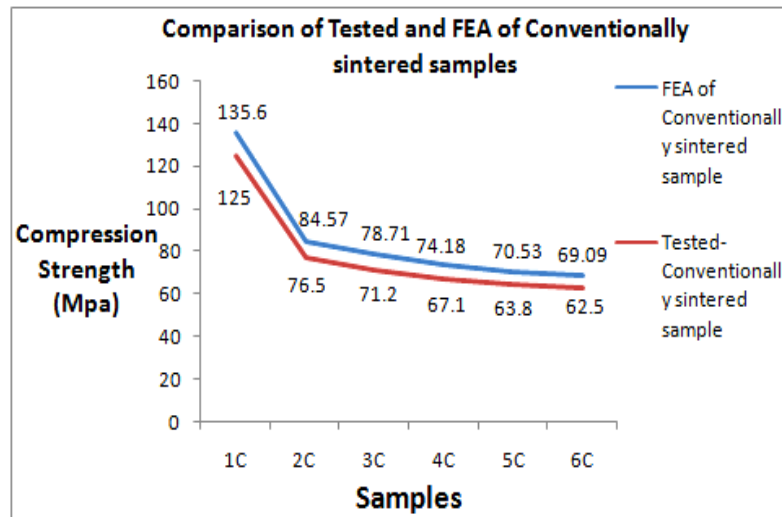


Fig.9.8: Comparison of tested and FEA of conventionally sintered composites

The graphs at Fig. 9.8 compare the compressive stress of conventionally sintered samples of the actual tested samples with that of the value obtained from FEM analysis of the samples. It is observed from the plots that the FEM analysis indicates

that the compressive stress values are higher by about 7.82 to 9.54 % compared to tested samples for the samples 1C to 5C.

9.1.2. Finite Element Method Analysis of microwave sintered samples

9.1.2.1 FEA Stress vs. Displacement analysis of 1M sample

The Fig. 9.9 indicates the stress vs. displacement plots analyzed for the 1M samples comprising of pure aluminium which has been sintered in microwave. It is observed from the plots that the maximum stress that the sample withstood was 155.1MPa and the displacement observed to be 0.023 mm. In this analysis too the maximum stress concentration is observed to be at the bottom edge at the periphery of the sample. The displacement also appears to be at the maximum at the top edges of the sample, both in the Y axis. The FEM analysis indicates that the calculated stress is higher by about 9.54 % compared to tested samples.

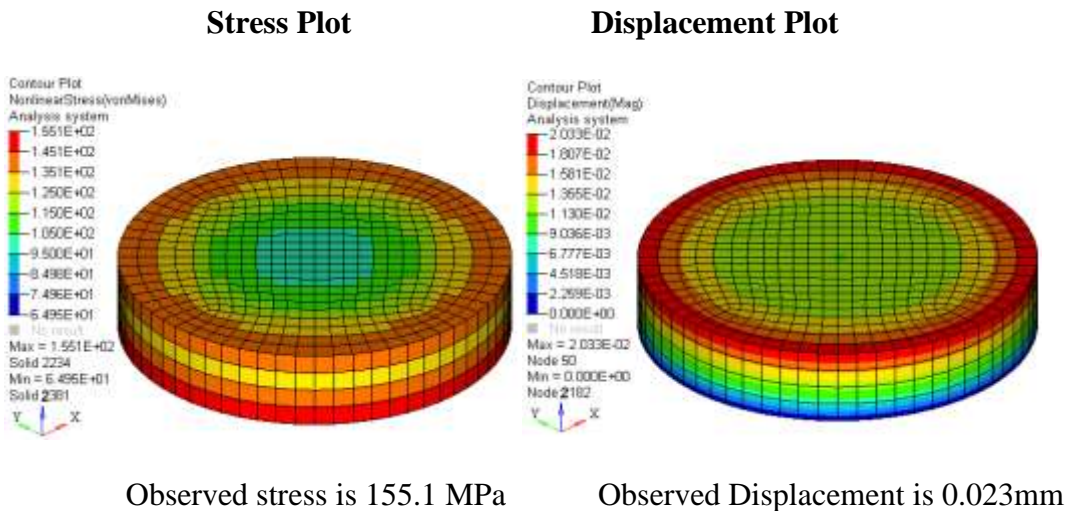
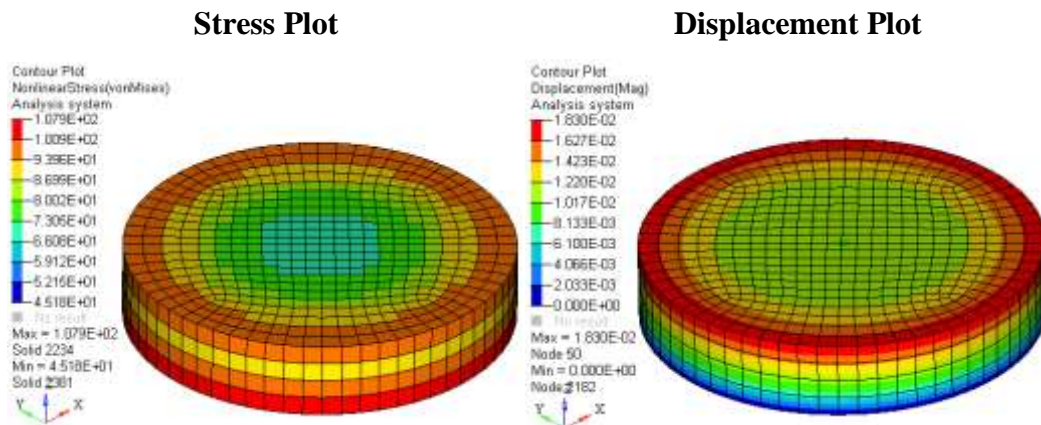


Fig. 9.9: FEA of Stress vs. Displacement of 1M sample

9.1.2.2 FEA Stress vs. Displacement analysis of 2M sample

The Fig. 9.10 indicate the stress vs. displacement plots analyzed for the 2M samples comprising of pure aluminium with 10 vol. % cenospheres and which has been sintered in microwave.



Observed stress is 107.9 MPa Observed Displacement is 0.0183 mm

Fig. 9.10: FEA of Stress vs. Displacement of 2M sample

It is observed from the plots that the maximum stress that the sample withstood was 107.9 MPa and the displacement observed to be 0.0183 mm. In this analysis the maximum stress concentration is observed to be at the bottom edge at the periphery of the sample. The displacement is observed to be at the maximum at top edge of the sample, both in the Y axis. The FEM analysis indicates that the stress has reduced by about 30.43 % compared to 1M with increase in the cenospheres content. The stress value calculated is higher by about 9.55 % compared to tested samples.

9.1.2.3 FEA Stress vs. Displacement analysis of 3M sample

The Fig. 9.11 indicate the stress vs. displacement plots analyzed for the 3M samples comprising of pure aluminium with 20 vol. % cenospheres and which has been sintered in microwave. It is observed from the plots that the maximum stress that the sample withstood was 98.72 MPa and the displacement observed to be 0.0183 mm. In this analysis the maximum stress concentration is observed to be at the bottom edge of the periphery of the sample. The displacement also appears to be at the maximum at the top edge of the sample, both in the Y axis. The FEM analysis indicates that the stress is lower by about 36.4 % compared to the 1M sample which has decreased with increasing cenospheres content. The stress value calculated is higher by about 9.52 % compared to tested samples.

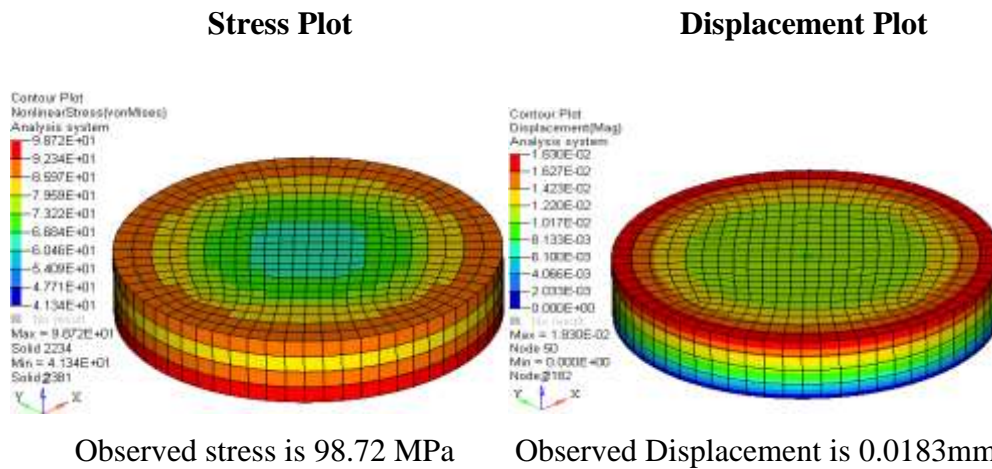


Fig. 9.11: FEA of Stress vs. Displacement of 3M sample

9.1.2.4 FEA Stress vs. Displacement analysis of 4M sample

The Fig. 9.12 indicate the stress vs. displacement plots analyzed for the 4M samples comprising of pure aluminium with 30 vol. % cenospheres and which has been sintered in microwave. It is observed from the plots that the maximum stress that the sample withstood was 95.29 MPa and the displacement observed to be 0.0172 mm. In this analysis too the maximum stress concentration is observed to be at the bottom edge of the periphery of the sample and the displacement also appears to be at the maximum at the top edge of the sample, both in the Y axis. The FEM analysis indicates that the stress is further lowered by about 38.6 % compared to the 1M sample which has decreased with increasing cenospheres content. The stress value calculated is higher by about 9.55 % compared to tested samples.

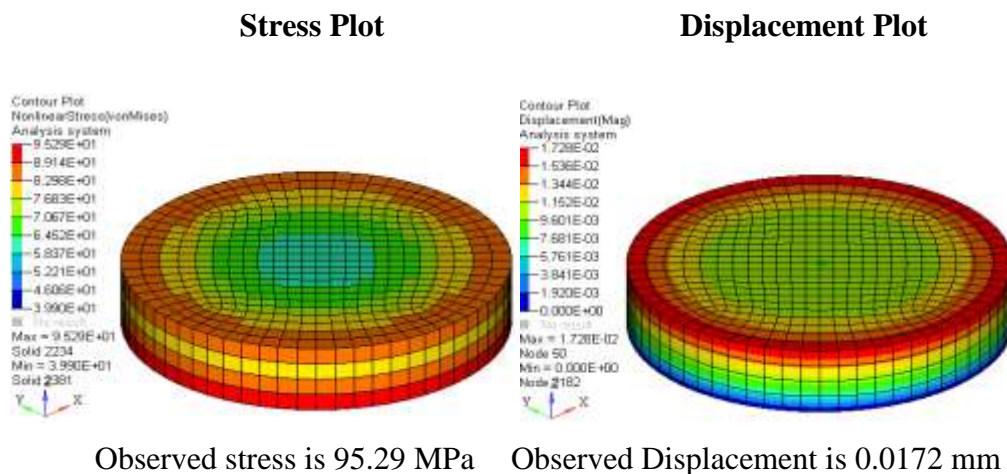


Fig. 9.12: FEA of Stress vs. Displacement of 4M sample

9.1.2.5 FEA Stress vs. Displacement analysis of 5M sample

The Fig. 9.13 indicate the stress vs. displacement plots analyzed for the 5M samples comprising of pure aluminium with 40 vol. % cenospheres and which has been sintered in microwave. It is observed from the plots that the maximum stress that the sample withstood was 84.68 MPa and the displacement observed to be 0.0162 mm. In this analysis also the maximum stress concentration is observed to be at the bottom edge of the periphery of the sample and the displacement also appears to be at the maximum at the top edge of the sample, both in the Y axis. The FEM analysis indicates that the stress is further lowered by about 45.4 % compared to the 1M sample which has decreased with increasing cenospheres content. The compressive stress value calculated is higher by about 9.56 % as compared to tested samples.

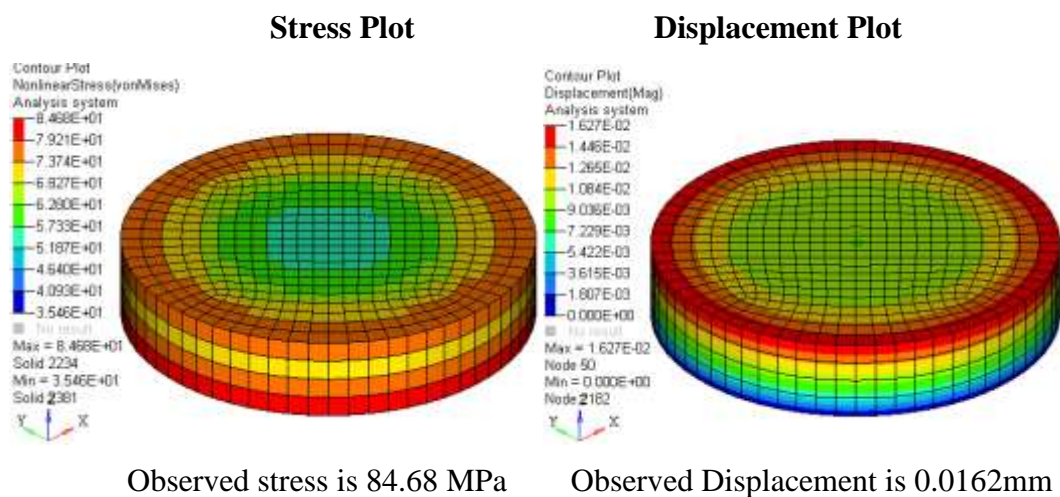


Fig. 9.13: FEA of Stress vs. Displacement of 5M sample

9.1.2.6 FEA Stress vs. Displacement analysis of 6M sample

The Fig. 9.14 indicate the stress vs. displacement plots analyzed for the 6M samples comprising of pure aluminium with 50 vol. % cenospheres and which has been sintered in microwave. It is observed from the plots that the maximum stress that the sample withstood was 79.26 MPa and the displacement observed to be 0.0161 mm.

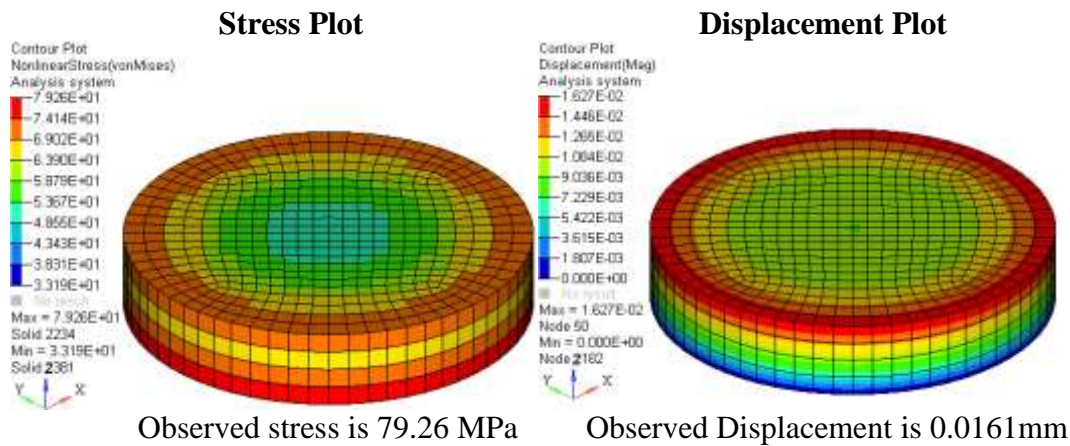


Fig. 9.14: FEA of Stress vs. Displacement of 6M sample

In this analysis also the maximum stress concentration is observed to be at the bottom edge of the periphery of the sample and the displacement also appears to be at the maximum at the top edge of the sample, both in the Y axis. The FEM analysis indicates that the stress is further lowered by about 48.9 % compared to the 1M sample which has decreased with increasing cenospheres content. The compressive stress value calculated is higher by about 9.58 % as compared to tested samples.

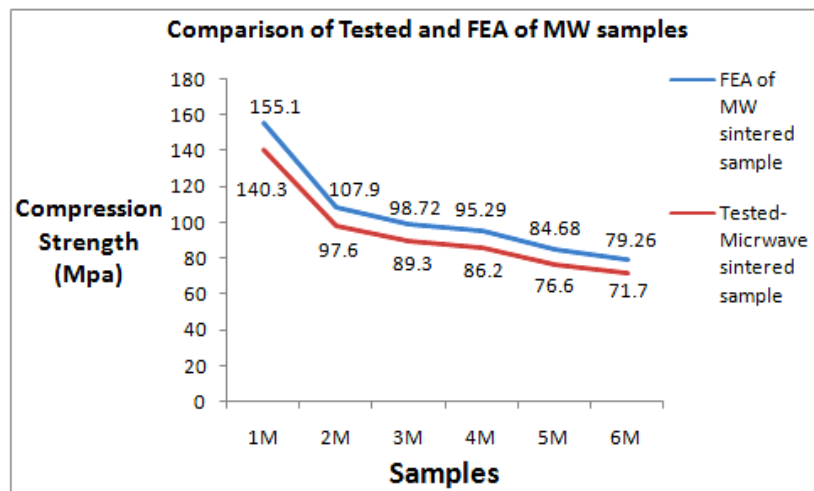


Fig. 9.15: Comparison of tested and FEA of Microwave sintered composites

The graphs at Fig. 9.15 compare the compressive stress of microwave sintered samples of the actual tested samples with that of the value obtained from FEM analysis of the samples. It is observed from the plots that the FEM analysis indicates

that the compressive stress values are higher by about 9.52 to 9.54 % compared to tested samples for the samples 1M to 5M.

9.2 Flexural strength (Modulus of Rupture)

Flexural strength, also known as Modulus of Rupture (MOR), bend strength, or fracture strength, is a mechanical parameter for brittle material. This is defined as material's ability to resist deformation under load. The transverse bending test is most frequently employed, in which a specimen having either a circular or rectangular cross-section is bent until fracture or yielding using a three point flexural test technique. The flexural strength represents the highest stress experienced within the material at its moment of rupture. It is measured in terms of stress, here given the symbol σ . was calculated as follows:

$$\text{Flexural Strength } \sigma \text{ or Modulus of Rupture} = 3PL/2BD^2$$

Where P= the actual load at the fracture point, L is the length of the supports holding the test specimen, B is the width of the test specimen and D is the depth or thickness of the test specimen and the units of flexural strength is kg/cm² or MPa.

The Fig. 9.16 illustrates the comparison in the flexural strength behavior of the conventionally sintered samples 1C to 6C and microwave sintered sample 1M to 6M. It is seen that the flexural strength of the conventionally sintered samples 1C which comprises of pure aluminium powder is 52.0 kg/cm². The flexural strength reduced to 47.7 kg/cm² when the cenospheres content was incorporated in the 2C sample to a tune of 10 vol. %. This shows a reduction of the flexural strength by 8.27%. When the cenospheres content was increased to 20 vol. % in the 3C sample the flexural strength reduced to 38.2 kg/cm² which is 26.5 % decrease in the strength compared to pure aluminium sample. When the cenospheres content was increased to 30 vol. % in the 4C sample the flexural strength reduced to 27.3 kg/cm² which is 47.5% decrease in the strength compared to pure aluminium 1C sample. The cenospheres content further when increased to 40 vol. % in the 5C sample the flexural strength reduced to 14.7 kg/cm² which is 71.7% decrease in the strength compared to pure aluminium 1C

sample. Further when the cenospheres content was increased to 50 vol. % in the 6C sample the flexural strength further reduced to 8.8 kg/cm² which is 83.0% decrease in the strength compared to pure aluminium 1C sample.

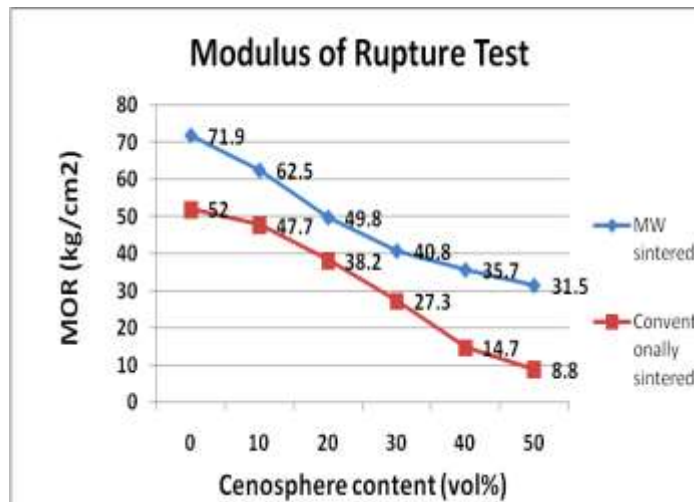


Fig. 9.16: Comparison of Modulus of Rupture of composites

It is seen that the flexural strength of the microwave sintered samples 1M which comprises of pure aluminium powder is 71.9 kg/cm². The flexural strength reduced to 62.5 kg/cm² when the cenospheres content was incorporated in the 2M sample to a tune of 10 vol. %. This shows a reduction of the flexural strength by 13.1%. When the cenospheres content was increased to 20 vol. % in the 3M sample the flexural strength reduced to 49.8 kg/cm² which is 30.7% decrease in the strength compared to pure aluminium sample. When the cenospheres content was increased to 30 vol. % in the 4M sample the flexural strength reduced to 40.8 kg/cm² which is 43.25% decrease in the strength compared to pure aluminium 1M sample. The cenospheres content further when increased to 40 vol. % in the 5M sample the flexural strength reduced to 35.7 kg/cm² which is 50.35% decrease in the strength compared to pure aluminium 1M sample. Further when the cenospheres content was increased to 50 vol. % in the 6M sample the flexural strength further reduced to 31.5 kg/cm² which is 56.19% decrease in the strength compared to pure aluminium 1M sample

A progressive decrease in flexural strength is observed for the both the conventionally and microwave sintered samples as the volume percent of cenospheres increased from

0 to 50. The sample appears to be more brittle than metallic with the increase in the ceramic phase by addition of cenospheres in both types of samples. The microwave sintered samples had a higher flexural strength by about 27.7%, 23.7%, 23.3%, 33.1%, 58.8% and 72.3% for 0, 10, 20, 30, 40 and 50 vol. % cenospheres content respectively compared to the conventionally sintered ones.

Microwave sintered samples had a overall higher flexural strength of about 26.8% compared to its counterpart, the conventionally sintered ones.

9.3 Study of the fracture surface

The microstructure at Fig.9.17 shows fracture surfaces of the 1C composite sample tested for flexural strength. The fracture surface of the composite which is comprised of 90 vol. % of aluminium and 10 vol. % of cenospheres sintered conventionally has been observed in the SEM for the fracture characteristic. The microstructure reveals a mixed mode of fracture surface which comprises of cup and cone type of contour at some places and cleavage steps with rough surface at other places, which supports the fact that this type of fracture is attributed to both the ductile material which is aluminium and the fracture happening in the tensile mode and the other type of fracture found is the coarse grained surface type which also supports the fact that the fracture surface is also composed of regions having brittle features contributed by cenospheres which are ceramic in nature, when seen at a magnification of 100 X.

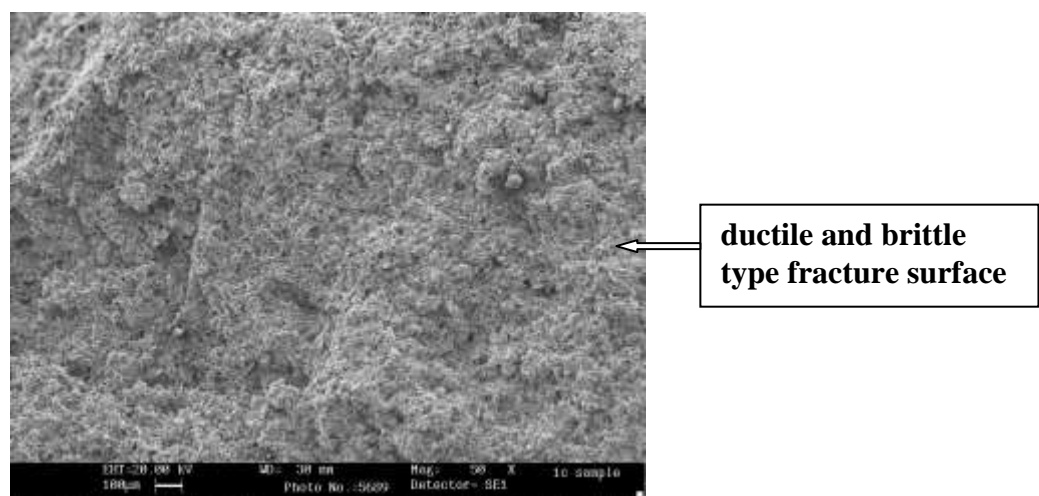


Fig. 9.17: Fracture surface of the 1C tested sample.

The microstructure at Fig.9.18 shows fracture surfaces of the 1M composite sample tested for flexural strength. The fracture surface of the composite which is comprised of 90 vol. % of aluminium and 10 vol. % of cenospheres sintered in microwave has been observed in the SEM for the fracture characteristic. Here too the microstructure reveals a mixed mode of fracture surface which comprises of cup and cone type of contour which supports the fact that this type of fracture is attributed to the ductile material which is aluminium. The other type of fracture i.e. coarse grained surface seen also supports the fact that the fracture surface is also composed of regions having brittle features contributed by cenospheres which are ceramic in nature, when seen at a magnification of 100 X.

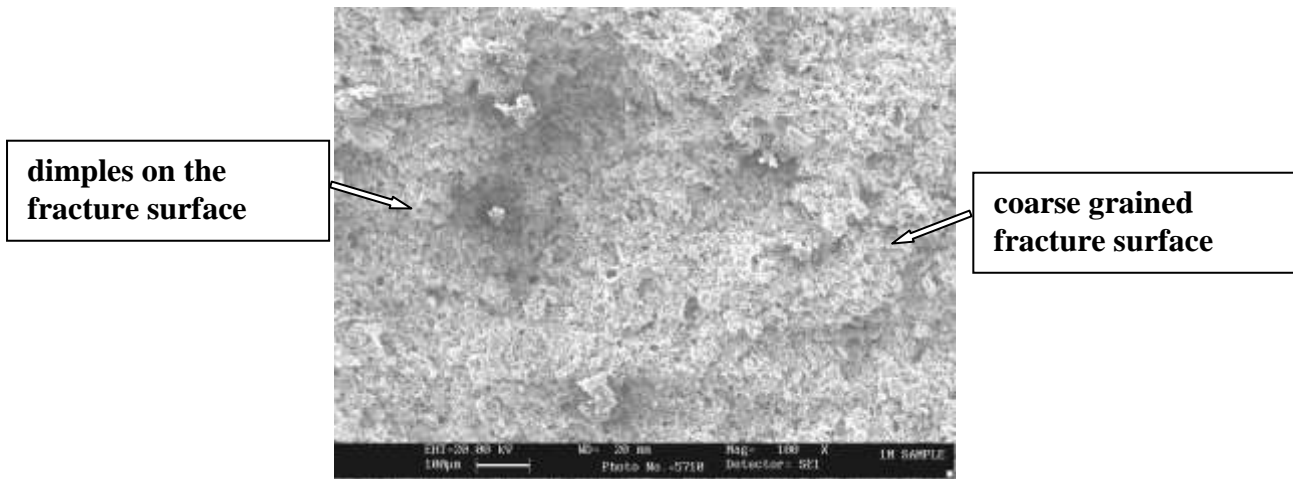


Fig. 9.18: Fracture surface of the 1M tested sample.

The microstructure at Fig.9.19 shows fracture surfaces of the 5C composite sample tested for flexural strength. The fracture surface of the composite which is comprised of 60 vol. % of aluminium and 40 vol. % of cenospheres sintered conventionally has been observed in the SEM for the fracture characteristic. The microstructure reveals more of brittle mode of fracture and less of cup and cone features representing ductile surface which is attributed to aluminium. The brittle mode seen from the coarse grain line fracture surface is mainly attributed to the materials of ceramic nature. In this case the sample has 40 vol. of cenospheres dispersed in the matrix which is supporting brittle type of fracture due to ceramic nature of the cenospheres.

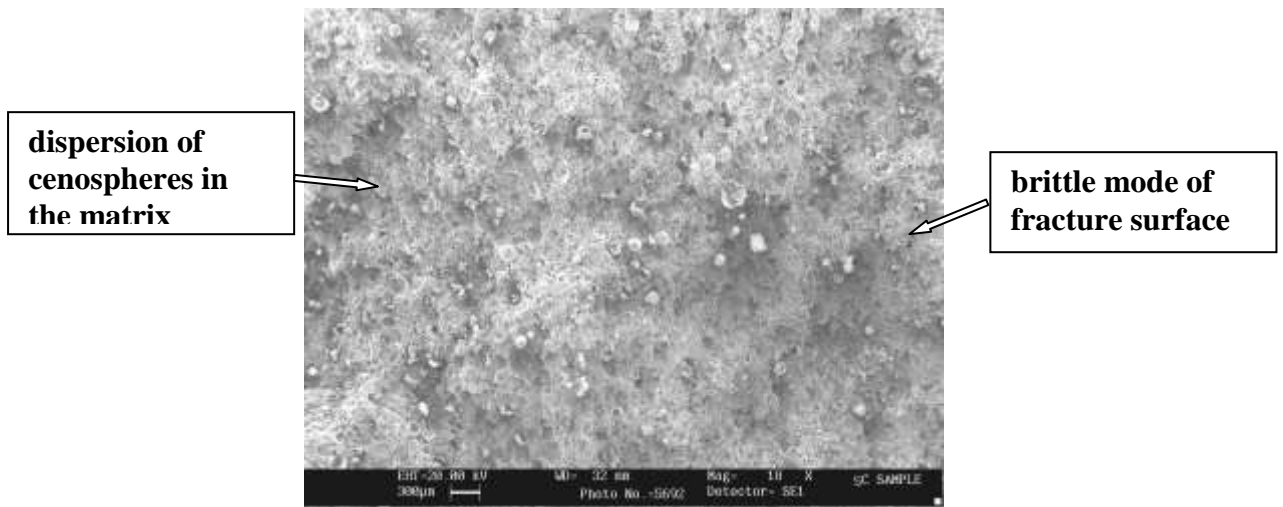


Fig. 9.19: Fracture surface of the 5C test sample.

The microstructure at Fig.9.20 shows fracture surfaces of the 5M composite sample tested for flexural strength. The fracture surface of the composite which is comprised of 60 vol. % of aluminium and 40 vol. % of cenospheres sintered in microwave has been observed in the SEM for the fracture characteristic. The microstructure reveals more of brittle mode of fracture and less of cup and cone features representing ductile surface which is attributed to aluminium. The brittle mode seen from the coarse grain line fracture surface is mainly attributed to the materials of ceramic nature. In this case the sample has 40 vol. of cenospheres dispersed in the matrix which is supporting brittle type of fracture due to ceramic nature of the cenospheres.

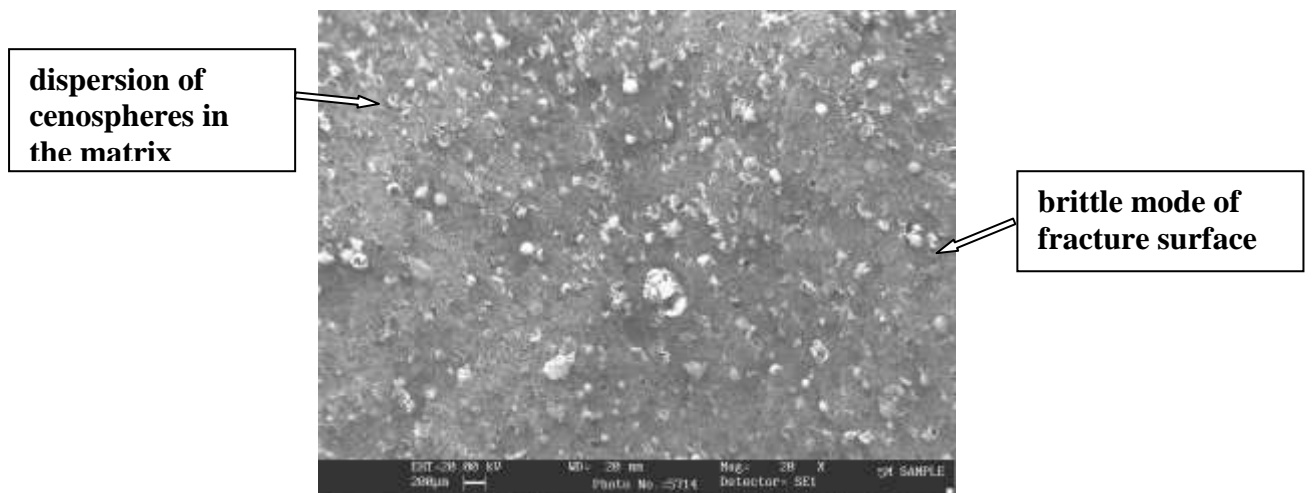


Fig. 9.20: Fracture surface of the 5M test sample

9.4 Brinell Hardness Number

It can be seen from the Fig.9.21 that BHN value for the pure aluminium composites without cenospheres addition were 32 and 46 for the 1C and 1M designated samples respectively. Microwave sintered samples showed higher BHN value by about 30.4% compared to conventionally sintered one.

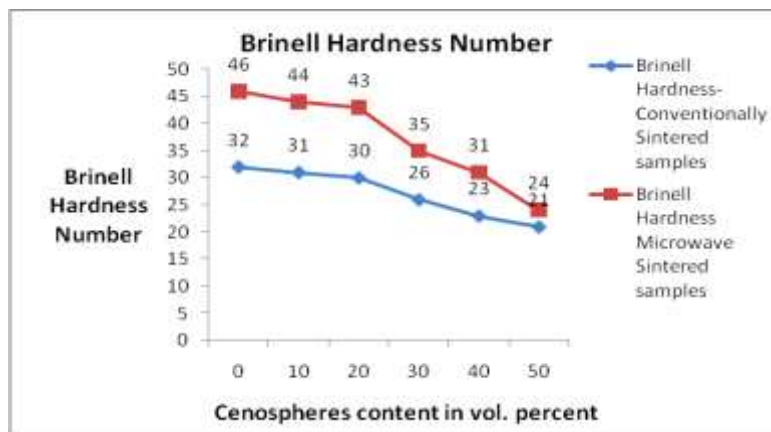


Table 9.21: Brinell Hardness Number (BHN) of samples

As the cenospheres content was increased from 0 to 10, 20, 30, 40 and 50 vol. %, the BHN value of the composites decreased proportionally. But the BHN values were on the lower side for all the microwave sintered samples compared conventionally sintered ones. The 2M samples exhibit 29.5 % less BHN value compared to 2C samples, 3M samples exhibit 30.2 % less BHN value compared to 3C samples, 4M samples exhibit 25.7 % less BHN value compared to 4C samples, 5M samples exhibit 25.8 % less BHN value compared to 5C samples and 6M samples exhibit 12.5 % less BHN value compared to 6C samples. The decreasing trend in the BHN values proportionally to the increase in cenospheres content can be seen in the Fig.6.10. The microwave sintered samples exhibiting increased values in the BHN compared to conventionally sintered samples which can also be seen from the table 5.4.

9.5 Discussions on mechanical properties

It is observed from the Fig.9.1 that as the volume fraction of the cenospheres increased from 0 to 50 vol. %, the mechanical properties in terms of compression and

flexural strength reduces proportionately to the increase in cenospheres content. The total fracture energy decreases as the volume fraction of cenospheres increases irrespective of the applied compact pressure. Several parameters such as porosity distribution, insufficient wetting of matrix material with reinforcement etc., play a role in deciding the strength of the composites. Under uniaxial compression test, fracture gets initiated at the bottom of the specimens. The detachment of the external walls from the test specimen from the main body core and formation of shear planes in discrete areas, were observed as the specimens' main failure mechanisms. This is well supported from the finding of the FEA undertaken for 2C to 6C and 2M to 6M samples with increased cenospheres content.

The density of the sample also strongly depends on the compaction pressure applied to the mix during fabrication (green body), as does porosity. Insufficient packing during compaction also result in unintended porosity within the matrix thereby contributing for the reduction in strength.

During compression testing it was observed that as the deformation increased, the external walls of the composite began to detach from the main body revealing the internal core of the material. This behavior may be attribute to the inhomogeneous distribution of porosity, since the walls and the bottom of the composite were less dense compared to the specimen's core.

Some reports also suggest that behavior of the fracture modulus E_f is mainly related both to the bonding between matrix and the reinforcement particles after sintering and to the volume fraction of the cenospheres in the composite. The ductility also reduces with increasing cenospheres content in the matrix there by leading to brittleness. The presence of micro-porosity (unintended porosity) from the composite as well as porosity from cenospheres interferes adversely to the sintering process because the distance between the matrix and the particle is increase, and it is likely that cenospheres as well as fractured cenospheres enhance imperfections in the composite, which can prevent a number of matrix particles to bond mechanically with the

reinforcement prior to sintering. The above reasons result in insufficient bonding between aluminium matrix and the cenospheres particles after sintering, which leads to the reduction of the ductility of the composite. [Vogiatzis et al 2015].

Since cenospheres are ceramic and brittle in nature, this brittle phase can lead to poor interfacial stress transfer and is detrimental to the quality of the composite in terms of mechanical strength. Differences are observed between compressive yield strength values in composites of different matrices, which may be related to the difference in the test techniques rather than the fundamental material behavior itself. It is important to note that most aluminum matrix syntactic foams have a compressive strength over 100 MPa. These observations are limited to the data reported in the literature but the numbers may be different for other compositions. The strength increases with foam density for all types of foams. [Dung D. Luong et al]

The extent, to which the compressive stress has reduced in the composite on increasing the cenospheres content after yielding, is either a measure of the degree of agglomeration or the tendency of breakage and collapse of cenospheres during yielding. At this condition, the cenospheres within in the composite deforms elasto-plastically which would lead to strain hardening in the matrix. But because of the mechanical bonding between cenospheres and the matrix, and also the porous nature of the cenospheres, the strain hardening is not so significant. The interface at cenospheres surface in the aluminium matrix as well as the porous nature of cenospheres shells acts as dislocation sink sites and thus the matrix strain hardening is expected to be very marginal or low.

Additionally, the cenospheres shells also gets shared and starts fracturing which results in the reduction in modulus and thus the stress starts decreasing. The cenospheres fraction in the matrix get shared, broken and collapsed and the matrix starts yielding as soon as the stress levels reach to that extent at which the next series of cenospheres starts cracking and sharing. Since the composites are also highly porous in nature as seen from the porosity graphs, the deformation is also expected to be highly inhomogeneous and localized. The collapse of cenospheres, shearing of the

matrix around the cenospheres and compaction of the cenospheres and the pores take place simultaneously during deformation of the composite during loading.

At the initial stage, during yielding a major fraction of cenospheres may get sheared, broken and collapsed leading to greater degree of stress reduction and hence reduces the compressive or flexural strength. During the deformation process, matrix undergoes strain hardening and as a result there would be a steady increase of stress with strain while deforming. This is attributed to the fact that collapse and breakage of cenospheres and in due course its densification nullifies the effect of strain hardening and is responsible for decrease in stress values. [D.P. Mondal et al 2009]

The metal matrix composites behave like any other foam when loaded in compression. During compression testing, there are three regimes of behavior when loading in compression. The first regime initially starts with a linear elasticity. on further loading, the linear elastic regime is followed by the second regime, the plateau strength. The third regime is the final regime which ends by the densification strain. The failure behavior of the metal matrix composite may be different either due to its compositions. The failure is controlled by the different plastic characteristics of the matrix and the reinforced material. The failure may be either due to ductile mode of failure, or may be collapsing of the structure of the cenospheres on loading. The failure may also occur due to shearing mode due to the crushing of the cenospheres which are ceramic in nature. [M. Altenaiji et al 2012]. Zhao et al, 2008 have reported that three factors affect the failure behaviour of metal matrix foam namely ductility of metal matrix, structure of ceramic cenospheres and, thirdly the volume fraction of ceramic cenospheres and metal matrix. It is also reported that the behaviour of metal matrix composite's performance failure depends on the type of the metal used for the matrix. Further it is stated that the strength of the cenospheres has also an effect on the strength of metal matrix composites.

It is observed from Table 2 that as the temperature of sintering increases, there is increase in bulk density and hardness with reduction in apparent porosity in the

sintered samples. The Porosity (%) values of microwave sintered composites are lower when compared to conventionally sintered composites. The Brinell Hardness Number of microwave sintered composites is higher compared to conventionally sintered composites.

At higher temperatures of sintering, pores become more closed because micro pores vanish during the sintering process of the material. The sintering temperature and the process influence the bulk density, mechanical strength, thermal stability, porosity and shrinkage of the samples [Morteza Oghbaei 2010]. The development of physical and mechanical properties is related to the phases formed due to reaction sintering between alumina and alumino-silicates and formation of compact microstructure [Satapathy et al 2012].

Material density is an important characteristic for predicting mechanical properties and permeability. As the density increases (and porosity decreases), the mechanical properties also increase with decrease in permeability. It is observed that there is formation of complex oxides in the composite matrix when sintering at higher temperatures beyond 650⁰C. The same has been observed by other authors, who have reported that the thermodynamic analysis of the Aluminum Cenosphere composite indicate a possibility of chemical reaction between the Alumium melt and Cenosphere particles leading to reduction of alumina, silica and iron oxide during their contact with the melt. The elemental Si formed by the reduction reaction would alloy with the matrix and that the Gibbs free energy and the heats of reaction of this reaction are highly exothermic in nature. As a result greater amount of eutectic silicon is seen in the composite and the chemical reaction indicates the increase in silicon level in the matrix [Ananda kumar et al 2014]. This may be possible since the XRD graphs of this study also indicate the presence of silicon and alumina peaks in the high temperature sintered samples.

Aluminium cenospheres metal matrix composite have similar structural characteristics as those of metal matrix syntactic foams. Under compression loading they may have different failure modes such as ductile which forms due to the collapse and crushing

of the cenospheres, brittle mode wherein the failure is due to shear failure or in the form of fracture which is caused due to initiation of cracks while loading the sample. The fracture mode of failure very much agrees with that of Griffith's Rupture theory. The main criteria available to predict the failure mode of MMCs under compression is the ductility nature of the metal matrix, volume fraction of matrix and the inner structure of the reinforcement particle[Zhao YY et al 2009].

Balch et al have proposed that the pure aluminium matrix fails by ductile plastic deformation whereas the aluminium alloy based composites failed by shear fracture. The matrix to reinforcement ratio has a bearing on the failure mode of the composite. The increase in the reinforcement content to that of matrix leads to the failure of the composite in the brittle mode while the increase in the matrix component leads the composite to fail in ductile mode. The reinforcement having varied structure and porosities may fail in different modes.

Metal matrix syntactic foams are particularly suited to applications where permanent deformation at low stresses is undesirable. To summarize, the Aluminium Cenospheres MMCs manufacture by different methods have different microstructures and properties. The manufacturing of the MMCs through melt Infiltration casting , though a simple process has a disadvantage of its inability to vary the volume fraction of the cenospheres[Zhao YY et al 2009].

The compressive strength of MMCs not only depends on the strength of the metal matrix but also on the ceramic reinforcement and its volume fraction, structure and distribution in the matrix. The interfacial bonding between the matrix and the reinforcement, amount of the defects present also have a bearing on the compressive strength of the composites. In metal matrix syntactic foams, both the metal matrix and the ceramic particles contribute to the compressive strength of the syntactic foams.

The same metal matrix in different forms and the different heat treatment procedures can also result in the difference in the compressive strengths of the composites. For example aluminium MMC fabricated through stir casting route may have different

compressive strengths compared to the PM route fabricated ones. [YY Zhao et al 2009].

Rohatgi et al have reported that the compressive yield strength of the Al matrix syntactic foams increased with increasing particle size of the ceramic spheres, while others have reported that larger ceramic spheres are had high compression strength. However, the variation in compressive strengths in both the cases were attributed to the different void contents in different sized ceramic cenospheres instead of different geometries. Porous cenospheres can also be used in producing MMCs with the same composition and porosity; however, porous ceramic spheres are much weaker than hollow cenospheres. The Al matrix syntactic foams containing porous ceramic spheres have much lower compressive strength than those containing hollow ceramic spheres. [YY Zhao et al 2009].

The aluminium cenospheres MMCs, produced by stir casting can have variable volume fractions of reinforcement but the distribution of the distribution of the same is inhomogeneous leading to varying properties which are not consistent and lacks repeatability of the process for consistent product. The production of aluminium cenospheres MMCs through liquid sintering can produce metal matrix composites with variable amounts of uniformly distributed ceramic particles. However, it has a high production cost and the as-produced syntactic foams often contain structural defects [Zhao YY et al 2009],

It is observed from the plots at Fig. 9.13 that the FEM analysis indicates that the compressive stress values are higher by about 7.82 to 9.54 % compared to tested samples for the samples 1C to 5C. It is also observed from the plots at Fig.9.20 that the FEM analysis indicates that the compressive stress values are higher by about 9.52 to 9.54 % compared to tested samples for the samples 1M to 5M. The marginally higher values predicted from FEM analysis is due to the assumptions taken for modeling such as perfect geometry of the test samples, no variation in the load vs. displacement values, and uniform property of the sintered composite throughout without much variation etc., but in practice, there may be deviations in the geometry

from sample to sample and also in the variations in the load vs. displacement values, which are reflected in the FEM analysis with marginal difference in the predicted values.

Relatively large volume fractions ($> 10\%$) of the ceramic reinforcement profoundly affect the behavior of aluminium matrix composites during manufacturing, sintering and during service. These changes can be further classified as intrinsic and extrinsic changes. Amongst the intrinsic effects which include micro structural alterations, change in the heat treatment characteristics, thermal stresses etc., which significantly affect the physical, mechanical, tribological and thermal properties. The ceramic reinforcement such as cenospheres alter the solidification behavior of the aluminium matrix by way acting as a thermal barrier to diffusion of heat. It catalyses the heterogeneous nucleation of the crystallizing phase from the melt and restricts convection of fluid thereby inducing morphological instability in the solid liquid interface [Surappa 2003]. The main reason as to why microwave sintering yields better mechanical properties in the composites fabricated through Powder Metallurgy route is that in case of powder metals, it produces finer grain size on sintering and the shape of the porosity is different compared to the conventionally sintered. Powder metal samples sintered through microwave show round edged porosities, producing higher ductility and toughness [Rustum Roy et al 1999].

All the properties of a given material are determined by its microstructure. The critical issue in micro structural development is the densification of the material and coarsening. The micro structural development depends on the parameters such as optimized temperature, sintering time, heating rate and the pressure. The rapid heating rate is the key to produce products with a high sintered density for a given microstructure and grain size compared to slow heating for the same sintered density. Conventional sintering has definite disadvantages accompanied with difficulties since conventional sintered product have differential sintering that give rise to differential densification leading to inconsistent properties. In this context, microwave sintering is an alternative sintering technique to overcome these problems of conventional sintering. Since microwave sintering is a non-contact sintering technique in which heat gets transferred to the product through electromagnetic radiation. By microwave

sintering large amount of heat can be transferred to the material's interior which reduces differential sintering to a large extent. The microwave sintered products also have finer micro-structural development, with average grain size and higher density which result in enhanced mechanical properties as compared to the conventionally sintered ones.

Morteza Oghbaei et al [2010] has reported that microwave sintering effectively assist the forward diffusion of ions which accelerates the sintering. This results in matrix densification by grain growth process. Sintering process aids re-crystallization, grain growth and densification at high temperatures in the body that is being sintered. This densification mechanism is strongly dependent on diffusion of ions between the same sample particles. The mechanism of grain growth rate is assisted by the grain boundary diffusion process. It has been found that intense microwave field concentration is active around the particles of the sample while sintering. The power of this microwave field between the particles of the sample in the bulk of the material is about 30 times higher than the external field and this is sufficient to ionize the sample particles at its surface. This accelerates ionic diffusion which promotes rapid densification of the material is promoted under microwave sintering.

Apart from the microwave radiation, the surrounding electromagnetic field also effectively enhances the ionic diffusion kinetics near the grain boundaries. The kinetic energy of the ions at the grain boundary increases which thereby decrease the activation energy required for the forward ion jump and in the process increases the barrier height for the reverse jump. This mechanism promotes forward diffusion of the inter grain ions which accelerates the grain growth during sintering.

An important feature of the aluminium alloy composite containing cenospheres is their distribution and interface between reinforcement and matrix. Disadvantages in the case of composites fabricated through stir casting or gravity casting route, is that the occurrence of agglomerations which may be caused by a characteristic limitation of the stirring technique. Porosity located in the neighborhood of interface is an effect of premature particle-matrix de-cohesion during crystallization. The cenospheres

distribution in the molten metal matrix is also influenced by the tendency of particles to float due to density differences and interactions with the solidifying metal. It is also pointed out that cenospheres that are present in the inter dendritic regions between aluminium dendrites, due to lack of nucleation site for aluminium on cenospheres particles and also due to pushing of cenospheres by growing aluminium dendrites during solidification, strains are developed in the matrix leading to stress concentrations, which affect the mechanical and other properties. [J. Bienias et al 2003]

An alternative to conventional alloys are metal matrix composites (MMCs), which have a high specific modulus, good wear resistance and a tailorable coefficient of thermal expansion. A major drawback to these MMCs is high cost. The reasons are twofold. First, the material itself is expensive because specially synthesized pre-alloyed powders are usually required and many processing steps are needed. The powders are typically cold pressed, then hot pressed or sintered and extruded. Canning and vacuum degassing are common. The second reason that these alloys are expensive is due to the high costs of secondary processing. They are not produced to near net shape and therefore require extensive forging or machining, which can be particularly problematical because of the ceramic component. Conventional P/M processing can overcome both these problems. Only two processing steps are required (pressing and sintering) and the part is formed into its final shape in one operation – it is the quintessential net shape process. Thus there is significant potential for press-and-sinter processed aluminium P/M composites in order to provide high stiffness at low cost. However, adding significant quantities of an inert ceramic reinforcement phase to an aluminium P/M matrix is problematical.

For optimum sintering, inclusions need to be equiaxed and uniformly distributed. Clustering of reinforcing particles should be avoided. This can be achieved by matching the particle size of the reinforcement powders to the particle size of the matrix powders. For very fine reinforcement particles, every aluminium particle will be completely surrounded by reinforcement particles and the system will be incompressible and non sinterable. As the particle size ratio is increased, the volume

fraction reinforcement can be increased. At a large particle size ratio, the reinforcement particles have a lower probability of being part of a cluster network and are evenly spaced through the aluminium matrix. Load bearing clusters do not impede compaction and the sintering rate is homogenised throughout the compact.

De-sintered zones are less likely to form and sintering cracks are less likely to develop. Improved sintered densities result. Coarse reinforcement particles are therefore preferred. A second distinct feature that can be clearly correlated with high performance sintered MMC's is that the reinforcing phase must be fully wet by the liquid phases produced during sintering in order to generate an effective, load bearing interface. In the absence of wetting, sintering is poor and the properties are much-reduced.

The toughness and higher ductility contributes to better mechanical properties. The distinct uniformly distributed pores in the microwave sintered samples lower the stress concentration factor there by contributing to increased mechanical properties due to increasing loads to fracture. Conventionally sintered samples exhibit uneven pore distribution with sharp, triangular and wedge shaped pores that The observed porosity in microwave sintered composites is round edged porosity which contributes act as stress concentrators thereby enabling the sample to fail due to fracture at lower loads.

Existence of the continuous metal phase makes it possible for the crack to propagate through the matrix. Moreover, good fracture toughness of the metal facilitates the crack deceleration in the binder phase. A dislocation pileup is formed and subsequently that induces the formation of the crack nuclei when the maximum shear stress is greater than the critical stress for dislocation generation. In the cermets, containing a high volume of the ceramic phase, the interfaces are the preferred site to produce micro cracks because of the presence of crystallographically disoriented boundaries and large residual stresses at those areas. [Maksim Antonov 2006].

Hence it is concluded from this study that the composites exhibit good properties only at a certain vol. % of cenospheres are present in the matrix. Most of the physical and mechanical properties decrease proportionally to increase in the cenospheres content. The mix design needs to be properly selected to fabricate composites with required properties for use in applications.

CHAPTER 10

CONCLUSIONS FROM THE STUDY

The study on the various properties of the Powder Metallurgy based Aluminium Cenospheres composites sintered in Microwave at 675⁰C have led to the following conclusions which are summarized as below:

1. Aluminum metal matrix composites can be fabricated through Powder Metallurgy route with Cenospheres as reinforcement and the densification of the composite achieved by Microwave sintering at a temperature of 665°C. The matrix formed is that of pure aluminum metal without undergoing oxide formation. The filler cenospheres are also evenly dispersed throughout the matrix with its shape intact. It was observed that the aluminium metal powder reacts with cenospheres to form alumino-silicates and alumina (Al₂O₃) at temperatures beyond 665°C and above, in the oxidizing atmosphere. Beyond this temperature the cenospheres undergo self-sintering to become complex oxides the matrix also ceases to be metallic.
2. The physical properties shown that the Bulk Density value was on the higher side for the microwave sintered samples compared conventionally sintered ones which varied from 2.1 to 2.7 % for various volume % of cenospheres. The Water Absorption values were on the lower side for all the microwave sintered samples by about 12.2 to 13.6% compared conventionally sintered ones, and the Porosity values were on the lower side the microwave sintered samples by 18.6 to 23.1% compared to its counterpart the conventionally sintered ones.
3. The erosion resistance properties of the composite samples show encouraging results up to 30 vol. % loading of cenospheres in the composites. The samples also exhibited sufficient ductility at this vol. % of cenospheres. The erosion loss seems to be more pronounced at acute erosion angle of 30⁰ for all the samples and the loss was comparatively less at impingement angles between

60 to 90⁰ deg for the conventionally sintered samples. The erosion loss was between 3.0-13.9 % lower for the microwave sintered samples at 30⁰, 2.1 to 43.8 % at 45⁰, 19.6 to 33.3% at 60⁰ and 6.2 to 62.6% wear loss at 60⁰ angles compared to the conventionally sintered samples.

4. The dry sliding wear loss increases as the cenospheres content increases in the composites and the wear rate also remarkably increases as the load increases. The wear loss is high at 3 kg loading of the sample. The wear loss in conventionally sintered composites is more pronounced than the microwave sintered samples. The wear loss is mild at lower cenospheres content and tends to become severe as the cenospheres content gets increased. The dry sliding wear loss was between 19 to 53.0 % lower for the microwave sintered samples at 1 kg load, 14.7 to 46.2 % at 2 kg load and 12.1 to 38.5% at 3 kg load compared to the conventionally sintered samples.
5. The Compression strength of the composites containing was found to decrease from 140.3 to 71.7 MPa with the increase in cenospheres content from 10 vol. % to 50 vol. %, for microwave sintered samples. For the conventionally sintered composites the strength reduced from 125.0 to 62.5 MPa. The compressive strength of microwave sintered samples was more by 12.8 to 22.2 % compared for 10 to 50 vol. % of cenospheres compared to the conventionally sintered samples. After 25 thermal shock cycles the compression strength decreased from 44.3 to 49.4% for the conventionally sintered samples and from 25.1 to 47.6% for the microwave sintered samples, containing 10 to 50 vol. % of cenospheres in the composites. Microwave sintered samples had better thermal shock resistance properties.
6. The Co-efficient of Thermal Expansion of the microwave sintered composites decreased with increase in the cenospheres content. The CTE values decreased from 16.3 to 3.6 x 10⁻⁶/⁰C for 10 to 50 vol % cenospheres increase respectively. The conventionally sintered samples showed high co-efficient of thermal expansion between 20.9 to 50.7 % compared to microwave sintered ones

which were on the lower side.

7. The Flexural strength of the conventionally sintered composites was seen decreasing from 52 to 8.8 MPa while Flexural strength of microwave sintered composites were decreasing from 71.9 to 31.5 MPa with increase in cenospheres content from 10 to 50 vol %. MW sintered was better by about 23.7 to 72.1 % in Flexural Strength compared to the conventionally sintered composites.
8. The Brinell Hardness Number of conventionally sintered samples for 10 to 50 vo.% of cenospheres composite was seen to reduce from 32 to 21 whereas microwave sintered sample showed BHN reducing from 46 to 24. The microwave sintered samples had high BHN values by about 12.5 to 35.4% compared to the conventionally sintered ones.
9. The aluminium powder in the mix does not get converted into alumina (oxide of aluminium) as had happened in the previous experiments when sintered in microwave or conventional sintering at temperatures above 665⁰C. The matrix is still metallic in all the composition of the composites sintered both in microwave and conventional sintering. This confirms that the matrix of the composite metallic comprises of aluminium metal. The microwave sintering has also shown that the sintering takes place uniformly throughout the bulk of the material. The sintering process is rapid, has high heating rates, reduced processing times, uniform temperature throughout with minimal thermal gradients. Aluminium metal matrix composites can be fabricated through powder metallurgy route sintered in microwave sintering which is found to be adoptive & effective rapid sintering method for development of aluminium-cenospheres composites fabricated through powder metallurgy route at lower temperatures. It is possible to fabricate Aluminium Cenospheres 'Syntactic Foams' through powder metallurgy microwave sintering and the properties for the same match with those materials for applications in automotives.

10.1 Scope for future work

The following are the scope for future works:

1. To extend the concept of fabrication of powder metallurgy based aluminium cenospheres MMCs for higher volume microwave sintering.
2. To comprehensive study of powder metallurgy based microwave sintered aluminium cenospheres interface in the composite.
3. To evaluate the thermal behavior of the composites with reference to heat capacity and thermal conductivity for use in thermal/ energy saving applications.
4. Evaluate the mechanical properties such as tensile strength, fracture toughness, fatigue and impact load studies.
5. Study of the composites for vibration damping characteristics and the soundness of the structure for use in damping materials.
6. Demonstration of the composite product in real time in syntactic foam applications for use in automobile industry

RESEARCH PUBLICATIONS

- 1) M. G. Ananda Kumar, S. Seetharamu, Jagannath Nayak & L. N. Satapathy ‘Study on Thermal Behavior of Aluminium Cenospheres Powder Metallurgy Composites Sintered in Microwave’ (2014) *Elsevier’s Science Direct Journal, Procedia Materials Science*, 5, pp 1066-1074.
- 2) M. G. Ananda Kumar, S. Seetharamu, P. Sampath Kumaran and Jagannath Nayak, ‘The influence of Microwave sintering on the Tribological performance of Powder Metallurgy based Aluminium Cenospheres composites’, (2015), Scientific.net, *Materials Science and Engineering*, Trans Tech Publications, Switzerland, Vol. 830-831, pp 71-74.
- 3) M. G. Ananda Kumar, S. Seetharamu & Jagannath Nayak, ‘A Study on the Physical and Morphological Characteristics of Aluminium Cenospheres Composite Sintered at High Temperature in Microwave’ , (2014) *Journal of CPRI*, Volume 10, Issue 02, March, pp 385-394.
- 4) M. G. Ananda Kumar, M. Shekhar Kumar, K. Suryanarayana, S. Vynatheya, T. R. Venkatesh, S. Seetharamu and Jagannath Nayak, ‘Fly Ash Cenospheres –A resourceful material for engineering applications’,(2015) *Journal of CPRI*, Volume 11, Issue No. 01, March, pp 207-222.
- 5) M G Ananda Kumar , Nataraj J R, S. Seetharamu, Jagannath Nayak, ‘A study on the mechanical behaviour of microwave sintered aluminium cenospheres based syntactic foams’ , (2016) *Journal of CPRI*, Volume- 12, Issue No. 2 – June 2016, pp
- 6) M G Ananda Kumar, Jagannath Nayak, ‘Microwave sintering: An energy efficient process for sintering aluminium metal powder’, (2016) *Journal of CPRI*, Volume- 12, Issue No. 2 – June 2016, pp.

References:

Adefemi O. Adeodu, Christopher O. Anyaeche, Oluleke O. Oluwole, Charles U. Omohimoria, (2015), “Effect of Microwave and Conventional Heating on the Cure Cycles of Particulate Reinforced Polymer Matrix Composites”, *International Journal of Materials Science and Applications*, Volume 4, Issue 4 , July 2015, 229-240.

Altenaiji M, Schleyer G K, Zhao YY, (2012), “Characterisation of Aluminium Matrix Syntactic Foams under Static and Dynamic Loading”, *Intech*, Chapter 19, 437 -456.

Ananda Kumar M.G, Seetharamu S. Jagannath Nayak, (2014), ‘A Study on the Physical and Morphological Characteristics of Aluminium Cenospheres Composite Sintered at High Temperature in Microwave’, *Journal of CPRI*, Volume 10, Issue 02, March, 385-394.

Ananda Kumar M.G, Seetharamu S. Jagannath Nayak, L. N. Satapathy, (2014), ‘Study on Thermal Behavior of Aluminium Cenosphere Powder Metallurgy Composites Sintered in Microwave’ (2014) *Elsevier’s Science Direct Journal, Procedia Materials Science*, 5, 1066-1074.

Ananda Kumar M.G, Seetharamu S. P. Sampath Kumaran and Jagannath Nayak, (2015), ‘The influence of Microwave sintering on the Tribological performance of Powder Metallurgy based Aluminium Cenospheres composites’, *Scientific.net, Materials Science and Engineering*, Trans Tech Publications, Switzerland, Vol. 830-831, 71-74.

Ananda Kumar M.G, Shekhar Kumar M., Suryanarayana K., Vynatheya S., Venkatesh T. R., Seetharamu S. and Jagannath Nayak,(2015), ‘Fly Ash Cenospheres –A resourceful material for engineering applications’, *Journal of CPRI*, Volume 11, Issue No. 01, March, 207-222.

Anklekar R.M, Bauer.K, Agrawal D.K, and Roy. R,(2005) “Improved mechanical properties and microstructural development of microwave sintered copper and nickel steel PM parts”, *Powder Metallurgy*, 48, No.1, 39-45.

Anthony Macke, Schultz B F, Rohatgi P K, (2012), Metal Matrix Composites: Offer the Automotive Industry an Opportunity to Reduce Vehicle Weight, Improve Performance, *Advanced Materials & Processes*, 19-23.

ASM Handbook Vol.7, (1998), Powder Metal Technologies- *Porous Powder Metallurgy Technology*, 2568-2582.

Asokan P., Mohini Saxena, Shyam R. Aslokar, (2005) “Coal combustion residues- environmental implications and recycling potentials”, *Resources Conservation & Recycling*, 43, 239-262.

ASTM G 76 – (2004) Standard, ‘Standard Test Method for Conducting Erosion Tests by Solid Particle Impingement Using Gas Jets’.

Baskar B, Handjezian, Satkthivel, 2015, “sound absorption and Noise Reduction Properties of Syntactic Aluminium Matrix Composites”, *Journal of chemical and Pharmaceutical Sciences*, Special Issue 6, 159- 162.

Bhattacharya A, Calmidi V.V, Mahajan R.L,(2002), “Thermo-physical properties of high porosity metal foams”, *International Journal of Heat and Mass Transfer*, 45, 1017-1031.

Bienias J, Walczak M, Surowska B and Sobczak J, (2003), “Microstructure and Corrosion Behaviour of Aluminium Fly Ash Composites”, *Journal of Optoelectronics and Advanced Materials*, Vol 5, No.2, June 2003, 493- 502.

Chandrakant R Kini, Shivaprakash YM, Gowrishankar MC, Sharma SS, Sreenivasa Prasad KV, (2015), “Investigation on the Behaviour of ALFA Composite in Pre and

Post Heat Treated Conditions”, *International Journal of Research in Engineering and Technology*, Vol.4, Issue 02, 28-37.

Chandrasekaran S, Tanmay Basak, Ramanathan S, (2011), “Experimental and theoretical investigation on microwave melting of metals”, *Elsevier Journal of Materials Processing Technology* 211, 482-487.

Chun Lin He, Shao Jian Ma, Xiu Juan Su, Yan Qing Chen, Yu Shi Liang, (2013), “Calorimetry Study of Microwave Absorption of Some Solid Materials”, *Journal of Microwave Power and Electromagnetic Energy*, 47 (4), 2013, 251-261.

Das S, (2004), “Development of Aluminium alloy Composites for Engineering Applications”, *Transactions, Indian Institute of Metals*, Vol.57, No. 4, . 325 - 334.

David Raja Selvam. J, Robinson Smart. D.S. Dinaharan.I, 2013, “Synthesis and characterization of Al6061-Fly Ashp -SiCp composites by stir casting and compocasting methods”, *Elsevier Energy Procedia*, 34 (2013) 637 – 646

Dinesh K Agrawal, (1998) “Microwave processing of ceramics”, *Current opinion in Solid State & Materials Science*, 3, 480-485.

Dorian K Balch, John G O Dwyer, Graham R Davis, Carl M Cady, George T Gray III, David C Dunand, (2005), “ Plasticity and damage in aluminium syntactic foams deformed under dynamic and quasi-static conditions”, *Elsevier-Materials Science and Engineering*, A 391, 408-417.

Dou Z.Y, Jiang L.T, Wu, G.H, Zhang Q, Xiu Z.Y and Chen G.Q, (2007) “High strain rate compression of cenospheres-pure Aluminium syntactic foams”, *Scripta Materialia*, 57, 945-948.

Dung D. Luong, Oliver M. Strbik III, Vincent H. Hammond, Nikhil Gupta, and Kyu Cho, “Development of high performance lightweight aluminum alloy/SiC hollow

sphere syntactic foams and compressive characterization at quasi-static and high strain rates', pdf, *Internet*.

Ebadzadeh T., M. H. Sarrafi, E. Salahi, (2009) "Microwave assisted synthesis and sintering of mullite", *Ceramics International*.

Fenelov V B, Melgunov M S, Parmon V N, (2010),"The Properties of Cenospheres and the Mechanism of Their Formation During High Temperature Coal Combustion at Thermal Power Plants, *Kona Powder and Particle Journal No.28*, 189-208.

Gaohui Wu, Xiaoli Huang, Zuoyong Dou, Su Chen, Longtao Jiang, (2007)" Electromagnetic interfering shielding of Aluminium alloy- cenospheres composite", *Mater Sci* 42: 2633 2636.

Ghosh S, K.S. Pal, N. Dandapat, A.K. Mukhopadhyay, S. Datta, D. Basu, (2011)," Characterization of microwave processed aluminium powder" *Ceramics International* 37 , 1115–1119.

Goldstein. A, Kaplan W.D, Singurindi A, (2002) "Liquid assisted sintering of SiC powders by MW (2.45 GHz) heating", *Journal of the European Ceramic Society* 22 1891 -1896.

Guo R.Q., Rohatgi P.K., (1997) "Preparation of Aluminium Fly ash particulate composite by powder metallurgy technique" *Journal of Materials Science-32 Engineering*, 3971-3974.

Guo R.Q., Venugopalan. D, Rohatgi P.K., (1998) "Differential thermal analysis to establish the stability of aluminium- fly ash composites during synthesis and reheating" *Materials Science & Engineering A* 241, 184-190.

Gupta M., Wong W.L.E., (2005), “Enhancing overall mechanical performance of metallic materials using two-directional microwave assisted rapid sintering”. *Scripta Materialia*, 52, 479-483.

Hermann Riedel, Jiri Svoboda, “Simulation of Microwave Sintering with Advanced Sintering Models”, *Proceedings of 8th International Conference on Microwave & High Frequency Heating*.

Hyo S. Lee, Kyung Y. Jeon, Hee Y. Kim, Soon H. Hong., (2000). ‘Fabrication process and thermal properties of SiCp/Al metal matrix composites for electronic packaging applications’, *Journal of Materials Science* 35, 6231 – 6236.

Idalia Gomez, Maryangel Hernandez, Juan Aguilar, Moises Hinojosa, (2004), “Comparative study of microwave and conventional processing of MgAl₂O₄- based materials”, *Ceramics International* 30, 893-900.

Imre Norbert Orbulov, (2012), “Compressive properties of aluminium matrix syntactic foams”, *Materials Science and Engineering*, Volume 555, 52–56.

James Cox, Dung D. Luong, Vasanth Chakravarthy Shunmugasamy, Nikhil Gupta, Oliver M. Strbik III and Kyu Cho,(2014), “Dynamic and Thermal Properties of Aluminum Alloy A356/Silicon Carbide Hollow Particle Syntactic Foams”, *Metals* 2014, 4, 530-548

Jiping Cheng, Dinesh Agrawal, Yunjin Zhang, Rustum Roy, (2002), “Microwave sintering of transparent alumina”, *Materials Letters* 56, 587-592.

Joseph J., Biernacki, Anil.K. Vazrala, Wayne Leimer H., (2008), “Sintering of a class F fly ash”. *Fuel* 87, 782-792.

Kiran Kumar Ekka, S. R. Chauhan, Varun, (2013), “Study on the effects of Ceramic particulates (SiC, Al₂O₃ and Cenospheres) on sliding wear behaviour of Aluminium matrix composites using Taguchi design and neural network”, *International Journal*

of Research in Engineering and Technology, Vol.2, Issue 11, 550-559.

Kok M, (2005), "Production and mechanical properties of Al₂O₃ particle- reinforced 2024 aluminium alloy composites", *Journal of Materials Processing Technology*, 16, 381- 387.

Kwak J.S, Kim Y.S, (2008), "Mechanical properties and grinding performance on Aluminium- based metal matrix composites", *Journal of Materials Processing Technology*, 201, 596- 600.

L.N. Satapathy, G. Swaminathan, S. Vijay Kumar, S. Dhar.,(2012), 'Large-Scale Microwave Sintering of Ceramic Components' , *Interceram* 61, 1–2.

Leszek A. Dobrzanski, (2006), "Significance of materials science for the future development of societies", *Journal of Materials Processing Technology*, 178, 133-148.

Lutgard C. DeJonghe and Mohamed N. Rahaman, "Sintering of Ceramics", *Handbook of Advanced Ceramics*, Chapter 4, 187-253.

Mahnicka, L (2012), 'Influence of Raw Materials Ratio and Sintering Temperature on the Properties of the Refractory Mullite-Corundum Ceramics' *World Academy of Science, Engineering and Technology* 63, 404-409.

Maksim Antonov and Irina Hussainova (2006), "Thermophysical properties and thermal shock resistance of chromium carbide based cermets", *Proceedings Estonian Academy of Science and Engineering*, 12, 4, 358–367

Matsunaga T., Kim J. K., Hardcastle S., Rohatgi P.K., (2002), "Crystallinity and selected properties of fly ash particles", *Materials Science & Engineering A* 325, 333-343.

Miracle D.B and S.L. Donaldson, (2001), “Composites”, *ASM Handbook* Vol.21, 3-17.

Miracle D.B, (2005), “Metal matrix composites- From science to technological significance”, *Composites Science and Technology* 65, 2526- 2540.

Mondal D.P, S. Das, N. Ramakrishnan, K. Uday Bhasker, (2009), “ Cenosphere filled Aluminum Syntactic Foam made through Stir Casting Technique”, *Elsevier: Composites Part A*” 40, 279-288.

Morteza Oghabaei, Omid Mirzaee.,(2010), ‘Microwave versus conventional sintering: A review of fundamentals, advantages and applications’, *Journal of Alloys and Compounds*, 494, 175-189.

Nath S. K., Sanjay Kumar, ‘Wear Resistant Ceramics from Fly Ash ’National Metallurgical Laboratory, Council of Scientific & Industrial Research, Jamshedpur-831007, 1-7. *Internet Search*.

Nawathe S., Wong W.L.E., Gupta M.,(2009), “Using microwaves to synthesize pure Aluminium and metastable Al/Cu nanocomposites with superior properties”, *Journal of Materials Processing Technology*, 209, 4890-4895.

Nikhil Gupta, Pradeep K. Rohatgi (2015), Book on ‘Metal Matrix Syntactic Foams: Processing, Microstructure, Properties and Applications’, *Destech Publications Inc.*, USA.

Nipendra P Singh, Lawrence C. Boyd Jr., Robert M. Purgert, Jerzy Sobczak, (2003), “ Aluminum Syntactic Foams ALFA for Automotive Applications’, *Journal of KONES, Internal Combustion Engines*, Vol.10, 3-4.

P.K. Rohatagi, (1997) “Preparation of Aluminium fly ash particulate composite by powder metallurgy technique”, *Journal of Materials Science*-32 3971-3974.

P.K. Rohatgi, Nikhil Gupta, Benjamin F Schultz and Dung D Luong, (2011), “ The Synthesis, Compressive Properties and Applications of Metal Matrix Syntactic Foams. *The Journal of the Minerals, Metals and Material Society*, Vol.63, No.2, 36-42.

Panneerselvam M and Rao K. J, “Preparation of Si₃N₄SiC composite by microwave route, *Bulletin of Materials Science*, Vol 25, No.7, December 2002, 593-598.

Peelamedu D. Ramesh, Rustum Roy, Dinesh K. Agrawal,(2002), “Microwave-induced reaction sintering of NiAl₂O₄”, *Materials Letters*, 55, 234-240.

Penn Stuart, Alford Neil, “Ceramic Dielectrics for Microwave Applications”, *Handbook of Low and High Dielectric Constant Materials and their applications*, chapter-10, volume 2, Academic Press, 493- 530.

Piluso P., Gaillard, Lequeux N, & Boch P., (1996), “Mullitization and Densification of (3Al₂O₃ + 2 SiO₂) Powder Compacts by Microwave Sintering”. *Journal of the European Ceramic Society*, 16, 121-125.

Raghavendra Khedle, D.P.Mondal, S.N. Verma, Sanjay Panthi, (2012), “FEM Modeling of compressive behavior of aluminium cenosphere syntactic foam (ACSF) under constrained condition”, *Indian Journal of Engineering and Materials Science*, Vol.19, 135- 143.

Rohatgi P.K, Gupta N and Simon Alaraj.,(2006), “Thermal Expansion of Aluminium-Fly Ash Cenospheres Composites Synthesized by Pressure Infiltration Technique”, *Journal of Composite Materials*, Volume 40, No.13, 1163- 1172.

Rohatgi, Schultz B.F, Daoud A, Zhang W.W, (2009) “Tribological performance of A206 Aluminium alloy containing silica sand particles”, *Tribological International*, 23rd July.

Rustum Roy, Dinesh Agrawal, Jiping Chang & Shalva Gedevanishvili, (1999), “Full sintering of powdered- metal bodies in a microwave field”, *Nature*, Vol.399, 668-670.

Sadeghi E, S Hsieh and M Bahrami, (2011), “Thermal conductivity and contact resistance of metal foams”, *Journal of Physics D: Applied Physics*, Vol. 44, pp 1-7.

Sampathkumaran P, Ranganathaiah C, Seetharamu S and Kishore, (1998), “Sliding wear studies in glass –epoxy system through scanning microscopic observation”, *Bull. Mater. Sci*, Vol 21, No.4, August, 335-339, Indian Academy of Sciences.

Schaffer G.B., “Powder Processed Aluminium Alloys”,(2004), *Materials Forum*, Volume -28

Shanmughasundaram P, Subramanian, G. Prabhu., (2011), ‘Some Studies on Aluminium – Fly Ash Composites Fabricated by Two Step Stir Casting Method’, *European Journal of Scientific Research* ISSN 1450-216X Vol.63 No.2, 204-218.

Shuvendu Tripathy, 2009, “Studies on Aluminum–Fly-Ash Composite Produced by Impeller Mixing Abrasion”, *M. Tech Thesis*, Department of Metallurgical & Materials Engineering, National Institute of Technology, Rourkela.

Souvignier C.W, Sercombe T.B, Huo S.H, Calvert P and Schaffer G. B,(2001), “Freeform fabrication of Aluminium metal matrix composites”, *Journal of Materials Research*, Volume 16, No.9, September, 2613- 2617.

Sudharshan, M.K. Surappa, (2007), “Dry sliding wear of fly ash particle reinforced A356 Al composites”, *Elsevier, Science Direct, Wear*, 349-360.

Sudharshan, M.K.Surappa., (2008), “Synthesis of fly ash particle reinforced A356 Al composites and their characterization”, *Materials Science & Engineering A* 480, 117-124.

Surappa M K, 2003, “Aluminium Metal Matrix Composites: Challenges and opportunities’, *Sadhana*, Vol. 28, Part 1 & 2, February/ April, 334-340.

Suresh N, S. Venkateswaran, S. Seetharamu, (2010), “ Influence of cenospheres of fly ash on the mechanical properties and wear of permanent moulded eutectic Al–Si alloys” *Materials Science-Poland*, Vol. 28, No. 1.

Tjong S.C, Ma Z.Y, (1999), “High temperature creep behaviour of powder-metallurgy aluminium composites reinforced with SiC particles of various sizes”, *Composites Science and Technology* 59, 1117- 1125.

Torralba J.M, C.E. da Costa, Velasco F, (2003), “P/M Aluminium matrix composites: an overview”, *Journal of Materials Processing Technology*, 133, 203- 206.

Vogiatzis C. A, Tsouknidas A, Kountouras D T, Skolianos S, (2015), ‘Aluminium – ceramic cenospheres syntactic foams produced by powder metallurgy route’, *Elsevier Materials and Design*, 85, 444-454

Website on Cenotechnologies.

Website: www.Aluminium.org

Website: www.apitco.com, ‘Cenospheres from fly ash’ pdf file.

Website: www.wikipedia.com

Willard. Sutton H., (1989), “Microwave Processing of Ceramic Materials”, *Ceramic Bulletin*, 68, No.2, 376- 385.

Wilson S, Ball A, “Wear Resistance of an Aluminium Matrix Composite”, Department of Materials Engineering, University of Cape Town, Rondebosch 7700. South Africa, report from the *Internet search*.

Wong Wai Leong Eugene, Manoj Gupta,(2010),”Characteristics of Aluminium and Magnesium Based Nanocomposites Processed Using Hybrid Microwave Sintering”, *Journal of Microwave Power and Electromagnetic Energy* , 44(1), 14-27.

Wu G. H, Dou Z.Y, Ding L.T, Cao J.H, (2008), “Damping properties of Aluminium matrix- fly ash composites”, *Elsevier Science Direct, Materials Letter* 60, 2945- 2948.

Wu G. H, Dou Z.Y, Sun, D.L, Jiang L.T, Ding B. S and He B.F, (2007), “Compression behaviors of cenospheres-pure Aluminium syntactic foams”, *Scripta Materialia*, 56, 221-224.

Yuyuan Zhao, “Metal Matrix Syntactic Foams: Manufacture, Matrix Material, Microstructure, Modulus and More”, Vol. 63 No. 2, TMS Society *Journal of Materials*

Zhao Y, Tao. X, Xue X., (2008), “Manufacture and Mechanical Properties of Metal Matrix Syntactic Foams”, *Materials Science and Technology*, October, 2607- 2615.

Zhao YY and X. F. Tao, (2009), ‘Behaviour of Metal Matrix Syntactic Foams in Compression’ *Materials Science and Technology (MS&T)*, 1785-1794.

BIO-DATA

Name : M G Ananda Kumar

Date of Birth : 15.11.1968

Permanent address : No. 108/1, 2nd A Main Road,
Nanjappa Layout, Vidyaranyapura,
Bengaluru- 560 097
Karnataka State, India
Mobile: 09986318844,
Phone: (O) 080-23601399

Email : mgananda@cpri.in

Academic qualification

1. Diploma in Ceramic Technology : S J Polytechnic (1987)
Board of Technical Education, GOK
2. A.M.I.I.Cer.by examination : Indian Institute of Ceramics, Kolkata
(1993)
3. M. Tech- Materials Engineering : National Institute of Technology
Karnataka (NITK), Surathkal
(2005)
4. Ph.D : National Institute of Technology
Karnataka (NITK), Surathkal
(presently from 2008 onwards)

Employment : Working as Engineering Officer Gr.4 in
Central Power Research Institute,
Sir C V Raman Road, Sadashivanagar
Bengaluru- 560 080

Experience : Working in Central Power Research
Institute, Bengaluru since 1989.
(27 years of research experience)

APPENDIX

Measured values for various properties of aluminium cenospheres Composite

Test	Composition	Aluminium Cenospheres Conventionally sintered	Aluminium Cenospheres Microwave sintered	Difference in value (%)
Porosity (%)	100 % Al	30.5	26.4	15.6
	Al-90- Ceno 10	39.6	34.1	23.1
	Al-80- Ceno 20	42.1	35.5	18.6
	Al-70- Ceno 30	44.1	36.2	21.8
	Al-60- Ceno 40	44.9	37.8	18.8
	Al-50- Ceno 50	46.2	38.7	19.6

Water Absorption (%)	100 % Al	17.5	14.8	18.2
	Al-90- Ceno 10	21.1	18.6	13.6
	Al-80- Ceno 20	20.9	18.5	13.1
	Al-70- Ceno 30	21.1	18.8	12.4
	Al-60- Ceno 40	21.2	18.9	12.5
	Al-50- Ceno 50	20.6	18.4	12.2

Bulk Density (g/cc)	100 % Al	2.15	2.2	2.3
	Al-90- Ceno 10	1.95	2.0	2.5
	Al-80- Ceno 20	1.91	1.95	2.1
	Al-70- Ceno 30	1.81	1.85	2.2
	Al-60- Ceno 40	1.78	1.83	2.7
	Al-50- Ceno 50	1.76	1.80	2.2

Erosion Loss (g)								
Composition	Aluminium Cenospheres Conventionally sintered				Aluminium Cenospheres Microwave sintered			
	Angle of Erosion							
	30	45	60	90	30	45	60	90
100 % Al	0.01	0.016	0.012	0.0187	0.009	0.0090	0.0080	0.007
Al-90- Ceno 10	0.495	0.86	0.443	0.397	0.480	0.66	0.356	0.277
Al-80- Ceno 20	1.386	1.81	1.13	0.871	1.194	1.635	0.821	0.716
Al-70- Ceno 30	2.4	3.15	1.86	1.23	2.080	2.650	1.366	1.126
Al-60- Ceno 40	2.9	3.52	2.3	2.3	2.560	3.300	1.800	1.780
Al-50- Ceno 50	3.2	3.88	2.8	3.2	2.900	3.800	2.100	3.400

Wear Loss (g)						
Composition	Aluminium Cenospheres Conventionally sintered			Aluminium Cenospheres Microwave sintered		
	Load in kg					
	1	2	3	1	2	3
100 % Al	0.02	0.03	0.19	0.01	0.02	0.14
Al-90- Ceno 10	0.17	0.26	0.52	0.08	0.14	0.32
Al-80- Ceno 20	0.42	0.68	0.98	0.34	0.58	0.72
Al-70- Ceno 30	0.72	1.30	1.80	0.55	0.81	1.3
Al-60- Ceno 40	1.23	1.90	2.60	0.95	1.6	2.2
Al-50- Ceno 50	2.11	2.80	3.30	1.15	2.3	2.9

Tests	Composition	Aluminium Cenospheres Conventionally sintered	Aluminium Cenospheres Microwave sintered	Difference in value (%)
Brinell Hardness Number	100 % Al	32	46	30.4
	Al-90- Ceno 10	31	44	29.5
	Al-80- Ceno 20	30	43	30.2
	Al-70- Ceno 30	26	35	25.7
	Al-60- Ceno 40	23	31	25.8
	Al-50- Ceno 50	21	24	12.5

Aluminium Cenospheres composites Conventionally sintered					
Tests	Composition	Compression strength before and after thermal shock cycles			
		Prior to sintering	5 cycles	10 cycles	25 cycles
Compression Strength (kg/cc)	100 % Al	125	123.8	121.7	120.1
	Al-90- Ceno 10	76.5	72.6	67.4	42.6
	Al-80- Ceno 20	71.2	67.3	63.3	39.9
	Al-70- Ceno 30	67.1	61.6	58.7	34
	Al-60- Ceno 40	63.8	57.7	54.9	32
	Al-50- Ceno 50	62.5	48.2	38.1	31.6

Aluminium Cenospheres composites Microwave sintered					
Tests	Composition	Compression strength before and after thermal shock cycles			
		Prior to sintering	5 cycles	10 cycles	25 cycles
Compression Strength (kg/cc)	100 % Al	140.3	138.8	133.7	131.1
	Al-90- Ceno 10	97.6	90.9	86.3	73.1
	Al-80- Ceno 20	89.3	87.3	81.3	58.5
	Al-70- Ceno 30	86.2	79.3	77.7	57
	Al-60- Ceno 40	76.6	68.9	62.7	46.6
	Al-50- Ceno 50	71.7	56.7	47.4	37.6

Test	Composition	Conventionally sintered	Microwave sintered	Difference in value (%)
Co-efficient of Thermal Expansion (W/m.K)	100 % Al	$25.6 \times 10^{-6}/^{\circ}\text{C}$	$25.6 \times 10^{-6}/^{\circ}\text{C}$	0
	Al-90- Ceno 10	$20.6 \times 10^{-6}/^{\circ}\text{C}$	$16.3 \times 10^{-6}/^{\circ}\text{C}$	20.9
	Al-80- Ceno 20	$16.3 \times 10^{-6}/^{\circ}\text{C}$	$10.4 \times 10^{-6}/^{\circ}\text{C}$	36.2
	Al-70- Ceno 30	$12.9 \times 10^{-6}/^{\circ}\text{C}$	$7.7 \times 10^{-6}/^{\circ}\text{C}$	40.3
	Al-60- Ceno 40	$9.3 \times 10^{-6}/^{\circ}\text{C}$	$4.7 \times 10^{-6}/^{\circ}\text{C}$	49.5
	Al-50- Ceno 50	$7.3 \times 10^{-6}/^{\circ}\text{C}$	$3.6 \times 10^{-6}/^{\circ}\text{C}$	50.7

Conventionally sintered							
	Prior to sinter	5 cycles	% loss in strength	10 cycles	% loss in strength	25 cycles	% loss in strength
1C	125	123.8	1.0	118.9	4.9	120.1	3.9
2C	76.5	72.6	5.1	67.4	11.9	42.6	44.3
3C	71.2	67.3	5.5	63.3	11.1	39.9	44.0
4C	67.1	61.6	8.2	58.7	12.5	34	49.3
5C	63.8	57.7	9.6	54.9	13.9	32	49.8
6C	62.5	48.2	22.9	38.1	39.0	31.6	49.4
Microwave sintered							
	Prior to sinter	5 cycles	% loss in strength	10cycles	% loss in strength	25 cycles	% loss in strength
1M	140.3	139.1	0.9	133.7	4.7	131.1	6.6
2M	97.6	93.1	4.6	86.3	11.6	73.1	25.1
3M	89.3	85.2	4.6	81.3	9.0	58.5	34.5
4M	86.2	79.3	8.0	77.7	9.9	57	33.9
4M	76.6	69.6	9.1	62.7	18.1	46.6	39.2
6M	71.7	56.7	20.9	47.4	33.9	37.6	47.6

Tests	Composition	Aluminium Cenospheres Conventionally sintered	Aluminium Cenospheres Microwave sintered	% loss in compression strength
Compression Strength (kg/cc)	100 % Al	125.0	140.3	10.9
	Al-90- Ceno 10	76.5	97.6	21.6
	Al-80- Ceno 20	71.2	89.3	20.3
	Al-70- Ceno 30	67.1	86.2	22.2
	Al-60- Ceno 40	63.8	76.6	16.7
	Al-50- Ceno 50	62.5	71.7	12.8

Tests	Composition	Aluminium Cenospheres Conventionally sintered	Aluminium Cenospheres Microwave sintered	Difference in value (%)
Flexural Strength (kg/cc)	100 % Al	52.0	71.9	27.7
	Al-90- Ceno 10	47.7	62.5	23.7
	Al-80- Ceno 20	38.2	49.8	23.3
	Al-70- Ceno 30	27.3	40.8	33.1
	Al-60- Ceno 40	14.7	35.7	58.8
	Al-50- Ceno 50	8.8	31.5	72.1